ORNL/SPR-2015/643

# Quantitative Assessment of Nuclear Data Uncertainties for National Security Applications

## FY2015 Report: Developing the Building Blocks and Tools for Comprehensive Nuclear Data Uncertainty Analysis

## Project OR15-V-OR-Nuclear Data Roadmap-PD3SL

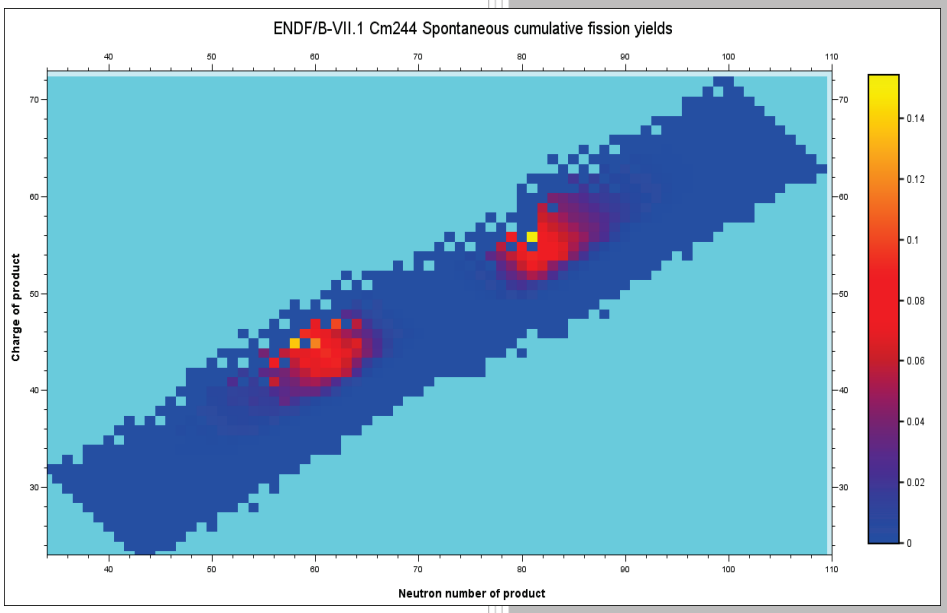


Oak Ridge National Laboratory
Ian Gauld
Stephen Croft
Dan Ilas
Andrew Nicholson
Marco Pigni
Ram Venkataraman
Louise Worrall

Los Alamos National Laboratory
Martyn Swinhoe

Lawrence Livermore National Laboratory
Caleb Matton
Dennis McNabb
Vladimir Mozin
Jerome Verbeke

**October 2015**



OAK RIDGE NATIONAL LABORATORY
MANAGED BY UT-BATTELLE FOR THE US DEPARTMENT OF ENERGY

**ORNL/SPR-2015/643**

Reactor and Nuclear Systems Division

# Quantitative Assessment of Nuclear Data Uncertainties for National Security Applications

## FY2015 Report: Developing the Building Blocks and Tools for Comprehensive Nuclear Data Uncertainty Analysis

## Project OR15-V-OR-Nuclear Data Roadmap-PD3SL

Ian Gauld,[1] Stephen Croft,[1] Dan Ilas,[1] Andrew Nicholson,[1] Marco Pigni,[1] Ram Venkatraman,[1] Louise Worrall,[1] Martyn Swinhoe,[2] Caleb Mattoon,[3] Dennis McNabb,[3] Vladimir Mozin,[3] Jerome Verbeke[3]

[1]Oak Ridge National Laboratory
[2]Los Alamos National Laboratory
[3]Lawrence Livermore National Laboratory

Date Published: October 2015

Prepared by
OAK RIDGE NATIONAL LABORATORY
Oak Ridge, TN 37831-6283
managed by
UT-BATTELLE, LLC
for the
US DEPARTMENT OF ENERGY
under contract DE-AC05-00OR22725

**CONTENTS**

## LIST OF FIGURES

## LIST OF TABLES

## EXECUTIVE SUMMARY

Nuclear data impacts virtually every aspect of nuclear nonproliferation modeling and simulation. From the design of nuclear detection instruments used in nondestructive and destructive technologies, to the interpretation of measurement data, reliable nuclear data are needed. Application areas include nuclear forensics, signature analysis, material verification, reactor-based materials production detection, treaty verification and nuclear test monitoring, and safeguards. However, nuclear data development has been driven almost entirely by the needs of the reactor physics and nuclear criticality community. When modeling applications extend into areas of national nuclear security, the validated range of data application can be easily exceeded. This leads to results that rely on nuclear data with gaps and inconsistencies or that are of a very low quality. Since full uncertainty analysis (inclusive of nuclear data) is not performed routinely, users are unlikely to be aware when results are unreliable. The need to improve nuclear data for a range of extended applications including national security is underscored by a recent workshop on Nuclear Data Needs for Applications organized by the Office of Science Nuclear Physics program and the Office of Defense Nuclear Nonproliferation R&D, and the formation of a working group on nuclear data to develop consensus data needs and advance activities leading to new measurements.

Efforts to compile nuclear data needs in the past are dominated by studies that typically address only a narrow application area, or are limited to evaluating a small subset of nuclear data. In addition, these studies are largely ad hoc and dominated by subjective experience. While expert opinion is valuable, intuition should not be the sole basis of prioritizing future experimental programs.

This project applies quantitative nuclear data uncertainty analysis tools to evaluate complex, often multi-physics problems that rely on a vast database of diverse nuclear data. Not only can these tools be applied to assess levels of uncertainty associated with the different components of current nuclear data, but the tools enable the identification of the specific nuclear data dominating the contribution to model uncertainty. Such tools represent a basic cross-cutting R&D capability that can be applied in any study to identify and prioritize nuclear data needs that are highly application dependent. This project focuses primarily on data for nondestructive assay using neutron and gamma-based measurement technologies, but also extends to include the nuclear data important to direct measurement of nuclear material (destructive techniques). These technologies are central to proliferation detection technologies. The types of nuclear data addressed in this project include a) neutron reaction cross sections, b) prompt neutron multiplicity distributions for fission, P($\nu$), c) prompt fission energy distribution (Chi), d) spontaneous fission neutron emission, e) neutron emission from ($\alpha$,n) reactions, f) delayed gamma ray emission, g) nuclear decay data, and h) fission product yields. These data underpin quantitative modeling and simulation applications for a broad range of nonproliferation problems, beyond the focus area of this project.

The first year of this project (FY 2015) has focused on compiling and developing the covariance information that describe the uncertainties in nuclear data and their correlations, and developing the tools to apply these covariances to analyze complex problems. The complexity arises because these problems are not analytic in nature, they generally involve many physics processes, use large amounts of data, are highly energy dependent, and data importance is very applications specific. A preliminary application of these tools and data is demonstrated for a neutron multiplicity counter instrument and $PuO_2$ samples as a case to exercise the methods and integrate the different data components of the uncertainty analysis. The major project accomplishments are summarized below:

- Neutron cross section covariance data from ENDF/B-VII.1 nuclear data files were applied to develop continuous-energy libraries for uncertainty analysis using the MCNP code. Several

strategies where investigated during this work to optimize and implement the procedure in the Kiwi code developed at LLNL. These libraries also include uncertainty in prompt fission neutron emissions. Initial demonstration of this method was applied to plutonium and oxygen isotopes.

- LLNL is developing data analysis tools to identify the important nuclear data contributing to the uncertainty by analyzing correlations between the system response and the nuclear data uncertainty variations (i.e., evaluating the system feedback due to each of the data uncertainty changes). This approach was successfully applied to the multiplicity counter model.

- Covariance data are generally not available for spontaneous fission neutron emission, and approximate uncertainty representations were developed and applied in this study to evaluate $^{240}$Pu. More rigorous theoretical approaches to spontaneous fission neutron uncertainty analysis and covariance data generation are currently being investigated by LLNL using the FREYA fission model code.

- Covariance data are not available for neutron emission from (α,n) reactions. Alpha reaction cross section covariance data were generated by ORNL using the SAMMY R-matrix code using a demonstration oxide matrix problem. Alpha particle stopping power uncertainty was also addressed. The work resulted in improved cross section evaluations for $^{17}$O and $^{18}$O, uncertainty estimates in the calculated neutron source, and better agreement with experimental data. Results of this work have been drafted for publication in a peer reviewed journal.

- Covariance data are similarly not available for nuclear decay data or fission product yields. However, retroactive development of covariance data has been performed previously by ORNL and the data have been compiled for application to this project.

- New approaches to nuclear data uncertainty analysis have been developed using perturbation theory and implemented in the ORIGEN isotope generation code by ORNL. This provides a powerful capability to identify the sensitivity of any calculated quantity to all nuclear data used in calculations for reactor based material production or complex decay problems such as post-detonation analysis. Development is continuing and the method is being applied to evaluate the Hanford production reactor experimental data. Additional support, beyond the current project, is likely needed to fully integrate uncertainty analysis using all available nuclear data covariance information.

- The analysis tools and covariance data were applied by LANL to the neutron multiplicity coincidence counter using $PuO_2$ as the measured nuclear material with different masses to similar different levels of neutron multiplication. This instrument exercises many of the nuclear data components addressed in this project and can be used for experimental confirmation of uncertainty results. The results identified the key nuclear data and uncertainties that influenced the neutron count rates and the derived Pu masses. This analysis also shows that the uncertainties are influenced by the method of measurement data analysis. Future work will extend the analysis of the multiplicity counter to address other nuclides and data.

Figure A shows the results of our uncertainty calculation for (α,n) production in uranium oxide. This analysis was used to demonstrate a general approach for uncertainty analysis as applied to (α,n) neutron yield calculations. However, this approach can be readily adapted to evaluate other source and matrix types, such as fluorides and many other compounds. The evaluation methodology also generates covariances that can be used to estimate uncertainties in the calculations. These uncertainties are observed to be consistent in comparisons to experimental data in Figure A. This uncertainty analysis methodology can be used in applications where measurements do not exist.

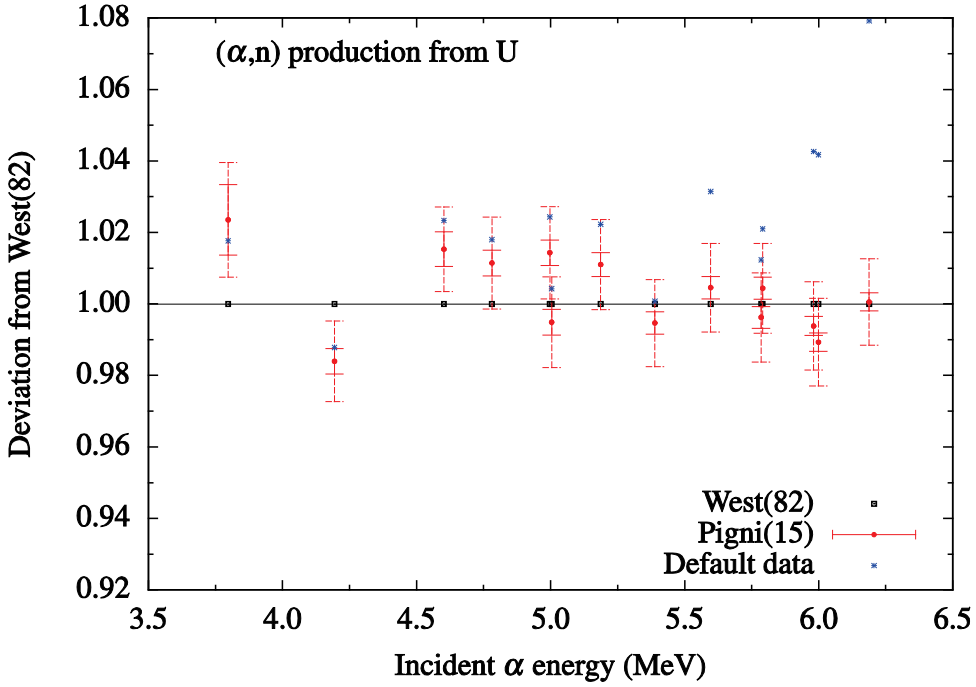


***Figure A. Comparison of calculations to West's measurements, showing deviations and estimated calculation uncertainty due to (α,n) cross section (red line), cross section plus stopping power coefficients (red dashed line), and results of calculations using default data in the SOURCES code.***

Figure B shows the estimated plutonium mass determined for the neutron multiplicity counter demonstration application from the calculated counting rates for 100 nuclear data perturbations that reflect the uncertainty in the data. The standard deviation of the resulting measured Pu mass is 0.04%, which corresponds to a 3-sigma input cross section variation.

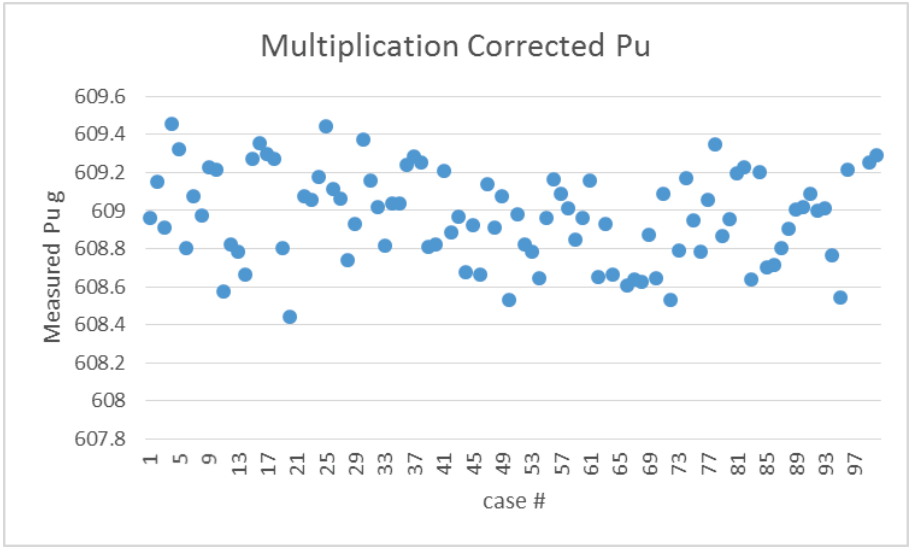


***Figure B. The derived Pu mass for the neutron multiplicity counter based on 100 samples of cross section data uncertainties.***

Table A summarizes the individual nuclear data contributions to the measurement of a medium-size plutonium sample. The results indicate that the uncertainty in the absolute intensity of spontaneous fission and (α,n) emission are the major contributors on this list.

***Table A. Summary of sensitivity study***

| | **Multiplication-corrected Pu mass uncertainty** | **Nonmultiplication-corrected Pu mass uncertainty** | **Multiplicity calculated Pu mass uncertainty** |
|---|---|---|---|
| SF intensity | 0.64% | 1.02% | 1.09% |
| (α,n) intensity | 0.62% | 0.10% | 0.00% |
| P(v) $^{240}$Pu | 0.16% | 0.44% | 0.38% |
| Energy spectrum $^{240}$Pu | 0.18% | 0.40% | 0.50% |
| Energy spectrum (α,n) | 0.27% | 0.04% | 0.00% |
| Global nuclear data [a] | 0.04% | 0.61% | 0.09% |

[a] Includes neutron cross sections and prompt fission parameters

Continued work to further develop the foundation for nuclear data uncertainty analysis is planned in FY 2016 with work focusing on a) expanding and finalizing the cross section analysis capability b) investigating use of the FREYA code for uncertainty analysis of the fission process, c) expanding the analysis of uncertainties in (α,n) reaction processes to include other matrix materials, d) initiating research on prompt and time-delayed gamma uncertainty analysis, e) continuing development of the tools for reactor based materials production analysis, and f) developing additional benchmark problems that exercise a broader range of nuclear data. The availability of these tools will provide important capability for defining nuclear data measurement needs and priorities for the activities on the Nuclear Data Working Group, and are readily transferable to other mission areas.

# 1. NUCLEAR DATA UNCERTAINTY R&D

## 1.1 INTRODUCTION

Nuclear data support all nuclear material measurement methods and serve as input to modeling and simulation tools that are used to represent detector systems and interpret measurement results. The accuracy of modeling and detector data analysis is limited by the accuracy of the nuclear data used in both nondestructive and destructive analyses. Therefore, accuracy is fundamental to the evaluation of nuclear material detection for forensics, signature analysis, nuclear material verification, reactor-based materials production detection, treaty verification and nuclear test monitoring, and safeguards.

Development of nuclear data has been driven primarily by the needs of the reactor physics and nuclear criticality safety communities. If modeling applications are extended into areas of national nuclear security, the validated range of the data can be exceeded, leading to results that rely on nuclear data with gaps and inconsistencies or of a very low quality. Since uncertainty analysis is not performed routinely, users are not likely aware when results are unreliable. To date, nuclear data deficiencies have been handled largely on a qualitative and ad hoc basis rather than with a structured, systematic approach that can assess the role of all nuclear data used in an analysis.

Unlike many previous studies, this project applies quantitative uncertainty tools to the broad class of all nuclear data used in support of modeling for national security missions. The methodologies and tools being developed under this project cross cut many areas of security research, as well as various measurement and instrument technologies. Although the nuclear data important to these different applications vary depending on the application, the tools developed under this project cover the major nuclear data categories common to many application areas:

- neutron reaction cross sections,
- nuclear decay data,
- fission product yields (production rates from fission),
- passive spontaneous fission neutron production data,
- passive (α,n) reaction neutron production data,
- passive gamma ray production data, and
- prompt neutron production and multiplicity data.

This project was established to develop

1. nuclear data uncertainties for the basic data used in nuclear security modeling applications (these data represent the fundamental building blocks of our approach to uncertainty analysis),
2. computational tools needed to apply these data in real applications,
3. experimental benchmarks to validate results from these tools and data, and
4. demonstration applications of high interest to nuclear nonproliferation detection.

Nondestructive assay (NDA) measurements using neutron and gamma emissions are emphasized in this work; however, the application space extends to include direct measurement of nuclides and isotopic ratios that can be detected, for example, in environmental airborne monitoring and nuclear facility sampling. This wide range of applications can be assessed because much of the nuclear data that define many of the physics processes and the observable signatures are common.

This report describes development of the codes, methods, uncertainty data, and analysis infrastructure that will be used to assess various proliferation detection and safeguards measurement systems. Ultimately,

these methods will be extended to systems that include irradiated nuclear materials (i.e., spent nuclear fuels and reactor-based materials production) and other fissioning systems. The ability to analyze irradiated materials is the grand challenge problem to demonstrate the analysis capability for a very broad range of nuclear data required for applications relevant to nuclear security.

The detector application studied in this report (part of the FY15 scope) includes analysis of the Epithermal Neutron Multiplicity Coincidence (ENMC) counter containing unirradiated $PuO_2$ material. The ENMC is an initial prototype system exercising a broad range of nuclear data. It is used as a platform to demonstrate modeling, development, and application of uncertainty analysis tools, and it can also be used as an experimental benchmark.

## 1.2 COLLABORATION ROLES AND RESPONSIBILITIES

Data and methods development draw on the considerable strengths and code experience of the partner laboratories.

- *Lawrence Livermore National Laboratory* (LLNL) analyzes uncertainties associated with continuous-energy nuclear data as used in transport codes such as Monte Carlo N-Particle (MCNP). In addition, LLNL brings considerable expertise in fission event modeling with development of the fission reaction yield event yield algorithm (FREYA) code for neutron-induced fission and spontaneous fission. FREYA is a critical tool or modeling and simulation of nuclear materials and analysis of uncertainties in these processes.
- *Los Alamos National Laboratory* (LANL) is central to developing the application models used in these studies, including instruments used in nuclear safeguards, arms control, nuclear proliferation detection, and post-detonation fallout analysis. LANL also has experience and access to data that will be used to validate individual components of nuclear data uncertainties. In this report, LANL developed the model for the ENMC used for preliminary methods integration and uncertainty analysis demonstration.
- *Oak Ridge National Laboratory* (ORNL) has primary responsibility for generating the uncertainty data and methods to analyze (1) passive neutron and gamma ray emissions from nuclear materials (i.e., the data not covered by the prompt nuclear process in MCNP being evaluated by LLNL) and (2) uncertainties in isotopic inventories and activities as related to fission event models (fallout) and reactor based materials production. ORNL has also provided independent verification of LLNL methods and data using SCALE. A detailed description of the work on data and uncertainties for (α,n) neutron production is included in this report.

Table 1 summarizes the code expertise and data development areas of each laboratory. This work will be discussed in more detail below.

**Table 1. Laboratory contributions to OR15-V-OR-Nuclear Data Roadmap-PD3SL**

| Lab | Code | Nuclear data and models |
|---|---|---|
| LANL | MCNP | Detector system model development and data application |
| LLNL | MCNP | Continuous-energy neutron reaction cross section data |
| | FREYA | Prompt neutron-induced fission data (nubar and Chi) |
| | | Prompt fission neutron multiplicity data |
| ORNL | SCALE/ORIGEN SOURCES | Nuclear decay data |
| | | Fission product yield data (production rates from fission) |
| | | Passive spontaneous fission neutron production data |
| | | Passive (alpha,n) reaction neutron production data |
| | | Passive gamma ray production data |
| | | Fission/transmutation based material production (inventories) |

## 1.3 A SYSTEMATIC FRAMEWORK FOR NUCLEAR DATA UNCERTAINTY ANALYSIS

Agencies that fund nuclear data measurement and sponsors of nuclear applications need objective information on data uncertainties to establish priority areas where improvements will most benefit their applications. Many efforts to identify nuclear data needs for safeguards and nonproliferation applications have suffered from a lack quantitative analysis. These efforts continue to be a largely ad hoc, failing to provide a comprehensive, systematic review of all nuclear data used in modeling. The result is subjective recommendations that vary depending on the source consulted, as well as findings that may not represent the broader problem.

Nuclear analysis models use a vast amount of data. A structured, systematic approach to data analysis is required to determine the levels of uncertainty associated with computational results (which are not currently reported in most cases). The systematic framework will also help determine which data are most important when defining the computational uncertainty needed to identify data measurements most likely to reduce modeling and simulation uncertainties.

As part of this project, the quantitative data uncertainty quantification process shown below is being developed to analyze key nuclear data used in nuclear security applications. The process includes the following main steps:

1. Define the end-use safeguards and nonproliferation applications of interest (e.g., detection technologies or instruments).
2. Develop representative models for simulation of these applications.
3. Identify the nuclear data required to analyze and compile available covariance data, including estimates of data uncertainty with their correlations.
4. Develop nuclear covariance data when data are not available.
5. Develop the software to analyze the impact of nuclear data on the applications and how current estimates of data uncertainty impact selected applications.
6. Compile experimental benchmarks to assess the reliability of uncertainty studies and conclusions (i.e., validation of uncertainty data and tools).

This project focuses on developing the foundational building blocks of nuclear data uncertainty and the modules necessary to apply these data to applications. The nuclear data and tools will be applied to several examples to demonstrate the methodology and illustrate the types of information that can be obtained for these studies. The larger effort to develop a fully automated, user friendly software framework for the broader community is not within the project scope. However, once the methods to

security applications of interest are successfully demonstrated, these components can be integrated within a unified analysis framework for use with other applications.

The quantitative analysis procedure is illustrated in Fig. 1. The process is (1) to clearly define the problem, (2) review previous findings to see if the problem has already been solved and to obtain any applicable information from previous studies, (3) model the problem, (4) collect output from the models, (5) analyze the results, and (6) clearly convey information in an understandable way that will result in action. A coordinated, clear, consistent message on nuclear data needs for security applications is needed.

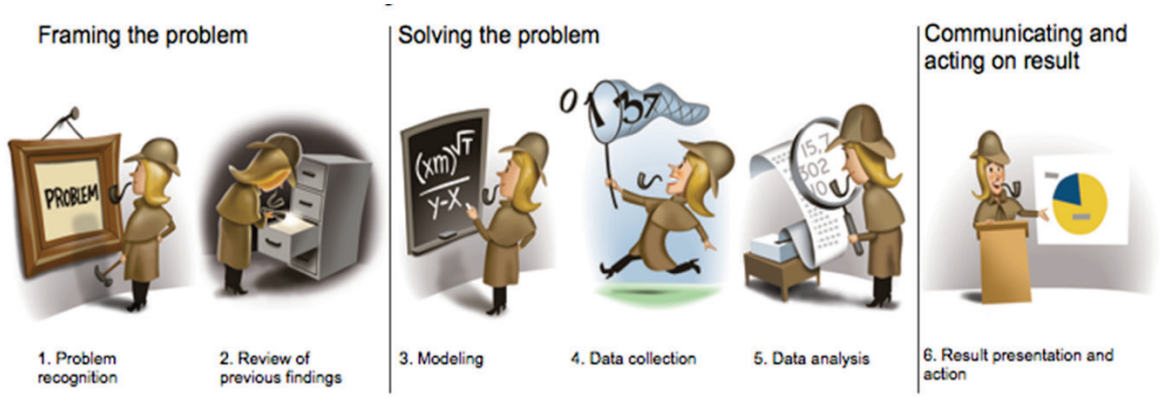


**Fig. 1. Steps in quantitative analysis developed for business data analytics.**[1]

## 1.4 EXPERIMENTAL VALIDATION

The approach to nuclear data assessment is based applying the uncertainties in the basic nuclear data as reported by the measurement laboratories. Approaches based on Monte Carlo sampling of these uncertainties re widely used and adopted in this work, along with other powerful adjoint-based (inverse) solutions for simulating isotopic evolution during irradiation and decay. These approaches rely on the availability of accurate uncertainty information and covariance data that describe correlations in the nuclear data uncertainties necessary for realistic uncertainty analysis. The reality of existing state-of-the-art nuclear data evaluations (e.g., ENDF/B-VII.1 [1]) is that while significant progress in the development of covariance data has been made [2], there are still important gaps and deficiencies in nuclear data uncertainty information. These gaps may be magnified in nuclear security applications that often rely on data very different than that needed in nuclear safety applications. Due to the unique nature of these data, they may not be very well known or extensively tested.

This raises the question that if covariance data are of unknown quality, how sound are the conclusions drawn from uncertainty analyses using these data? To address this concern, experimental benchmarks are integrated into the project where available to validate uncertainty analysis outcomes. Benchmarks provide an experimental basis to assess the quality of the data information and ensure that uncertainty conclusions obtained when extending an analysis beyond the range of the experimental data are accurate.

This report describes an initial venture into methods validation in which uncertainties developed for modeling neutron production from (α,n) reactions on oxygen are validated against measurements. The ENMC multiplicity counter was selected to demonstrate initial data and methods integration since it is available to provide experimental data for validation. An important aspect of this work is that the

[1] Used with permission from Thomas Davenport, "Keeping Up with the Quants: Your Guide to Understanding and Using Analytics," (Harvard Business Review Press) 2013.

uncertainty data applied in these studies do not have to be precise. As in probabilistic risk assessment, the exact value of a component failure rate is not of paramount importance to fault analysis. The critical factor is the ability to use the information to identify critical weaknesses that contribute most to the outcome. The failure rate on a particular system component does not need to be known precisely in order to identify priority areas for improvement.

## 1.5 RELATIONSHIP TO OTHER PROJECTS

This project is unique relative to other uncertainty projects funded by the Office of Defense Nuclear Nonproliferation Research and Development because it focuses exclusively on nuclear data and nuclear data uncertainty in applications. Project OR14-V-Uncertainty-PD2La "Uncertainty Quantification for Nuclear Safeguards and Non-Destructive Assay," focuses on nondestructive assay (NDA) measurements, with particular emphasis on uncertainty in instrument calibration. There are related technical areas of nuclear data in these projects; however, these areas are primarily limited to nuclear data in calibration sources (e.g., $^{252}$Cf, which is not addressed in this project). This project focuses exclusively on nuclear data uncertainty quantification for nuclear security and nonproliferation applications.

## 1.6 REVIEW OF PRIOR RESEARCH

Several investigations have evaluated and prioritized nuclear data needs for nuclear safeguards and nonproliferation applications. These studies were usually limited to a narrow applications space, and they only considered a small subset of the nuclear data needs relevant for a particular application. In contrast, the current project provides a comprehensive nuclear data review and considers the data and the uncertainty important to a broad range of potential applications that include both nondestructive assay (NDA), destructive assay (DA), or direct measurement of nuclear material by other methods (e.g., mass spectrometry of effluents). A comprehensive data analysis approach is necessary since various instruments and methods may be required in nuclear security measurements.

While previous works have examined the impact of nuclear data uncertainties and the sensitivity of methods to the nuclear data, little attention has been given to the covariances that define the correlations between the different components of data uncertainty. For accurate uncertainty quantification, it is essential to consider covariances in nuclear data. The current work examines the availability of covariance data and evaluates their impact on applications. For cases in which covariance data are not available (i.e., they are not reported with the data measurements), the data are generated using retroactive techniques. This is the case for passive neutron emission data, such as neutron yields from (α,n) reactions and spontaneous fission.

These previous works provide valuable insight to the impact of nuclear data parameters, and they indicate where research has previously been directed to address nuclear data needs. This project extends the foundations of previous studies by expanding the types of nuclear data considered, applying quantitative uncertainty analysis tools, and integrating these tools to address real-world applications.

Brief reviews of some earlier major works on nuclear data needs are presented in the following sections.

### 1.6.1 Schillebeeckx, et al., "Nuclear Data Requirements for Non-Destructive Assay of Fissile and Fertile Material" (1999)

As early as 1999, Schillebeeckx et al. [3] evaluated the impact of variations in nuclear data found in the literature on gamma- and neutron-based NDA methods, as well as on nuclear calorimetry. The gamma application focused on isotopic ratios using gamma spectroscopy. For this, the authors considered the differences among the half-lives reported in the literature for Pu isotopes and $^{241}$Am. They also considered

the differences in branching ratios for key gamma lines. Schillebeeckx et al. concluded that the contribution of nuclear data uncertainty to Pu isotopic ratio results (and $^{235}$U and $^{238}$U) is as high as ±1%. The authors observed that the $^{241}$Pu ratio reported prior to 1999 suffered a systematic uncertainty of >0.4%. Furthermore, the uncertainty in $^{241}$Pu half-life reported in American National Standards Institute (ANSI) standard 15.22 [4] was deemed unreliable by De Bièvre and Verbruggen [5].

For the nuclear calorimetry application, Schillebeeckx et al. examined the impact of differences in the specific power (heat) of different Pu isotopes and $^{241}$Am. They calculated the specific power by using literature values of the half-life, atomic mass, and disintegration energy for alpha decay, and then compared the specific power to the values directly measured using calorimetry. The authors reported a negligible difference. One of the reasons for the negligible difference was that the half-life values in the literature were obtained from calorimetry measurements and hence were not independent determinations.

The neutron application focused on passive neutron multiplicity counting. The nuclear data examined in the study were the half-life for spontaneous fission and the fission moments. The authors examined the triples neutron counting rates results and concluded that the accuracy was limited to 3%, which was approaching the nuclear data uncertainties. Schillebeeckx et al. also examined the (α,n) production yields from plutonium oxide. They compared the values based on thick target yields reported by Croft [6] to the values reported by Perry [7], which were based on microscopic cross section values. The two sets of results were systematically different by 3–6% for the different Pu isotopes and 2% for $^{241}$Am. Many of these nuclear data issues remain unresolved after 15 years.

### 1.6.2 Santi, "Sensitivity of Modeling Neutron Emissions to Uncertainties in Nuclear Data" (2008)

Santi [8] performed a study to understand how uncertainties in the fundamental nuclear data may affect the precision of radiation transport codes in modeling the correlated neutron emissions from nuclear materials. This study was conducted to explore new and advanced NDA techniques for the reprocessing technologies being considered for the former Advanced Fuel Cycle Initiative (AFCI). Since this scenario would keep various actinides commingled with plutonium at all times throughout the separation process, the resulting recycled nuclear fuel intended for the Advanced Burner Reactor (ABR) was thought to pose some unique measurement challenges. Robust, accurate modeling capabilities are paramount for predicting the neutron emission characteristics of the AFCI nuclear material during the various phases of separating and fabricating the material deemed relevant for safeguards. Calculations were performed to determine the sensitivity of modeling neutron emissions from nuclear materials associated with an UREX+1a separation process to uncertainties associated with the two prime sources of neutrons from nuclear material—spontaneous fission and (α,n) reactions.

MCNPX calculations were performed to determine the sensitivity in modeling the singles, doubles, and triples rates for UREX+1a nuclear materials to the uncertainties in the spontaneous fission multiplicity distributions. The spontaneous fission neutron multiplicity distributions for $^{238,240,242}$Pu and $^{244,246}$Cm were varied based on the measured uncertainties associated with the first, second, and third factorial moments of their respective distributions. The results of the calculations showed that the uncertainties in the $^{244}$Cm distribution produced the only measurable effect on the counting rates, with a ± 0.5% variation seen in the singles rate, a ± 1% variation seen in the doubles rate, and up to a ± 3.4% variation in the triples rate.

Because several of the possible separation technologies that were considered for AFCI would remove Cm from the nuclear material at some point in the process, a second set of calculations was performed with the Cm removed from the UREX+1a process. With no Cm present within the nuclear material, minor variations were observed with the calculated counting rates due to the uncertainties in the $^{240}$Pu neutron multiplicity distribution. Variations due to uncertainties in the $^{240}$Pu neutron multiplicity distribution depended on whether the high burnup or low burnup Pu was used in the calculation. The variations in the

count rates ranged from ±0.1–0.2% in the singles rate, ±0.3–0.5% in the doubles rate, and ±0.4–0.7% in the triples rate for high burnup Pu and low burnup, respectively. In the case of the calculations for high burnup Pu, which assumed a 4% $^{238}$Pu weight fraction and 29% weight fraction for $^{240}$Pu, variations of ±0.7% in the singles rate, ±1.5% in the doubles rate, and ±2.4% in the triples rate were observed due the uncertainties associated with the $^{238}$Pu neutron multiplicity distribution.

Calculations were performed using the SOURCES4C code to determine the sensitivity of modeling the total neutron production rate from (α,n) reactions on the uncertainties associated with the $^{17}$O(α,n), $^{18}$O(α,n) and $^{19}$F(α,n) cross sections. The effect of the uncertainties in the various cross sections on the neutron production rate varied depending on the separation stage being considered, with a 4–7 % variation observed due to uncertainties in the $^{18}$O cross section, a 0.1–11% variation due to the $^{19}$F cross section, and a 0.2–0.6% variation for the $^{17}$O cross section. Similar variations in the neutron production rates were observed when the Cm was removed from the material.

The study described above focused on the impact of nuclear data uncertainties on a particular NDA method for a specific application. The nuclear data considered were the spontaneous fission neutron multiplicity distribution for Pu and Cm isotopes and the $^{17}$O(α,n), $^{18}$O(α,n) and $^{19}$F(α,n) cross sections. The study did not consider the impact of covariances.

### 1.6.3 Parker, "Nuclear Data Needs: Source Term Library/Uncertainty Analysis" (2009)

Parker [9] evaluated nuclear data needs focused on energies and intensities of gamma ray lines of interest in safeguards. The objective of this study was to "produce a best library of γ rays emitted from isotopes of interest to be used as a reliable reference in safeguards work" and to "provide uncertainties for energies and branching intensities." Parker set out to evaluate the needs for actinides, fission products, and activation products, but funding constraints limited the work to actinide isotopes. As part of the work, a computer code called RADSRC was written to create a list of gamma ray lines for input to MCNP and other Monte Carlo codes.

Parker reported that the first investigations were done on U, Np, Am, and Pu. Early work compared National Nuclear Data Center (NNDC) gamma ray lists with the list generated by RADSRC. The study concluded that "with a few exceptions, the sources agree."

This study was completed in 2009, taking into consideration the actinide isotopes only. Parker recommended that "future work should include fission and activation products." A variety of fission products can be found in spent fuel. Some fission products with characteristic γ rays include $^{89,90}$Sr, $^{91}$Y, $^{95,97}$Zr, $^{111}$Ag, $^{136,137}$Cs, $^{141,143,144}$Ce, $^{153}$Sm, $^{156}$Eu, $^{161}$Tb, Rh, Pd, Nb, etc. A library of these isotopes would be useful to the safeguards community. Any analysis package could select isotopes from the library for specific use. A variety of activation products will be generated due to the presence of various structural materials from a variety of neutron induced reactions (n,γ), (n,p), (n,n'), (n,2n), etc. The activation products emit characteristic gamma lines. Cross sections for the creation of activation products depend on the neutron energy spectra. Some cross sections are well known, while others are not. Accurate cross sections and their uncertainties are needed for modeling radiation signatures.

### 1.6.4 Bahran et al., "A Survey of Nuclear Data Deficiencies Affecting Nuclear Non-Proliferation" (2014)

Bahran et al. [10] performed a general survey across various academic and research institutions in order to identify the most significant nuclear data deficiencies affecting applications in nuclear nonproliferation. The authors observe that in recent years, such deficiencies have become increasingly apparent in the nuclear nonproliferation community, where accurate interpretation of physical applied nuclear

measurements depends on the availability of nuclear data fit for this purpose. Well-known examples include data in applications key to nonproliferation, such as special nuclear material characterization through neutron multiplicity measurements, spent fuel assay techniques, and γ-ray spectroscopy for isotope identification, among others.

The authors capture a number of deficient nuclear data parameters, including isotopic determination for nuclear safeguards (which requires data on half-lives), relative emission probabilities (branching ratios), and accurate energy differences. Passive neutron multiplicity counting for special nuclear material characterization is limited by the accuracy of certain data on multiplicity distributions, energy spectra, isotopic correlations asymmetric neutron emission, spectrum-multiplicity correlation, and fission n-γ correlations and (α,n) yields.

Bahran et al. point to nuclear data deficiencies in $^{252}$Cf, which is used ubiquitously as a calibration surrogate for Pu, and Cm isotopes $^{244}$Cm and $^{248}$Cm, which are important in the fuel cycle.

The most widely reported general issues based on survey responses were related to correlated particle emissions from fissile nuclear material (neutron and gamma-ray multiplicity), fission product data, total and partial neutron cross sections of various isotopes, and (α,n) yields from light elements. The most widely reported specific deficiencies were those related to nubar for $^{239}$Pu in the fast energy range, and data associated with fission products (yield, energy spectrum, half-lives, emission, branching ratios, etc.). Other recurring issues included photonuclear data and S(α,β) thermal scattering datasets. Standalone issues reported consisted of deficiencies in the electronic excitation cross section libraries, critical mass values, and specific heat for nuclear calorimetry.

Bahran's review is indeed comprehensive, with expert input from practitioners in safeguards, nuclear nonproliferation, forensics, and nuclear data communities. However, these reviews are qualitative and subjective; results depend on the experts surveyed and their particular experiences with data deficiencies. While studies by survey represent a significant compilation of experiences, they are not systematic, and they generally lack quantitative analysis of the impacts of the uncertainties for defined end use applications. Consequently, it is difficult to develop nuclear data acquisition prioritizes or to rank data needs according to their importance and benefit to the community.

### 1.6.5 Sleaford, Gamma Spectroscopic Data for Non-Proliferation Applications (2015)

The Sleaford study [11] provides upgrades to the Evaluated Nuclear Data File (ENDF) database for transport modeling for neutron induced gamma ray spectrometry, e.g., the Neutron Activation Analysis (NAA) or the Prompt Gamma Neutron Activation Analysis (PGNAA). Sleaford observes that while some libraries have no photon spectra in the database for actinides, others have poor resolution or missing lines. For several thermal neutron capture reactions, such as $^{183}$W(n,γ) and $^{32}$S(n,γ), the study added new gamma lines in the capture gamma library. The Evaluated Gamma-Ray Activation File (EGAF) was cross-correlated with the Evaluated Nuclear Structure Data File (ENSDF) database decay schemes and then input into ENDF library for transport modeling. The ENSDF contains evaluated nuclear structure and decay data in a standard format. An international network of evaluators contributes to the database, which is maintained by the National Nuclear Data Center at Brookhaven National Laboratory. Information in the database is regularly updated to reflect revised evaluation results. Most recently completed evaluations are published in *Nuclear Data Sheets*. For each nuclide, all known experimental data used to deduce nuclear structure information are included. Each type of experiment is presented as a separate dataset. In addition, there is a dataset of "adopted" level and gamma-ray transition properties. These properties represent the evaluator's determination of the best values for these properties based on all available experimental data. The ENDF/B files are the core evaluated nuclear reaction data containing

recommended cross sections, spectra, angular distributions, fission product yields, thermal neutron scattering, photo-atomic data, and other data, with emphasis on neutron-induced reactions.

The update by Sleaford will be part of the next ENDF/B release. The study is evaluating new experimental data from thermal capture gamma from $^{235}U(n,\gamma)$ and $^{237}Np(n,\gamma)$. There are no high resolution capture gamma lines in the ENDF library for major actinides: the thrust of the study seems to be toward high resolution nuclear data (gamma lines) for neutron activation methods. Discussion on uncertainties is limited, although better quality data can be expected to lead to lower uncertainties.

### 1.6.6 Office of Science Workshop on Nuclear Data Needs for Applications (2015)

A recent workshop organized by the Office of Science on Nuclear Data Needs for Applications [12] highlights the growing recognition of the need to improve nuclear data for applications beyond just nuclear energy. The workshop specifically included presentations and breakout sessions on national security and isotope production.

Recurring cross cutting data themes emphasized during the workshop included deficiencies in fission product yield data, the prompt fission neutron spectrum, a lack of comprehensive covariance data for uncertainty analysis, and gamma ray emission and decay data. These themes are similar to those from the recent safeguards and nonproliferation community survey conducted by Bahran [10].

While numerous deficiencies in the data for nuclear security applications are identified, the situation for medical isotope production is particularly bleak; the isotope community has largely abandoning use of nuclear data libraries such as ENDF/B-VII due to the poor performance and inability to predict many basic isotope production quantities from irradiated targets. Instead, the community relies heavily on empirically based nuclear data developed from their own production campaigns. However, limitations in this approach are that the empirical nuclear data cannot necessarily be extended to assess production or uncertainties in other facilities or different target designs, other irradiation configurations, or used for production optimization studies. In other words, the data cannot be extended beyond the range where experimental data are available because the underlying data and uncertainties are not based on the physics of the nuclear processes.

The workshop organizers prepared a report on the findings that include both application-specific and cross cutting data needs. The result is a massive list of data deficiencies and areas for future research. However, the impacts of these deficiencies have not been quantified, and there has been little attempt to show how improvements in these data would benefit the applications community. Ultimately, sponsors and the nuclear data measurement community will be challenged to identify priority research areas from these findings.

# 2. THE SCIENCE OF NONPROLIFERATION TECHNOLOGY IS DEPENDENT ON NUCLEAR DATA

## 2.1 THE IMPORTANTANCE OF NUCLEAR DATA

Measurements are the foundation of technical investigation and verification, and nuclear data provide the fundamental information that underpins nuclear modeling and simulation software used for the design of detection technologies, to interpret measured results, and to extend calibrations for applications beyond experimental data. Uncertainties in nuclear data are one of the primary contributions to measurement uncertainty.

Understanding current levels of uncertainties in nuclear data and developing improved data are essential steps to developing robust methods that can be applied to conditions not routinely encountered. Data improvement leads to more efficient, more effective decision making because conclusions from nuclear material measurements can be made with greater confidence.

## 2.2 DATA FOR NUCLEAR MATERIAL MEASUREMENTS

Nuclear data necessary for the interpretation of data from the measurement of nuclear material can be grouped into broad categories of (1) nuclear material inventory, (2) source emission processes, (3) radiation transport and interactions, and (4) instrument detection (or response function).

- **Nuclear material inventory** encompasses the nuclear data required to determine the nuclear isotope compositions for time-dependent problems related to nuclear reactor materials production and decay, and it also applies measurements following a fission event, such as post-detonation nuclear forensics. The material compositions have a direct impact on the passive emission sources (activities), transport within the nuclear item (e.g., subcritical neutron multiplication), and on direct measurement of nuclear material (rather than the material emission characteristics) by mass spectrometry or other means.
- **Radiation emission** encompasses the nuclear data required to describe the isotope composition within the item (if unknown) and the types and yields of the passive radiation emitted from the item caused by nuclear decay processes. For NDA measurements, the source term is generally either the neutron or gamma-ray emission from the nuclear material being measured. Nuclear heat generation may also be included in this category but is not considered here.
- **Radiation transport** encompasses the nuclear data required to describe the radiation interactions within the item and surrounding environment, and governs their transport (e.g., scattering) and removal (i.e., absorption or leakage), and subcritical neutron multiplication caused by fission due to passive neutron emission. The combination of passive emissions and subsequent interactions with the nuclear material ultimately determines the intensity and spectra of the radiation impinging on a detector. For NDA measurements, this usually refers to neutron or photon transport through the nuclear material item, through surrounding or intervening materials, or through the counter materials. Nuclear data in this category are frequently used to derive instrument correction factors which can be calculated using Monte Carlo radiation transport codes to compensate for radiation losses in the item-detector system, such as self-attenuation (gamma-rays) or self-shielding (neutrons) that are difficult to measure directly.
- **Instrument detection** encompasses the nuclear data required to describe the detected response. For NDA measurements, this may be a neutron and/or gamma-ray counting rate or spectral quantity used to derive nuclear material quantity, quality, and, sometimes, origin.

These nuclear data categories apply to many areas of nuclear security and nonproliferation measurements. However, the importance and emphasis of the nuclear data set will vary depending on the source characteristics and type of instrument used to obtain the data.

Figure 2 illustrates how design, calibration, and interpretation of measurement depend on nuclear data. The ENMC neutron multiplicity counter was the example chosen because it is the application subject of this study. However, its principles translate to many nuclear material measurements. Figure 2 shows the ENMC modeled for the study documented in this report, and it illustrates how the defined categories relate to the physical processes occurring within the counter.

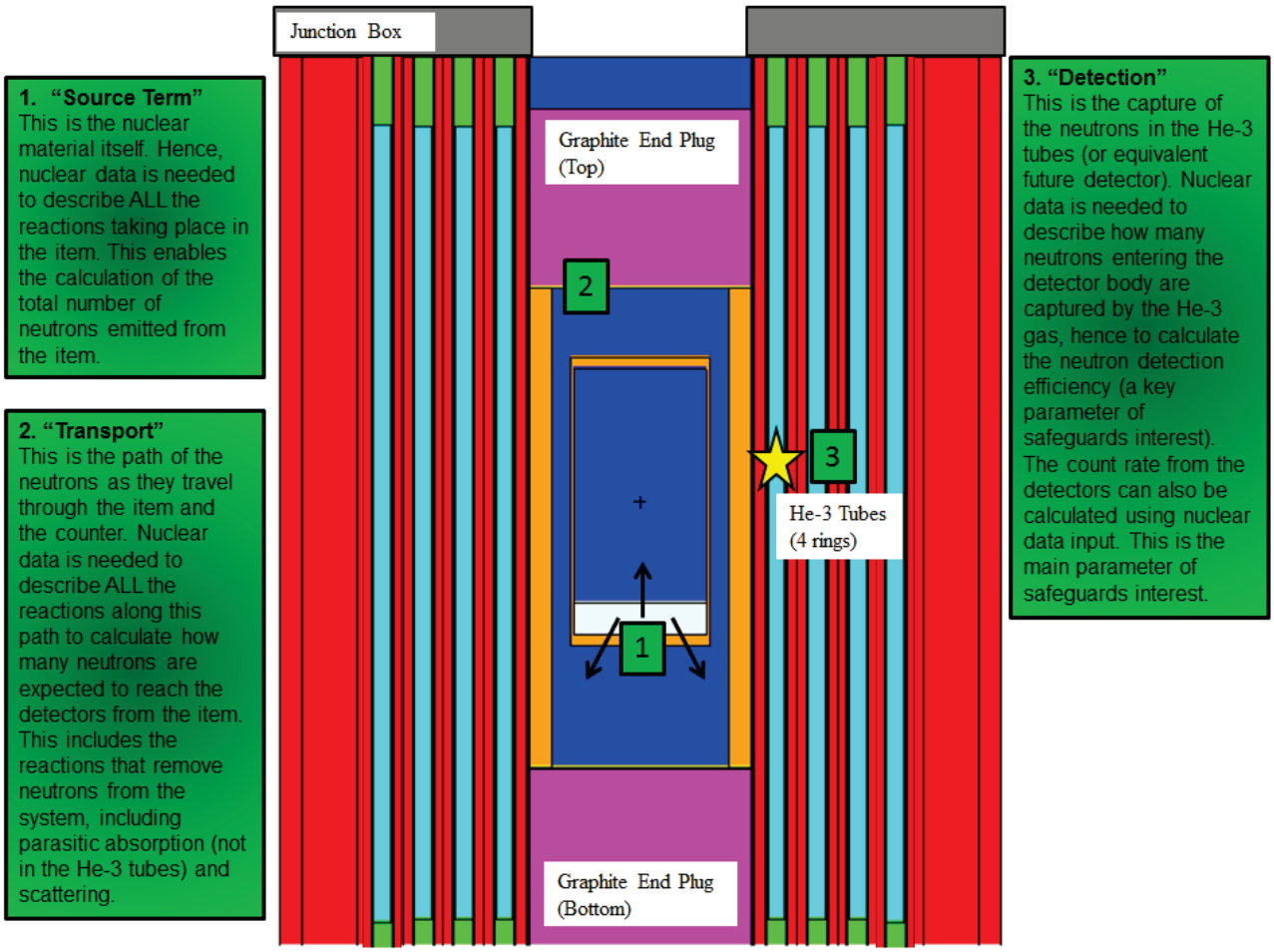


**Fig. 2. Nuclear data requirements for the ENMC neutron counter.**

Table 2 summarizes the nuclear data requirements for many measurements technologies. Each entry considers the physical processes and nuclear reactions taking place within the measurement system from first principles, and pairs these processes with the associated nuclear data requirements. Nuclear data requirements for neutron and gamma-ray based measurements are considered.

**Table 2. Review of nuclear data requirements for nuclear material measurements**

| Data category | Nuclear data type | | |
|---|---|---|---|
| **Nuclear material inventory** (fission products and actinides of interest for a nuclear security measurement and interferences) | **Fission process** | **Neutron capture reaction** | **Radioactive decay** |
| | Fission cross sections | Neutron capture (n, γ) cross sections | Decay half-lives |
| | Fission product yields (independent and cumulative fission yields) | Neutron absorption cross sections such as (n,2n) production | Decay branching fractions |
| **Radiation emission** | **Neutron emission** | **Gamma emission** | |
| | **Isotope inventory**<br>Isotopes of interest include: $^{244}$Cm, $^{238,240,242}$Pu, $^{239,241}$Pu, $^{233,235}$U, $^{252}$Cf | **Isotope inventory**<br>- Actinides: $^{238,239,240,241,242}$Pu, $^{233,235,238}$U, $^{241}$Am<br>- Short lived fission products: 100s<br>- Longer lived fission products: $^{106}$Ru, $^{144}$Ce, $^{125}$Sb, $^{134}$Cs, $^{137}$Cs, $^{154}$Eu | |
| | **Active neutron emission**<br>- Neutron-induced fission<br>- γ induced fission | **Gamma ray emission**<br>- γ energy (keV)<br>- Emission probability (per decay)<br>- Half-life (s)<br>Decay branching ratio | |
| | **Prompt fission process data**<br>- Prompt neutron emission<br>- Prompt neutron spectra<br>- Prompt neutron multiplicity distributions<br>- Number of neutrons per fission<br>- Prompt gamma ray emission<br>- Delayed neutron yields and spectra | **X ray emission**<br>- K x-rays of uranium and plutonium<br>- $K_\alpha$ x-ray energies, intensities and intrinsic line width<br>- X-ray florescence | |
| | **Passive spontaneous fission**<br>- Spontaneous fission neutron yields<br>- Spontaneous fission neutron spectra | **Bremsstrahlung radiation**<br>- β decay characteristics<br>- β particle $E_{max}$<br>- β decay transition type | |
| | **Passive (α, n) reactions**<br>- (α, n) cross sections for neutron production<br>- α-particle stopping powers<br>- (α, n) neutron spectra<br>- α reaction excitation energies | | |
| **Transport and detector response** | **Neutron transport**<br>- Neutron cross sections<br>- Prompt fission process (see above)<br>- Multiplication (fission, other)<br>- Neutron absorption and leakage<br>- S(α, β) thermal-treatment | **Gamma transport**<br>- Mass attenuation coefficients<br>- Photoelectric absorption cross section<br>- Compton scattering cross section<br>- Pair production cross section | |

A more detailed, general breakdown of the data is presented in Appendix A to describe the current status of each of the nuclear data items presented in Table 2. The approach borrows from the process of Phenomena Identification and Ranking Tables (PIRT) to identify relevant phenomena and to assess and rank the importance and knowledge base for each phenomenon. This approach is based on expert assessment and is therefore qualitative in nature. However, the process serves as a starting point upon which quantitative approaches can be developed, and it helps ensure that relevant phenomena and processes are not overlooked.

The phenomena are divided into categories of (1) direct measurement of nuclear material inventory, (2) indirect measurements based on neutron emission, and (3) indirect measurements based on gamma emission. The tables in Appendix A examine the status of the nuclear data and identify the state of knowledge of those data in each category.

## 2.3 NUCLEAR DATA FOR MEASUREMENTS

### 2.3.1 Neutron Reaction Cross Sections

Neutron reaction cross sections constitute a category of data that has received the greatest attention due primarily to their importance to reactor design, operation, and safety. In many cases, evaluations of the cross sections, neutron multiplicity, prompt fission neutron spectrum, and other parameters have been performed without complete quantification of uncertainties and covariance data. While it is clear that major efforts have been undertaken in recent evaluations, particularly in the representation of covariance matrices in the ENDF/B-VII.1 library [1], use of covariance data is still emerging, and these data are not considered accurate enough for use in assessing uncertainties in a scientific approach [13]. In many cases covariance data have been developed using a retroactive approach [14] independent of the original evaluation, thereby creating a somewhat inconsistent approach. Much work remains to improve covariance data in order to represent the full evaluation process as faithfully as possible and to ensure that the data provide accurate descriptions of uncertainty in applications.

### 2.3.2 Fission Product Yields

Fission product yield data used in ENDF/B-VII.1 are based primarily on the evaluations performed by England and Rider in 1992 [15]. The data are therefore more than 20 years old, and they describe the distribution of nuclides resulting from neutron-induced fission. The fission yields depend on the actinide being fissioned and the energy of the neutron causing fission. These data are tabulated as direct fission product yields and cumulative fission product yields which represent the direct yield to that fission product plus all yields to the decay precursors.

There is broad consensus in the international community for the need to sustain the capability to evaluate fission product yields and improve the data for many applications [16],[17]. However, there are currently no coordinated efforts in this area domestically. Recent studies of the ENDF/B-VII.1 fission yields and nuclear decay data identified significant inconsistencies in the fission yields [18]. The direct and cumulative yields are highly correlated by the nuclear decay schemes. Changes in the nuclear decay data in ENDF/B-VII.1 (2011) after the original evaluations in 1992 have resulted in direct fission yields that no longer produce correct values for several importance observable fission product nuclides. This has resulted in the need for retroactive adjustment of the fission yield data to reproduce experimental data. However, the adjusted data are not broadly distributed in ENDF/B.

Uncertainties are published with the England and Rider fission yield data. The fission yields are very highly correlated in charge (Z) and mass (A); however, no covariance data are available in the literature. Several retroactive approaches to fission yield covariance data development have been established and

demonstrated. The retroactive approaches are performed without access to all information and models using in the original fission yield evaluations and the results are generally sensitive to assumptions used in data reconstruction. Covariance data for fission product yields have been developed to perform uncertainty analysis using the Oak Ridge Isotope Generation (ORIGEN) code [18].

### 2.3.3 Spontaneous Fission Neutron Emission

ENDF/B-VII.1 contains no covariance data for spontaneous fission except for $^{252}$Cf. Therefore, codes used for spontaneous fission neutron source term definition (e.g., SOURCES4C) generally provide no uncertainty information. The fission spectrum is frequently represented analytically as a Watt fission spectrum using two spectral parameters. This representation is used, for example, in SOURCES4C and MCNP codes. Limited uncertainty analysis can be performed using these parameters.

Fission models such as those embedded in the FREYA code [19] developed at LLNL could provide additional uncertainty information and correlations in the energy distributions. The FREYA code includes both neutron-induced (prompt fission) and spontaneous fission. FREYA using a stochastic event model is currently being assessed under this project for spontaneous fission uncertainty analysis.

### 2.3.4 Passive Neutron Emission by (α,n) Reactions

Neutrons emitted by α-particle reactions with light element constituents are frequently encountered in nuclear security and nonproliferation problems. The SOURCES4C code [20] is used almost exclusively by the safeguards and nonproliferation community to calculate the passive neutron yields and energy spectra. However, SOURCES4C contains no uncertainty data to assess the accuracy of the calculations. Since the neutrons originate from α-particle reactions instead of neutron reactions, they are usually not considered in calculations using ENDF/B-VII.1 data.

The nuclear data for (α,n) reactions do not include covariance data. Therefore, covariances must be generated to provide a complete uncertainty analysis. This project specifically focuses on addressing uncertainty analysis data and methods for (α,n) calculations. These methods are demonstrated for the case of (α,n) reactions for oxide compounds ($^{17}$O and $^{18}$O) and applied to an experimental benchmark. Additional studies for the analysis of uncertainties for fluoride compounds will also be targeted next year. Nuclear data for $^{19}$F(α,n)$^{22}$Na reaction are not well known, and data on emission spectra are sparse. The thick-target yield from the $^{19}$F(α,n) reaction reported in the literature [21] is systematically different by more than 50%. The systematic uncertainties for materials such as $PuF_4$ and $UF_6$ are important to nonproliferation studies and should be quantified.

### 2.3.5 Nuclear Decay Data

Nuclear decay data include nuclide decay modes, half-lives, and branching fractions. These data are some of the best know nuclear data quantities and generally have very small uncertainties. Uncertainties are available for most nuclides, but covariance data are not available. In many cases, the decay data are uncorrelated between different nuclides. Therefore, studies of nuclear decay data uncertainty are possible using existing uncertainty data without the covariances.

One area of decay data of particular consequence has been the uncertainties in delayed neutron ($\beta^-$,n) decay (beta and neutron emission) that occur with short-lived, neutron-rich fission products. Revision of probabilities for delayed neutron emission in ENDF/B-VII.1 resulted in the inconsistencies observed in the calculated fission product yield. However, some recent experiments [22] have suggested that the probabilities for many of these fission products, currently based largely on theoretical calculations, are inconsistent with some theoretical predictions now being used.

### 2.3.6 Delayed Neutron Emission

In principle, each fissile isotope has a unique delayed neutron signature which can be exploited for isotope identification and quantification. However, delayed neutron group abundances are relatively poorly known nuclear data and have large associated uncertainties. The large uncertainties in the group abundances manifest as large uncertainties in fissile mass quantification in methods using delayed neutron measurements. The method of detecting delayed neutrons is a cross cutting measurement technique with applications in nuclear forensics, nonproliferation, and safeguards.

### 2.3.7 Photon Emission

Better knowledge of emission probabilities of x-rays and gamma rays will result lower systematic uncertainties in the results generated by the isotopic codes such as multigroup analysis for uranium (MGAU), multigroup analysis (MGA), and fixed-energy response function analysis with multiple efficiency (FRAM). One key line used by the isotopic codes is the 258.227 keV gamma emitted by $^{234m}$Pa, a daughter of $^{238}$U. The gamma ray intensity in the NuDAT is 0.0764%, with a relative uncertainty of 21%. The 258.227 keV line bridges the gap between the low and high energy sides of the relative efficiency curve when determining uranium isotopics.

### 2.3.8 Mass Attenuation Coefficients

Currently, uncertainty in the mass attenuation coefficients of actinide elements is a limiting factor in the overall accuracies that can be achieved by measurement methods such as Hybrid K-Edge Densitometry (HKED), which is used in safeguards.

### 2.3.9 $^{242}$Pu Correlations

The plutonium isotopic abundances in unirradiated nuclear material are frequently determined by gamma ray spectroscopy. Because $^{242}$Pu has no gamma emissions, it cannot be measured and must be inferred via correlations to other plutonium isotopes. Correlation algorithms have been developed for standard reactor types [23]. However, for nonstandard reactor types or unusual operating conditions such as those encountered in short-cycle research reactors, the plutonium production cycle must be understood in order to establish these correlations. Inaccurate predictions of $^{242}$Pu will impact the evaluation of total Pu content and make it difficult to verify material inventory. Although the $^{242}$Pu problem is not a nuclear data item itself, it is mentioned here since computational methods are required to develop the necessary correlations and their uncertainties, and these calculations require accurate nuclear data.

# 3. UNCERTAINTY ANALYSIS TOOLS AND DATA

This section focuses on methodologies and tools developed under this project for analysis of nuclear data uncertainties. This section describes LLNL developments in nuclear data uncertainty representations for MCNP calculations (radiation transport and prompt neutron/gamma emissions), analysis of uncertainties in neutron induced and spontaneous fission sources and spectra using the FREYA code, ORNL developments in nuclear data, and the application of data uncertainties for passive neutron emission from ($\alpha$,n) reactions, spontaneous fission, and isotope inventories generated from fission and neutron transmutation processes.

## 3.1 ANALYSIS APPROACHES

Several approaches can be used when performing nuclear data uncertainty studies. One option is to vary each data parameter independently to determine how much the calculated outputs change due to that perturbation. By varying the data parameter within the range of the measurement uncertainty, the impact of the data uncertainty on a calculated quantity is directly determined. This approach is appropriate when analyzing a small number of data parameters, but it can rapidly overwhelm computing resources as the amount of data increases.

Another option is to vary all input parameters simultaneously, creating multiple random "realizations" of the data parameter space. These realizations are created by statistically sampling all data parameters within the range as determined by measurement uncertainty. Each realization is put through the model to generate many sets of simulated results. Therefore, the distribution in computed results represents the total uncertainty due to the nuclear data as used in the calculations. In this approach, it is essential to include covariance information that defines the relationship between one parameter and the others.

Determining the contribution from each data parameter to the total uncertainty becomes more complex, as many different data parameters may be contributing to the results. Therefore, this approach requires post analysis of calculated results by searching for statistical correlations between model outputs and corresponding variations for each input parameter to identify the main components that drive the uncertainty. Despite the additional complexity, this approach has several advantages in that it scales easily to handle many input parameters, and it can reveal nonlinear responses that would remain hidden if parameters were only varied by a fixed amount. Both single parameter variations and simultaneous variation of multiple parameters are applied, depending on the complexity of the specific nuclear data being evaluated.

A third approach used specifically for the analysis of isotopic inventories is based on the adjoint (inverse) solution to the isotopic transmutation equations that define isotope formation and destruction. This approach is only applied to isotopic transmutation and decay since it requires development and solutions to the adjoint equations. The adjoint solution has been implemented in the isotope generation code ORIGEN [24]. This approach directly yields the sensitivities and uncertainties associated with all nuclear data in the transmutation calculations. The techniques and the nuclear data covariance data used to analyze each component of uncertainty are described in this section.

## 3.2 NEUTRON CROSS SECTION UNCERTAINTIES

To explore the large cross section nuclear data parameter space efficiently with a UQ study, the selected approach was to generate random realizations of the continuous-energy ENDF/B-VII.1-based nuclear data libraries used by the MCNP code [25]. The amount of nuclear data in these libraries is too vast to make varying individual data parameters computationally practical. Instead, random realizations vary all

nuclear cross sections and data associated with prompt fission processes by their measurement uncertainties. Therefore, analysis of the MCNP results obtained using these libraries is required to identify correlations between the results and the input nuclear data. This will help to determine the dominant nuclear data contributing to the results.

Covariance data in the ENDF/B-VII.1 evaluated nuclear data library [1] were applied to prepare random realizations of the neutron cross section reactions and fission parameters. ENDF/B-VII.1 contains nuclear cross section data for 423 target materials. Covariance data are available for 190 of these materials. The number of materials with covariance data has increased significantly from the previous release of ENDF/B-VII.0 that contained data for 26 materials (only 14 of them complete). This reflects the increasing priority of uncertainty estimation in nuclear analyses. The quantities in ENDF/B-VII.1 with covariance data include:

- total cross sections,
- elastic scattering cross sections,
- neutron capture (n,γ) cross sections,
- fission (n,f) cross sections,
- inelastic scattering (n,n') cross sections,
- cross sections for (n,xn),
- charged particle producing (n,p), (n,d), (n,t), (n,α) cross sections,
- number of neutrons per fission (nubar), and
- prompt fission neutron spectrum (PFNS).

Not all neutron reactions and nuclear processes in ENDF/B-VII.1 have covariance data.

Preprocessing of covariance data was performed first since the ENDF-6 format supports multiple methods for storing covariance data, including covariances between resonance parameters. The covariance matrices were projected onto a common energy grid using NJOY-2012 [26]. NJOY converts all of these different formats into a single standard matrix format so that uncertainty sampling can be performed using one matrix type.

Examples of the preprocessed covariance matrices produced by NJOY are shown in Fig. 3, along with correlations (ranging from -1 to 1). The covariance matrix can be reconstructed from the correlations and uncertainties. There are strong correlations in energy for each reaction, and there are also correlations between (n,f) and (n,γ) reactions. In this case, the full (n,f) vs. (n,γ) matrix is observed to be only partially complete; cross terms between reactions are present in the resonance region, but not at higher energies. In each subsection of Fig. 3, neutron energies extend from 10-5 eV to 20 MeV. Cross correlations between the two reactions are included in the resonance region only.

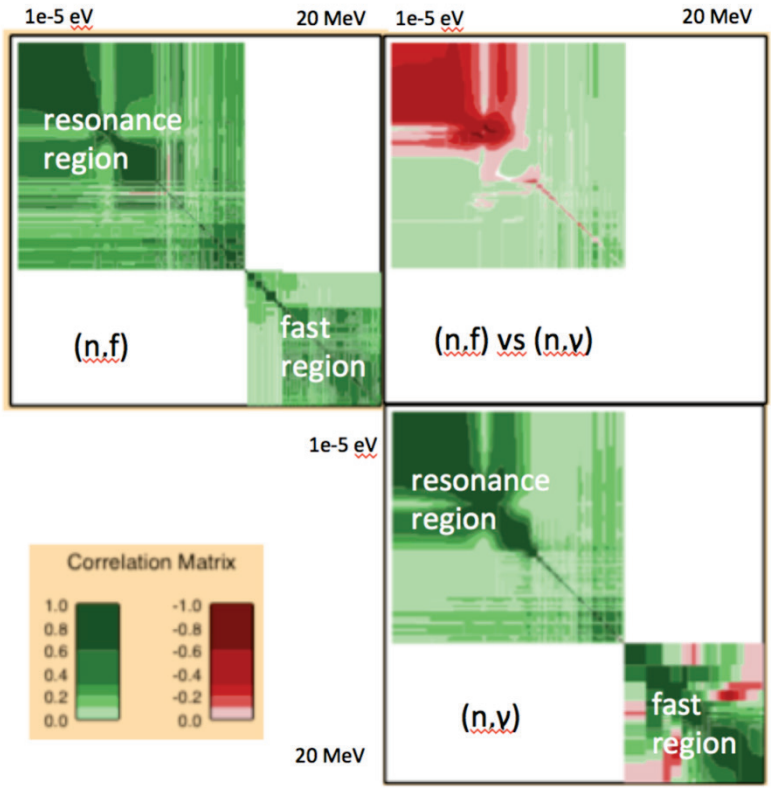


**Fig. 3. Correlations between $^{239}$Pu(n,f) and (n,γ) cross sections at different incident neutron energies.**

After processing covariances onto a common grid, random library realizations were generated using the LLNL code Kiwi [27]. The underlying algorithm for Kiwi is fairly simple. Given a covariance matrix $M$, Kiwi extracts the eigenvalues $\lambda$ and eigenvectors $\Lambda$ (where the i$^{th}$ column of $\Lambda$ is the eigenvector corresponding to eigenvalue $\lambda_i$). The most important eigenvectors correspond to the largest eigenvalues, whether positive or negative. (Nuclear data covariances are mostly positive-definite except for round-off errors due to floating-point arithmetic, so the dominant eigenvalues are expected to be positive).

After obtaining the eigenvalues and eigenvectors, Kiwi draws a random vector $V$ (drawn by default from a Gaussian distribution with σ = 1.0) and constructs a random realization vector $R$ such that:

$$R_i = \sum_j \eta_j \Lambda_{j,i} \quad , \tag{1}$$

where

$$\eta_j = \sqrt{\lambda_j} V_j. \tag{2}$$

Vector $R$ is a linear combination of eigenvectors, where each eigenvector is weighted by $\eta_j$. The principal eigenvectors (with large $\lambda_j$) receive larger weights on average. Small negative eigenvalues are assumed to come from round-off error and are discarded prior to constructing vector η, to avoid complex realizations.

The new realization is constructed from the original library $L$ and vector $R$:

- If the original matrix $M$ is absolute (i.e., cross section covariance matrix with units of barn$^2$), the realization is produced by adding $L + R$.
- If the original matrix $M$ is relative (i.e., unitless), the realization is produced by multiplication: $L\ (1 + R)$.

If a suitable number of nuclear data realizations is produced, the covariance between those samples should converge on the original matrix $M$.

Both approaches were investigated in the course of this work. However, only the selected final multiplicative approach using a relative covariance matrix is discussed in this report.

To gain more insight into the results of Kiwi, some of the principal eigenvectors of nuclear reaction covariance matrices are illustrated. The plot in Fig. 4 shows examples of principal components for the fission cross section covariance. Since these vectors correspond to the largest eigenvalues, they have the largest impact on Kiwi realizations. Low-energy features dominate their behavior, mainly because the cross section (and corresponding absolute uncertainty) is much higher at low energy.

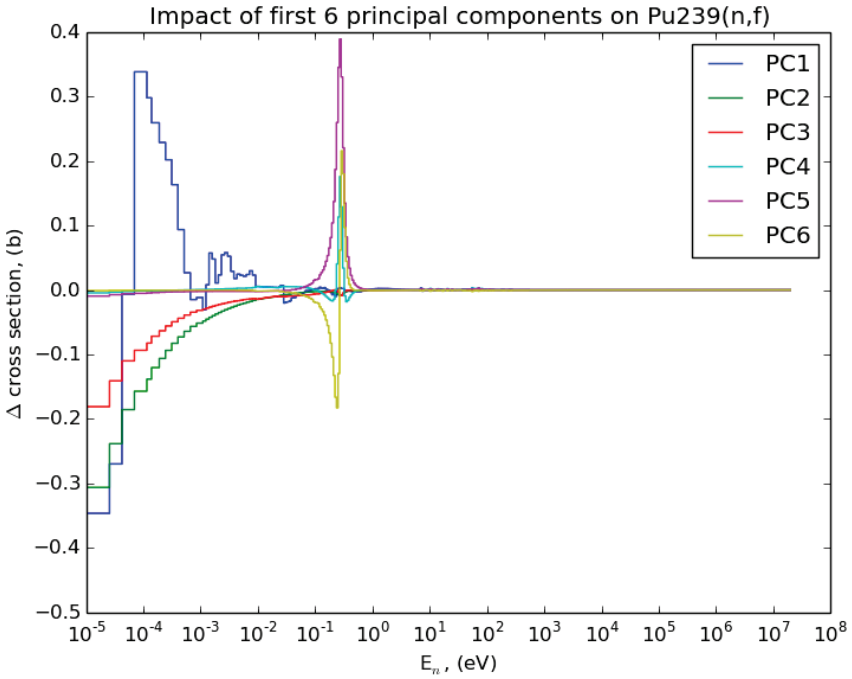


**Fig. 4. Principal eigenvectors of the $^{239}$Pu(n,f) absolute covariance matrix.**

Fig. 5 shows the prompt fission neutron spectrum covariance. Component 1 (in blue) shifts the peak of the spectrum to higher outgoing energy; components 2 and 3 change shape near the peak of the spectrum.

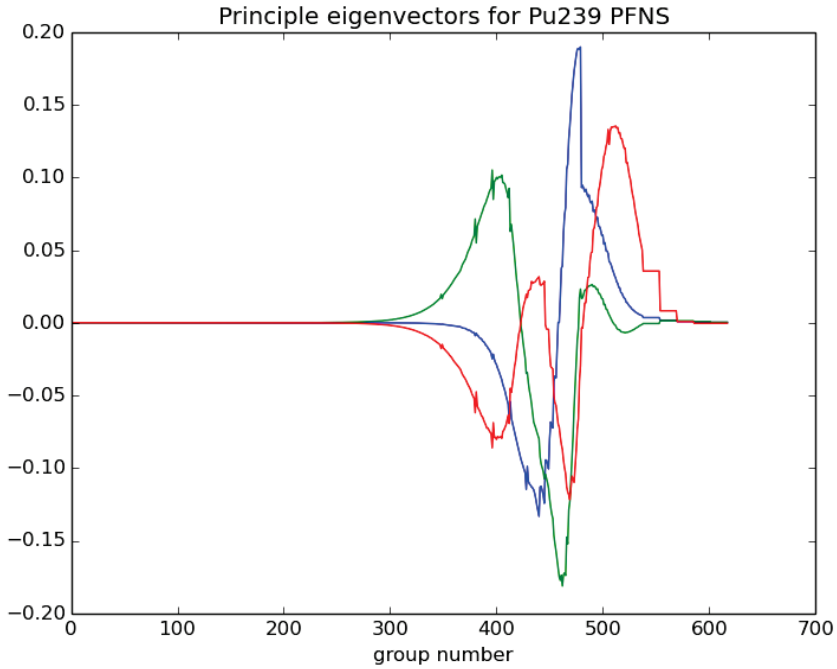


**Fig. 5. Principal components for the prompt fission neutron spectrum (PFNS).**

There are some potential issues that must be addressed after using Kiwi to create variations in the nuclear data:

- The total cross section for the realization may not equal the sum of individual reaction cross sections. If Kiwi had access to a full covariance matrix, including all cross reaction terms at all incident energies, then the realizations should, in principal, preserve consistency between the total cross section and its reaction components. However, in practice, additional steps must be taken to ensure consistency. These steps are discussed further below.
- The covariances are represented by normal distributions, and sampling from theses distributions can produce unwanted negative cross sections or probabilities. Kiwi handles these cases by truncating the distribution at 0 (i.e., setting any negative results to 0).
- Realizations for a probability distribution (such as the prompt fission neutron spectrum as a function of outgoing energy $E'$) likely will not integrate to 1 after running Kiwi and will consequently require renormalization.

While generating these realizations, Kiwi also captures details on how much each quantity was varied in each energy bin. These details are stored for later use in the analysis phase.

Once nuclear data realizations are generated, they are merged with ENDF/B-VII.1 evaluations using the LLNL code FUDGE [28] to create new ENDF-6 formatted nuclear data evaluations for each realization. These evaluations are then processed into ACE format using NJOY-2012 (since MCNP uses nuclear data stored in ACE format). The process of generating realizations and processing results into ACE format has been automated.

The tools for generating and analyzing library realizations were refined over the course of this work, and several different library realizations generated by LLNL and were investigated using MCNP simulations. Covariance data processing options studied are briefly described here:

- Energy bands of the covariance matrix data were initially grouped into 618 energy bins (spanning $10^{-5}$ eV to 20 MeV). For the later studies and for those used in this report, covariance matrices were grouped into 40 energy bins from $10^{-5}$ eV to 30 MeV. This change trades off detailed information about the energy dependence of correlations for more statistically significant correlations.
- Initially, absolute covariance matrices were used so that the resulting realizations were additive. However, this resulted in some nonphysical behavior of the uncertainties in the thermal region. The processing was later revised to use relative covariance matrices so that resultant realizations were multiplied rather than added to central values.
- When sampling, the random vector $V$ was initially generated from a normal distribution with $\sigma = 1$. This was later revised to use a normal distribution with $\sigma = 3$ rather than $\sigma = 1$ to capture a wider range of data variations.

The cross section realization for $^{237}$Pu fission is illustrated in Fig. 6 as obtained using the relative covariance matrix method. As observed, it does not entirely preserve the $1/v$ behavior in the thermal range since the cross section is multiplied by a different constant in each incident energy bin as defined by covariance data. This may indicate a potential problem with the original covariance estimate, where the entire thermal region is expected to be strongly correlated and exhibit $1/v$ shape.

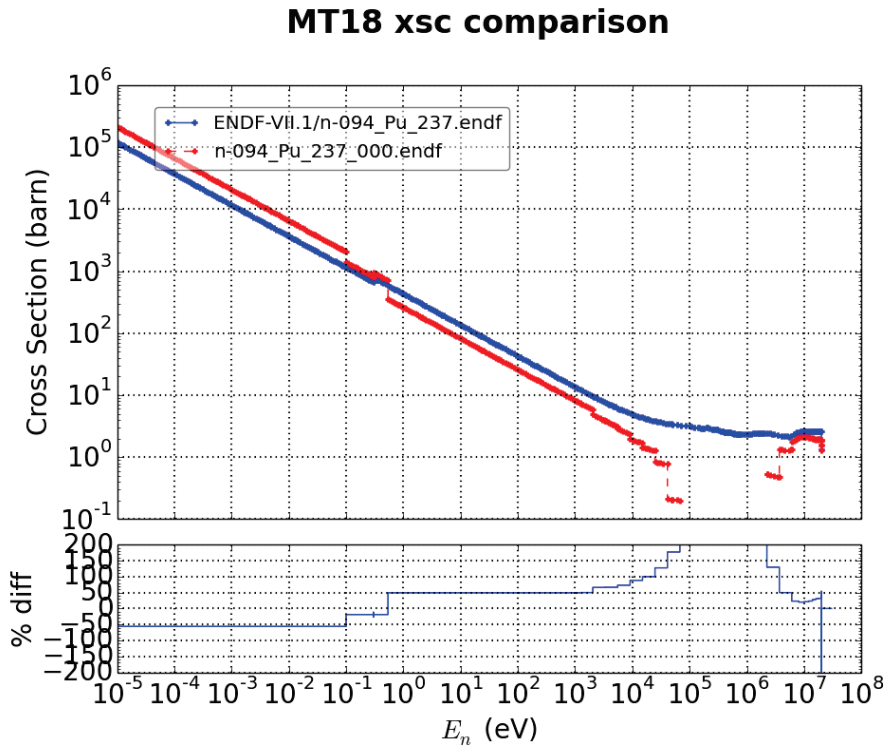


**Fig. 6. ENDF-VII.1 $^{237}$Pu (n,f) cross section versus random realization obtained by multiplying the cross section by a constant factor in each energy bin (better preserving the 1/v behavior at low incident energy).**

A total of 100 nuclear data libraries were generated and used in MCNP to simulate detection of neutron signals for the ENMC multiplicity counter model as described in Sect. 4 to extract the estimated Pu mass with and without neutron multiplication correction. The variation in the results obtained using these 100 MCNP calculations therefore represents the uncertainty associated in the calculation due to the underlying nuclear data as represented in the covariance files. The uncertainty reported in MCNP calculations includes only the contribution to the statistical Monte Carlo method and not the nuclear data. An example of the results for the estimated Pu masses obtained for each library iteration is shown in Fig. 7, which corresponds to the ENMC counter configuration for a plutonium mass of about 5 kg and two different plutonium isotopic compositions (reactor grade and weapons grade). The declared mass for this large sample was 5.056 kg for the reactor grade case and 5.116 kg for the weapons grade case. A few outlier runs produced lower estimated Pu mass and are discussed further in this report.

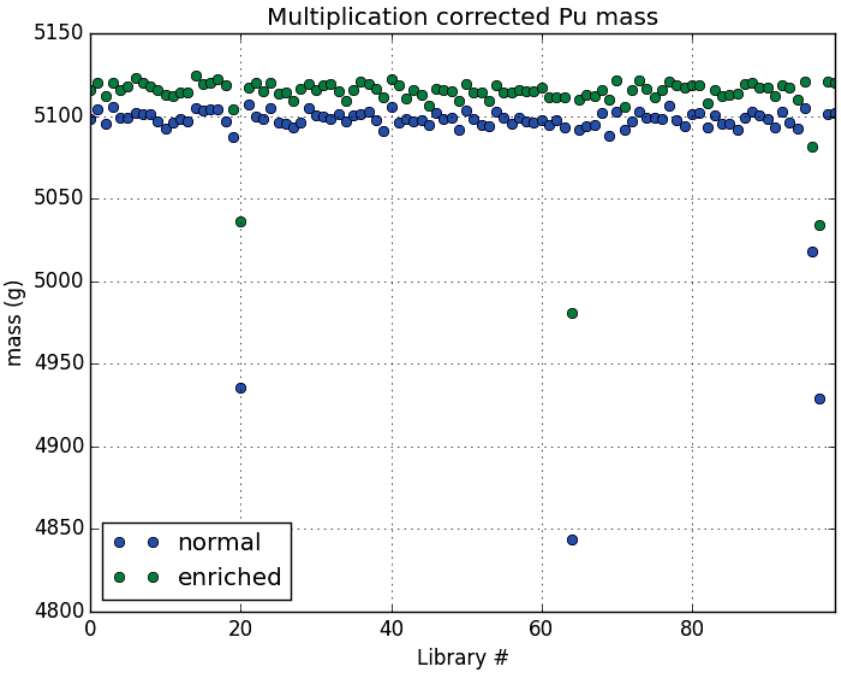


**Fig. 7. Multiplication-corrected Pu masses for the third library iteration for two isotopic composition ("normal" refers to reactor grade and "enriched" refers to weapons grade plutonium).**

These results do not provide information on the specific components of the nuclear data causing the largest contributions to the total uncertainty. To obtain this information, further analysis of the MCNP results is required. The approach applied in this work was to identify the nuclear data variations with the highest correlations or anticorrelations with simulation MCNP outputs. The number of input data parameters is large, so the task of searching for significant correlations was automated using Python scripts based on the *scipy* and *pandas* data analysis frameworks.

Small correlations (with absolute value < 0.3) were discarded as not being statistically significant. With a sample size of 100 simulations, a correlation > 0.3 or < -0.3 was considered significant at the $p < 0.01$ level (i.e., less than 1% chance that the correlation occurs due to normal random variation). This threshold is actually conservative and could be dropped to 0.26 while still preserving a significance of $p < 0.01$.

These libraries and the post analysis correlation methodology were applied to the ENMC demonstration problem described in Sect. 4.

### 3.3 SPONTANEOUS FISSION NEUTRON EMISSION

ENDF/B-VII.1 contains no covariance data for spontaneous fission processes for materials other than $^{252}$Cf (decay rates, neutron multiplicity, or energy spectra). Therefore, uncertainties in the number of emitted neutrons per fission and the energy spectrum of the neutrons are not included in the analyses described in the previous section. Spontaneous fission may be highly important to nuclear material measurements. The spontaneous fission neutron spectrum $N(E)$ is typically represented analytically as a Watt spectrum using spectral parameters $A$ and $B$, where

$$N(E) = C\, e^{-E/a} sinh\sqrt{bE} \qquad (3)$$

This representation is used in the SOURCES4C code [20] and is usually used in MCNP to represent the neutron energy distribution for these calculations. Uncertainties for some spectral parameters have been published; however, no covariances for these parameters are available. A preliminary approach investigated in this work, while not rigorous, was to assess the effect of different parameters sets that have been published and used.

General-purpose Monte Carlo codes such as MCNP, TART, COG, and TRIPOLI employ an *average fission model* which is characterized by outgoing secondary particles that are uncorrelated and sampled from the same probability density functions. This approximation is generally sufficient for the calculation of average quantities such as flux, energy deposition, and multiplication. It is however unsuitable for studying detailed correlations between neutrons on an event-by-event basis. For modeling neutron multiplicity counters, for instance, these correlations are important because determination of multiplication and mass of unknown objects is based on measuring time-correlated neutrons.

To address these correlations, FREYA [19] has been developed as a fission event generator which models complete fission reactions. Neutrons and photons are emitted sequentially from individual fission fragments in binary fission. Employing nuclear data for fragment mass and kinetic-energy distributions using statistical evaporation models for neutron and photon emission and conserving energy, momentum, and angular momentum throughout, FREYA can predict a host of correlation observables, including correlations in neutron multiplicity, energy, and angles, and the energy sharing between neutrons and photons.

FREYA can currently handle neutron-induced fissions of $^{233}$U, $^{235}$U, $^{239}$Pu, as well as the spontaneous fissions of $^{238}$U, $^{240}$Pu, $^{244}$Cm and $^{252}$Cf. For example, Figs. 8 and 9 show how the fission neutron energy spectrum varies with the number of fission neutrons emitted. Monte Carlo codes do not include such dependence. In addition, covariance data for the energy distributions can be generated by FREYA.

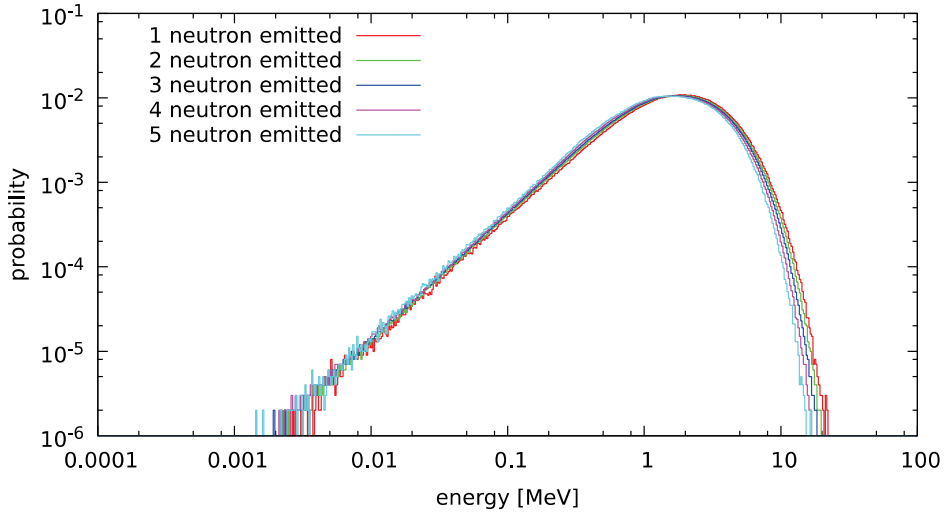


**Fig. 8. Dependence of fission neutron spectrum on number of fission neutrons emitted (1 MeV neutrons inducing fission in $^{235}$U).**

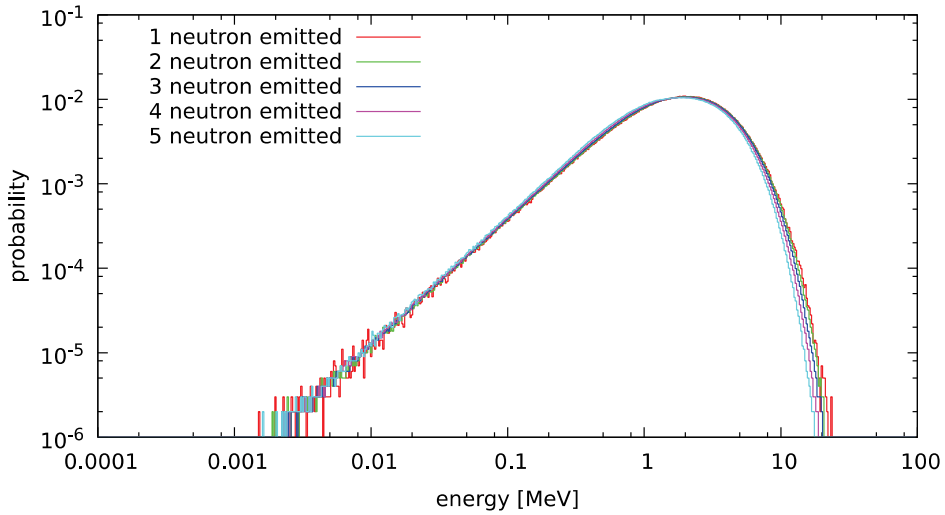


**Fig. 9. Dependence of fission neutron spectrum on number of fission neutrons emitted (1.85 MeV neutrons inducing fission in $^{239}$Pu).**

Table 3 lists the average fission neutron energy as a function of the number of fission neutrons emitted. This dependence will affect the responses of many neutron detectors.

**Table 3. Average neutron energy for different number of fission neutrons emitted (1 MeV neutrons inducing fission in $^{235}$U and 1.85 MeV neutrons inducing fission in $^{239}$Pu**

| # neutrons | Average fission neutron energy (MeV) | |
|---|---|---|
| | $^{235}$U ($E_n$=1 MeV) | $^{239}$Pu ($E_n$=1.85 MeV) |
| 1 | 2.11134 | 2.21853 |
| 2 | 2.02482 | 2.19571 |
| 3 | 1.95759 | 2.15156 |
| 4 | 1.87272 | 2.07703 |
| 5 | 1.78299 | 1.99027 |
| 6 | 1.73340 | 1.89826 |

Angular correlations between fission neutrons are also included in the FREYA model. Fig. 10 shows these correlations for $^{252}$Cf spontaneous fission neutrons.

FREYA is a fission model containing multiple tunable fission parameters. These parameters are determined from fitting measured quantities such as fission fragment mass distributions, kinetic-energy distributions, and average fission neutron multiplicities. Fitting these distributions results in correlated distributions for the tunable parameters. These correlated distributions of input parameters can be sampled to determine the effect on nuclear data uncertainties on the fission process and the overall Monte Carlo transport simulations.

FREYA is therefore being investigated in this project in FY2016 for application to uncertainty analysis for both improving neutron-induced fission process data and correlations and also for generating improved spontaneous fission data and uncertainties currently not available from other sources.

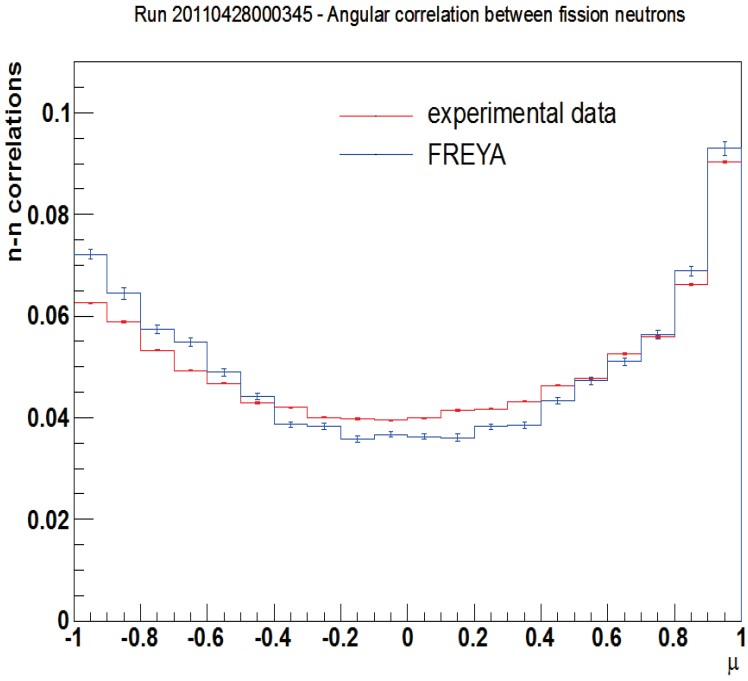


**Fig. 10. Angular distribution of $^{252}$Cf spontaneous fission neutrons (experimental measurements versus FREYA).**

## 3.4 (ALPHA,N) NEUTRON EMISSION

Nuclear data describing α-particle interactions on light nuclei are essential for calculating neutron emission via the (α,n) processes. Neutron emission by (α,n) reactions can represent a significant neutron source in neutron-based measurements of unirradiated nuclear material. In irradiated nuclear fuel that achieves a moderately high burnup, neutron emission is dominated by spontaneous fission of $^{242}$Cm and $^{244}$Cm generated by neutron transmutation on uranium and plutonium. However, for low burnup nuclear material such as in reactor-based weapons material production, the (α,n) processes can represent a large component of the total neutron source, so (α,n) neutron emission is important in any neutron-based measurement system.

ENDF/B-VII.1 contains no covariance data for processes related to passive neutron production via (α,n) reactions. The effort to develop covariance data to quantify uncertainties in nuclear data important to passive neutron emission is described in this section.

In the nuclear nonproliferation and safeguards community, the SOURCES4C code [20] is widely used to simulate the passive neutron emission sources and spectra. The methods and nuclear data in SOURCES4C are integrated in the ORIGEN code [24] that performs neutron transmutation and decay calculations, allowing time-dependent neutron sources to be calculated during material production and decay. The nuclear data used in SOURCES does not include uncertainties or covariance data. Therefore, uncertainties are not provided for the estimated neutron source intensities or in the emission spectra.

The potential importance of uncertainties in the nuclear data used in calculating (α,n) sources was investigated for the case of alpha-emitting actinides in an oxide matrix to demonstrate a methodology to generate the necessary covariance data (not reported in the measurements) and then propagate the uncertainties to the neutron source emission characteristics. In addition to providing uncertainty estimates, the methodology can also be used to generate improved nuclear data evaluations that can be adopted in the SOURCES4C code to yield lower systematic uncertainty compared to the existing nuclear data. As part of this project, new (α,n) cross section evaluations have been generated for $^{17}$O and $^{18}$O, and the results of neutron emission calculations are compared to experimental data. This work is described in the following sections.

### 3.4.1 Theory of (α,n) Neutron Source Emission

The SOURCE4C code (and therefore ORIGEN) incorporates a large amount of nuclear data as precompiled data libraries for the alpha particle stopping power cross sections, (α,n) reaction cross sections (compiled from experimental data or based on nuclear physics model calculations), and information related to the decay library such as branching ratios. It also incorporates spontaneous fission decay constants and α-particle emission energy yields. This section defines the theory leading to (α,n) reactions and the related neutron production function to clearly identify the role of nuclear data in the neutron yield.

The model used to calculate the average number of neutrons emitted from (α, n) reactions by the definition of thick-target neutron production function is defined by

$$p_i(E_\alpha) = \frac{N_i}{N} \int_0^{E_\alpha} \sigma_i(E)\epsilon(E)^{-1} \mathrm{d}E \,, \tag{4}$$

where $p_i(E_\alpha)$ represents the probability of an α-particle undergoing an (α,n) reaction with nuclide i normalized by the ratio of the atom density of nuclide, Ni, and the total density of the material, N. The integral of Eq. (1) is defined by $\sigma_i(E)$, the (α,n) cross section (in barns) for the nuclide $i$, and, $\epsilon(E)$ is the stopping cross section (in eV/$10^{15}$/cm$^2$) which is approximated by the Bragg-Kleeman relationship.

The integral is performed from $E_\alpha$ (the initial energy of the emitted α-particle) to $E = 0$ (when the α-particle has completely lost its energy). Eq. (1) shows that the nuclear data contributing to the uncertainty in the neutron yield are the (α,n) reaction cross section and the α-particle stopping power of the medium.

### 3.4.2 (α,n) Cross Section Evaluation

The procedure used to generate nuclear data covariance information from experimental (α,n) cross-sections data is based on the R-matrix code SAMMY [29]. These covariance data can then be used to assess uncertainties in the neutron yield. The SAMMY code is a modern tool for calculating reaction cross sections mainly used for nuclear data evaluations in the resolved neutron resonance region. However, SAMMY has built-in capabilities that also allow the code to evaluate cross sections for other incident particles, including charged particles [30]. The SAMMY code incorporates selected R-matrix approximations coupled to the Bayesian method in order to fit experimental data and ultimately to generate a set of resonance parameters with related parameter covariance matrix. For this task, results were based on the Reich-Moore formalism, which approximates the expression for elastic and reaction cross sections better than other single- and multi-level variants of the R-matrix theory.

In order to demonstrate the feasibility of the method for uncertainty analysis, SAMMY was applied to the case of an oxide matrix, where the light element targets that generate neutrons are $^{17}$O and $^{18}$O. Although this study was limited to oxides, the approach is general and can be easily extended to other target materials.

The $^{17,18}$O(α,n) cross sections measured by Bair et al. [31],[32] for thin targets were used to estimate a preliminary set of resonance parameters and related covariance matrix (see Table 4). The analysis of the $^{18}$O isotope was based on two thin target measurements of (α,n) cross section data. The first set was limited over the incident α energy range 1.06–2.50 MeV, and the second set was limited from 2.43–5.14 MeV. For the $^{17}$O, a single data set was used, with cross sections extending over the energy range 0.92–5.31 MeV. The reported overall uncertainty for these experimental data sets in the high energy region was at least 25%. The same relative uncertainty was assumed for the $^{18}$O data set measured at low energy since no error analysis was reported. Because of the large uncertainties in the thin-target measurements, the cross sections were scaled by Bair et al. using a normalization factor of 1.35 applied to all data sets on the basis of more accurate thick-target measurements on $^{nat}$O(α,n) [33]. After normalizing, the relative error reported for these data sets was about 7%. Note that the data in the experimental nuclear data archive EXFOR does not include the normalization factor applied by Bair.

**Table 4. $^{17,18}$O(α,n) experimental cross section data sets used in SAMMY R-matrix calculations**

| Nucleus | Author | E (MeV) | Error (%) | Norm.[a] | Unc.(%)[b] |
|---|---|---|---|---|---|
| $^{17}$O | Bair [32] | 0.92–5.31 | 25[c] | 1.35 | 7 |
| $^{18}$O | Bair [31] | 1.06–2.50 | 25[d] | 1.35 | 7 |
| $^{18}$O | Bair [32] | 2.43–5.14 | 25 | 1.35 | 7 |
| $^{nat}$O | West [35] | 3.80–10.0 | 1.5 | 1.00 | – |

[a] = Uncertainty was not included in the Bayesian update.
[b] = Uncertainty as assigned after normalization [33].
[c] = Excludes uncertainty of graphite sphere detector efficiency.
[d] = Assumed uncertainty since no error analysis was reported.

For incident α energies above 5.14 MeV, up 10 MeV, a constant 20% uncertainty was assigned to the JENDL $^{17}$O (α, n) cross sections. Experimental data for natural oxygen were used to evaluate $^{18}$O(α,n) cross sections above 5.14 MeV. The uncertainty of $^{18}$O (α,n) is based on the accuracy of $^{nat}$O cross sections estimated at 1.5% [34].

The results of the SAMMY R-matrix cross section analysis for $^{18}$O are shown in Fig. 11. Relative cross section uncertainties (in percent) are shown in a continuous red line along with their average relative uncertainty (5.8%) in a dashed red line. The SAMMY Bayesian procedure used to update the preliminary set of resonance parameters derived from the experimental data sets shows that the relative cross section uncertainties over the analyzed energy range (in a red continuous line) are, on average, 5.6% and 5.8% for $^{17}$O and $^{18}$O. These uncertainties are slightly smaller than those originally reported for the experimental data (7%) as a consequence of the constraint from the energy-dependent correlations deriving from the R-matrix model.

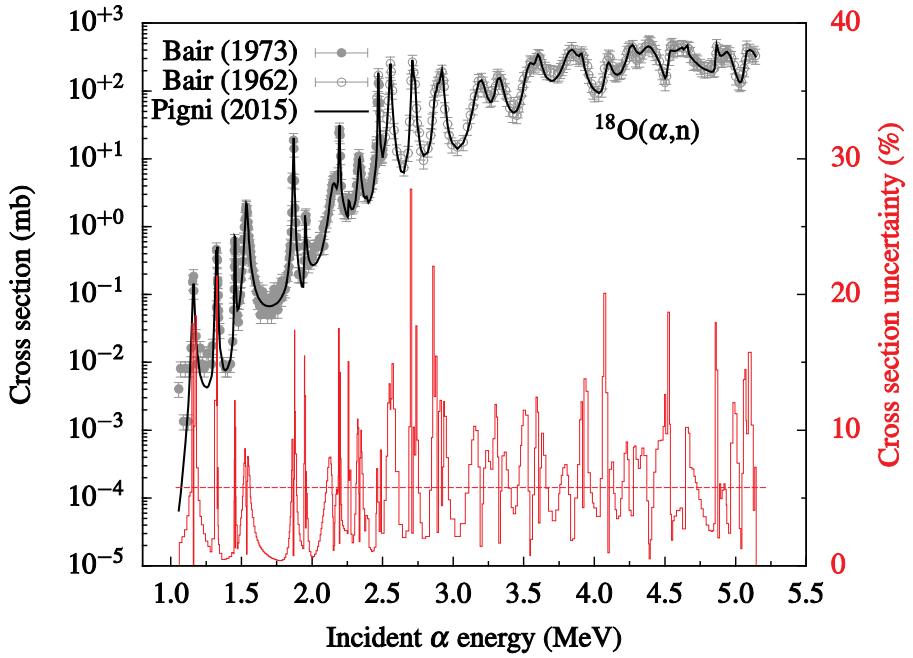


**Fig. 11. $^{18}$O(α,n) cross sections reconstructed by SAMMY from the preliminary set of resonance parameters in the energy range of 1–5 MeV compared with Bair's experimental data.**

Further normalization of the thin-target measurement data from Bair et al. were performed using thick-target yield measurements for natural oxygen targets reported by West and Sherwood [35] that have much smaller uncertainties of 1.5%. However, these measurements are only reported for energies above 3.80 MeV (Table 4). Normalization of the Bair et al. data between the two sets of measurements was performed over the common energy range of 3.80–5.14 MeV using $^{nat}$O (α,n) cross section data derived with the Bair et al. thin target measurements (Fig. 12). Data from West and Sherwood are indicated by red dots. The black line shows the reconstructed cross sections averaged over the group structure used in West's data. This procedure resulted in a small change in the original dataset in the energy range below about 5 MeV by +3%, which is well within the reported uncertainty of the original data of 7%.

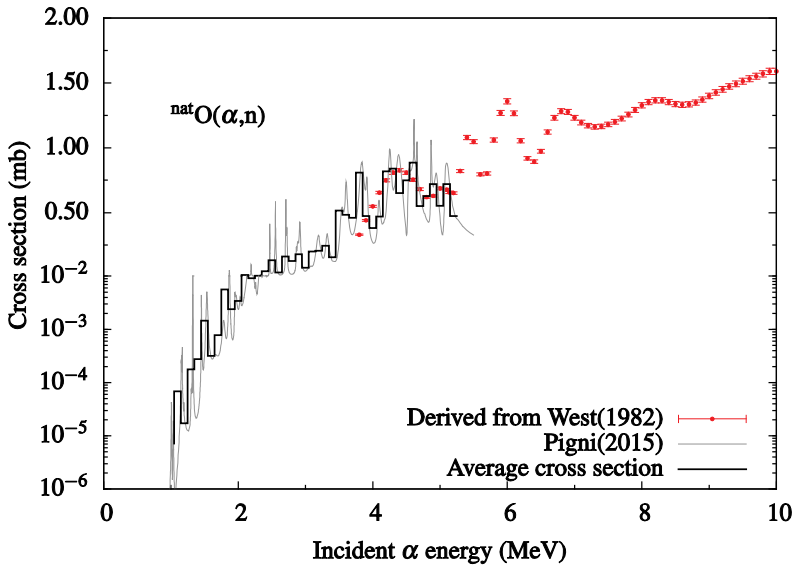


**Fig. 12. $^{nat}O(\alpha,n)$ cross sections reconstructed from the preliminary set of $^{17,18}O(\alpha,n)$ resonance parameters in the energy range of 1–5 MeV compared with derived data from West and Sherwood.**

The energy-dependent cross section covariance matrix generated by the R-matrix procedure for $^{18}O$ is shown in Fig. 13. The matrix contains the correlations the (α,n) cross section data as a function of energy necessary to perform correlated uncertainty analysis.

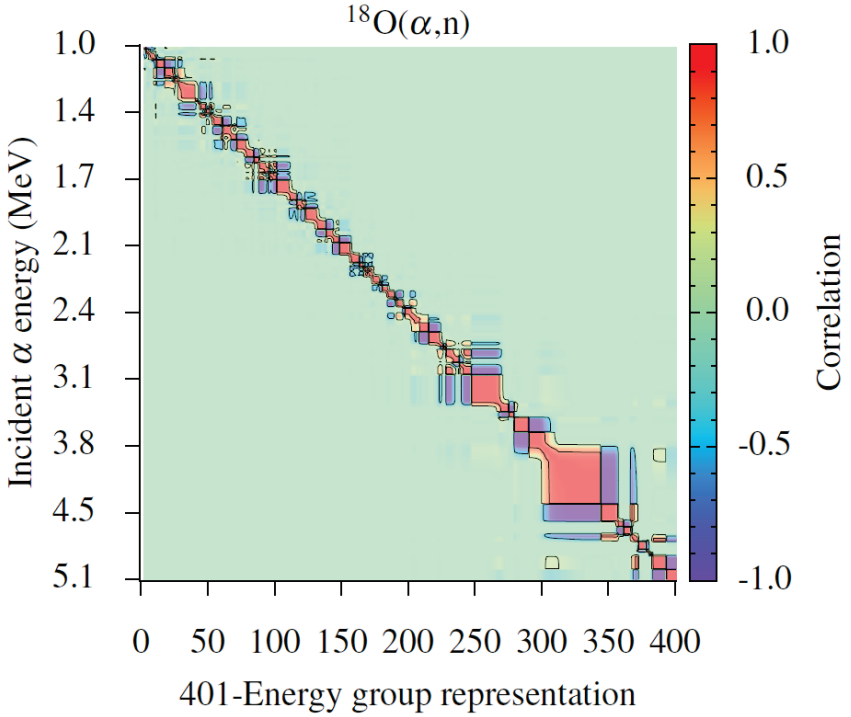


**Fig. 13. Correlation matrix and contour lines of $^{18}O(\alpha,n)$ cross sections in 401-Energy group representation (correlations below 1% not displayed).**

### 3.4.3 Stopping Power Evaluation

Uncertainty data are not available for the stopping power coefficients used to calculate neutron yield as in Eq. (4). In order to quantify the contribution of the stopping power cross sections on the uncertainty of the output (α,n) source responses, stopping power cross sections based on ASTAR data [36] for oxygen and uranium were fitted to the analytic function,

$$\varepsilon(E) = s_L(E) \cdot s_H(E) \cdot [s_L(E) + s_H(E)]^{-1}\ , \tag{5}$$

where $s_H$ and $s_L$ are stopping power functions defined in the SOURCES code by a set of five coefficient factors, c1, . . . , c5 such that

$$s_H(E) = c1\ (1000 \cdot E)^{c2}, \tag{6}$$

and

$$s_L(E) = c3E^{-1} \ln\ (1 + c4E^{-1} + c5E), \tag{7}$$

where E is the incident α-energy in MeV.

In the fitting procedure, the uncertainty on the ASTAR data was taken as 2.5% [34]. The results of the fitting procedure for uranium are shown in Fig. 14. This procedure was also used to generate fit coefficients and covariance information for the stopping power fit parameters.

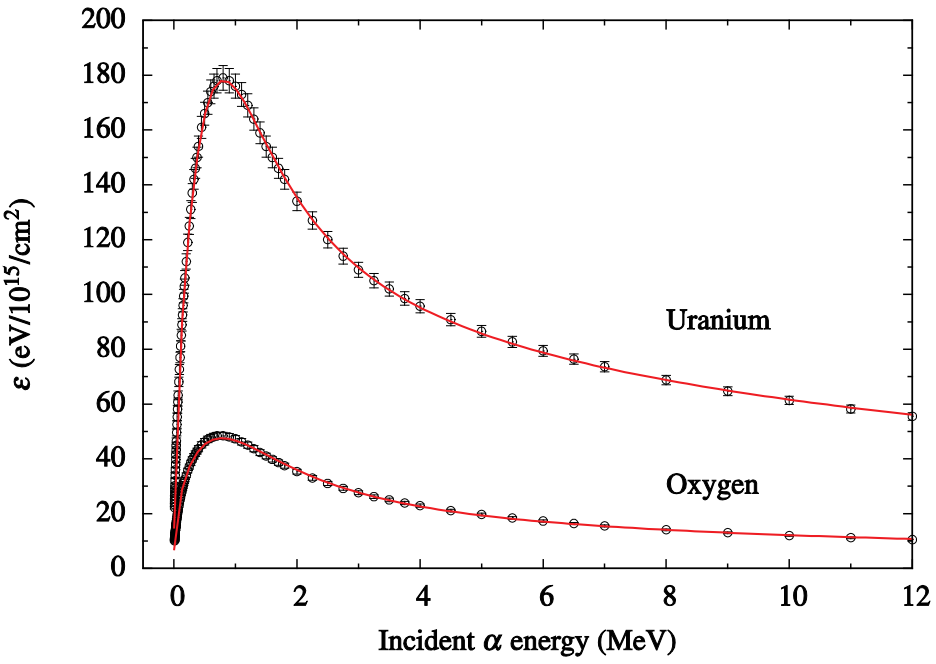


**Fig. 14. Stopping power cross sections for oxygen and uranium obtained from the parameterization defined by Eq. (2) (in red) and ASTAR data (black dots).**

### 3.4.4 Validation for Uranium Oxide Matrix

The cross section and stopping power data and uncertainties developed in this work were applied to analyze the measured neutron yields from alpha bombardment of a uranium oxide target. The precompiled data libraries of the ORIGEN code (using SOURCES methods) are provided with no covariance information. Therefore, no uncertainty can be estimated on neutron source intensities in the current version of these codes.

Based on the evaluation methodology described, revised nuclear data evaluations for $^{17,18}$O (α,n) cross sections and updated stopping power data were compiled, and associated covariance files for these data were generated for use in uncertainty analysis. Uncertainty results were generated by performing 50 ORIGEN calculations of the neutron yield, and for each calculation, a randomly sampled cross section library and stopping power coefficient library was used. The set of 50 libraries was generated by random perturbation factors obtained from the multivariate (normal) distribution based on the covariance information relative to the evaluated $^{17,18}$O(α,n) cross sections in the α-energy range between 1–10 MeV. The same procedure was used to generate the perturbation factors for the coefficient factors used to compute the stopping power cross sections for oxygen and uranium.

Uncertainties in calculated (α,n) production for uranium oxide are compared to the thick target experimental data of West [35] in Fig. 15. The uncertainty in the experimental data is reported as about 1.5% over this energy range. The error bars on the calculated values shown in the comparisons of Fig. 15 reflect the impact of uncertainties in both the (α,n) cross sections and the stopping power coefficients. These uncertainty estimates are not provided using the existing version of the SOURCES4C code or data. The impact due to (α,n) cross sections alone are also shown (smaller than the total uncertainty). Overall, the calculations show good agreement with the measurements and are generally within the reported measurement error. Somewhat larger deviations are observed for lower energy α-particles. The estimated relative error in the calculations of about 1% is consistent with the observed differences with measurements.

Figure 15 also includes comparisons of the results using the default version of SOURCES relative to the experimental data of West, showing overprediction in the neutron yields for alpha energies later than about 5.5 MeV of up to 8%. This overprediction is largely corrected using the new SAMMY evaluation of the cross sections.

This analysis for uranium oxide was used to demonstrate the approach of uncertainty analysis as applied to (α,n) neutron yield calculations. However, this approach can be readily adapted to evaluate other source and matrix types, such as fluoride and many other compounds. The methodology was used to develop new data with improved performance compared to the data currently in the SOURCES code. The methodology can also be used to estimate uncertainties in the calculations. These uncertainties are observed to be consistent in comparisons to experimental data. The same uncertainties can be used for extended range of applications where measurements do not exist. A journal paper describing the detailed methods and analysis results is currently in preparation.

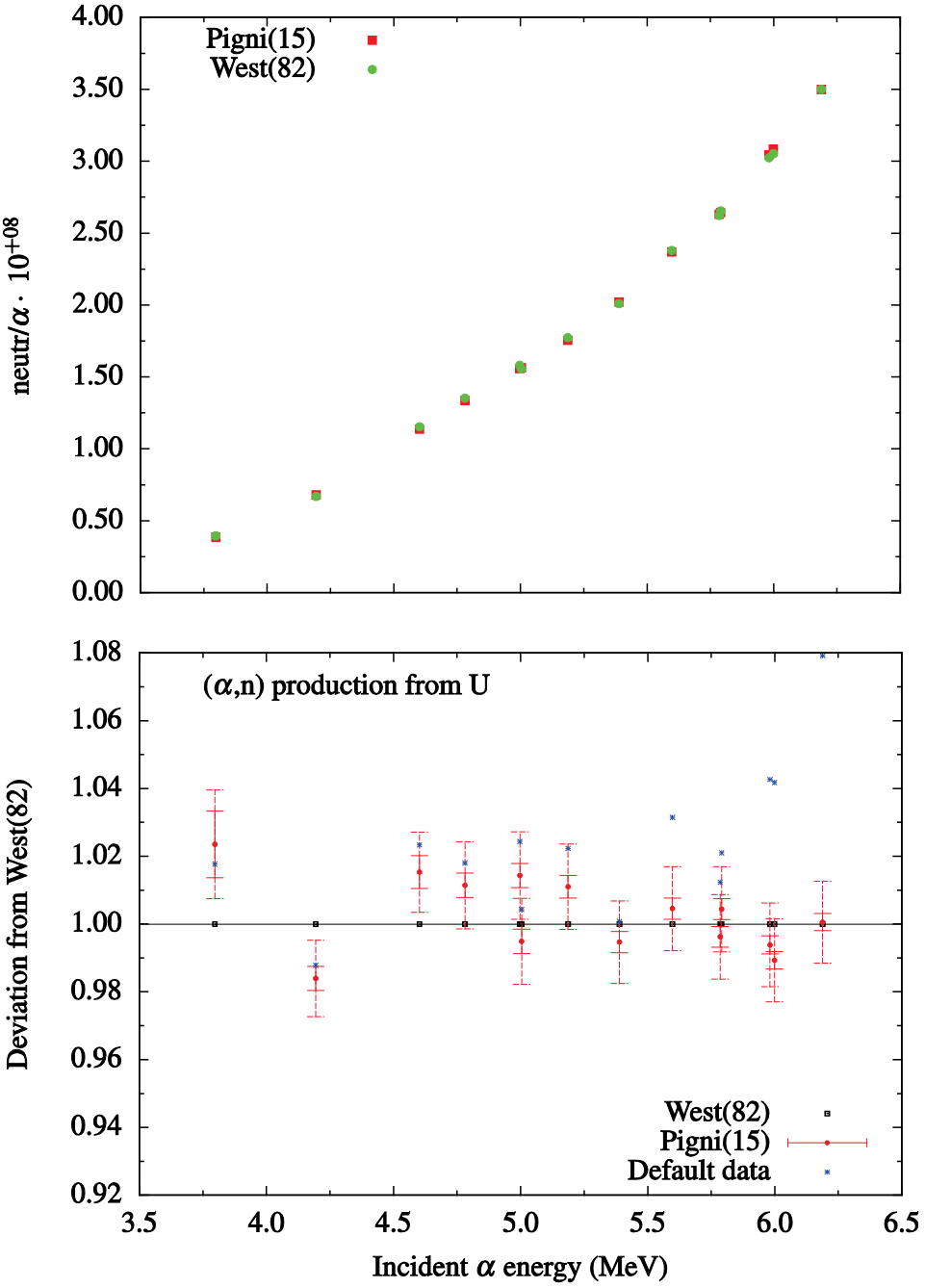


**Fig. 15. Comparison of calculations using evaluations of this work to West's measurements [35], showing deviations and estimated calculation uncertainty due to (α,n) cross section (red line), cross section plus stopping power coefficients (red dashed line), and comparison to the results of SOURCES using default data to West's data (blue data points with no uncertainties).**

## 3.5 REACTOR BASED MATERIALS PRODUCTION

Analysis of inventories from fission events or irradiated nuclear material can provide important information on possible proliferation activities, as measurements of environmental effluents or nuclear facility samples can be correlated to reactor activities using modeling and simulation codes. The concentrations of actinide and fission products, as well as radiation spectral analysis, can be used to infer anomalies in expected reactor operation or undeclared reprocessing activities. These types of studies rely heavily on burnup calculations to model isotope generation and decay following fission and establish baseline results and to determine potential signatures for identifying proliferation scenarios. These burnup calculations use a large amount of input nuclear data, and it is beneficial to identify which data have the largest response-sensitivities and which are most the responsible for uncertainties in the results.

The burnup code used in this project is ORIGEN [24]. ORIGEN tracks more than 2,300 individual nuclides formed by neutron transmutation, decay, fission, and activation. A preliminary version of a new code, ORIGEN Sensitivities (ORSEN), has been developed to compute sensitivity coefficients with ORIGEN that relate data perturbations to perturbations in nuclide concentrations after some specified burnup and/or decay period. The methodology used by ORSEN is described in this section.

The composition of nuclear material during irradiation is obtained by solving the nuclide transmutation equation, an initial-value problem consisting of a set of coupled first-order differential equations (Bateman equations) that describe time-dependent changes in the nuclide field caused by neutron irradiation and decay. These equations can be written using matrix notation as,

$$\boldsymbol{A}(\alpha)\,\mathbf{N}(t) = \frac{d\mathbf{N}(t)}{dt} \quad ; \qquad t \in (0, T_f) \tag{8}$$

$$\text{and} \quad \mathbf{N}(t=0) \rightarrow \mathbf{N_0} \quad ; \tag{9}$$

where:

A($t$) is the transmutation matrix, a function of input data parameters represented by $\alpha$, which include spectrum-averaged cross sections, decay constants and branching ratios, fission product yield data, decay emission spectra for gammas, alphas, betas and neutrons, nuclide initial conditions, and time-dependent total flux values;

N($t$) is the nuclide vector whose components correspond to the respective concentrations of every nuclide during the time period from initial-time t = 0 to final-time t = $T_f$ ; and

$N_0$ is the known initial nuclide concentration vector at time t = 0.

The ORIGEN module of the SCALE code system solves Eq. (5) for a given initial composition and specified nuclear data values in the ORIGEN data libraries that define the transmutation and decay process. For full simulation with all available nuclides, the dimension of N in ORIGEN is on the order of 1,500, and the transmutation matrix A contains approximately 50,000 nuclear data coefficients.

Typically, ORIGEN transmutation calculations are used to evaluate the time-dependent nuclide concentrations or some response that depends on nuclide concentrations at the final time ($T_f$) of the simulation; i.e., R → R(N($T_f$)). For all types of linear responses of interest in this study, the response can be expressed as the inner product of the final nuclide concentration vector N($T_f$) and a response-function

vector, $h_R$. The response-function vector has the same number of components as the nuclide vector, and the values of the components define the form of the response. Writing the response as an inner product gives,

$$R \rightarrow \mathbf{h}_R^T \mathbf{N}(T_f) = \sum_{i=1}^{L} h_{R,i} N_i(T_f). \quad (10)$$

Following are some examples of responses that can be evaluated at $T_f$, and their corresponding response-function vectors:

a) $^{239}$Pu concentration:
$h_{R,i} = 1$ where i = $^{239}$Pu index; and $h_{R,i} = 0$ for all isotope indices

b) sum of $^{235}$U + $^{239}$Pu mass:
$h_{R,i} = 1$ for i = $^{239}$Pu and for $^{235}$U indices; and $h_{R,i} = 0$ for all other isotope indices

c) fission product decay energy release (heat):
$h_{R,i} = Q_i \lambda_i$ for i = the requested fission product nuclide; and $h_{R,i} = 0$ for all other fission products; where $Q_i$ is the decay energy and $\lambda_i$ is the decay constant (half life), for fission product i

Uncertainties in these types of calculations due to the nuclear data uncertainty are frequently not considered because of the complexity of the transmutation process and the vast amount of nuclear data used in the calculations. The solution to this problem requires analysis of how a particular response of interest changes due to a change in any specified data parameter (i.e., due to the uncertainty in the data) appearing in the transmutation equation. This is indicated by the relative sensitivity coefficient, $S_\alpha^{(R)}$, which is defined for a particular response $R$ and an arbitrary data parameter $\alpha$ to be

$$S_\alpha^{(R)} = \frac{\Delta R / R}{\Delta \alpha / \alpha} \quad . \quad (11)$$

Sensitivity coefficients provide much insight about the transmutation physics, and they are required for numerous applications, including experiment similarity analysis and data adjustment procedures. They also can be used for response uncertainty analysis. Uncertainties in input nuclear data propagate through the transmutation calculations and produce uncertainties in computed nuclide concentrations, resulting in uncertainties in the responses. Sensitivities can be used to determine the overall uncertainty in a response and to identify the relative contributions of individual nuclear data parameters.

One straightforward method to compute sensitivities is to vary the value of one of the input parameters α by the fractional amount $\Delta\alpha/\alpha$; rerun the ORIGEN calculation with the perturbed data value to compute fractional response change, $\Delta R/R$, and then directly evaluate Eq. (8). This direct perturbation approach is sufficient if only a small number of input data are of interest. However, the general transmutation equation contains about 50,000 data parameters, so a massive computational effort would be required to compute sensitivities for all data by perturbing each individual parameter. A much more efficient approach for computing sensitivities is to use perturbation theory for the transmutation equations. Perturbation theory requires solving the *adjoint* transmutation equation, which is given by

$$A^T(\alpha)\mathbf{N}^*(t) = -\frac{d\mathbf{N}^*(t)}{dt} ; \qquad t \in (T_f, 0) \quad (12)$$

and $$\mathbf{N}^*(t = T_f) \rightarrow \mathbf{h}_R. \quad (13)$$

The adjoint equation in Eq. (9) is very similar to the forward transmutation equation in Eq. (5), except the time derivative is negative, and the transmutation matrix is transposed. Due to the negative derivative in Eq. (9), the *adjoint is solved backwards in time* as a final-value problem, where the final condition is equal to the response-function vector.

Recently, a new solution algorithm [37] has been implemented in ORIGEN which provides the capability to solve the adjoint transmutation calculations. After performing the forward and adjoint transmutation calculations, sensitivity coefficients can be computed for an arbitrary data parameter α using the expression

$$S_\alpha^{(R)} = \frac{\alpha}{R} \int_0^{T_f} \mathbf{N}_R^*(t) \frac{\partial \mathbf{M}(\alpha(t))}{\partial \alpha} \mathbf{N}^T(t)\, dt. \quad (14)$$

Therefore, one forward and one adjoint solution can provide sensitivities for *all* data in the ~50,000 coefficients of the transmutation matrix for any single response of interest.

From Eq. (11), it can be seen that the change in response R caused by a change in an arbitrary data parameter α is expressed as

$$\frac{\Delta R}{R} = S_\alpha^{(R)} \frac{\Delta \alpha}{\alpha}. \quad (15)$$

The sensitivity coefficient is a first order approximation which assumes a linear relationship between the response uncertainty and the nuclear data parameter uncertainty. Therefore, the above equation is limited to analyzing small relative changes. Under this condition, the sensitivities are calculated as the percent change in the response caused by a 1% change in data parameter α.

In FY15, a prototypic version of ORSEN was developed for this project to compute response sensitivities using depletion perturbation theory for reactor burnup calculations. This code was initially developed for other applications and was not capable of performing representative reactor simulations. ORSEN leverages recent improvements made to ORIGEN, allowing forward and adjoint transmutation calculations to be performed by calling ORGEN application program interfaces (APIs) from inside of ORSEN. After obtaining the forward and adjoint solutions, ORSEN evaluates Eq. (11) to obtain sensitivities for all nuclear data appearing in the ORIGEN transmutation computation.

As an example application, sensitivity coefficients were computed for the $^{238}$Pu concentration in low-enrichment uranium fuel after 3 years of irradiation to a burnup of 33 GWd/t fuel followed by 3 years of cooling time. Fig. 16 illustrates the complex dominant production paths from neutron reactions and decay that define the concentrations of uranium and trans-uranium products from irradiation. In the example case of the $^{238}$Pu concentration, the final condition for the nuclide adjoint vector at $T_f$ is zero for all nuclides except for $^{238}$Pu, which has a value of 1. Equation (9) is solved backwards in time, starting with the final condition, so it begins with 3 years of decay followed by 3 years of irradiation.

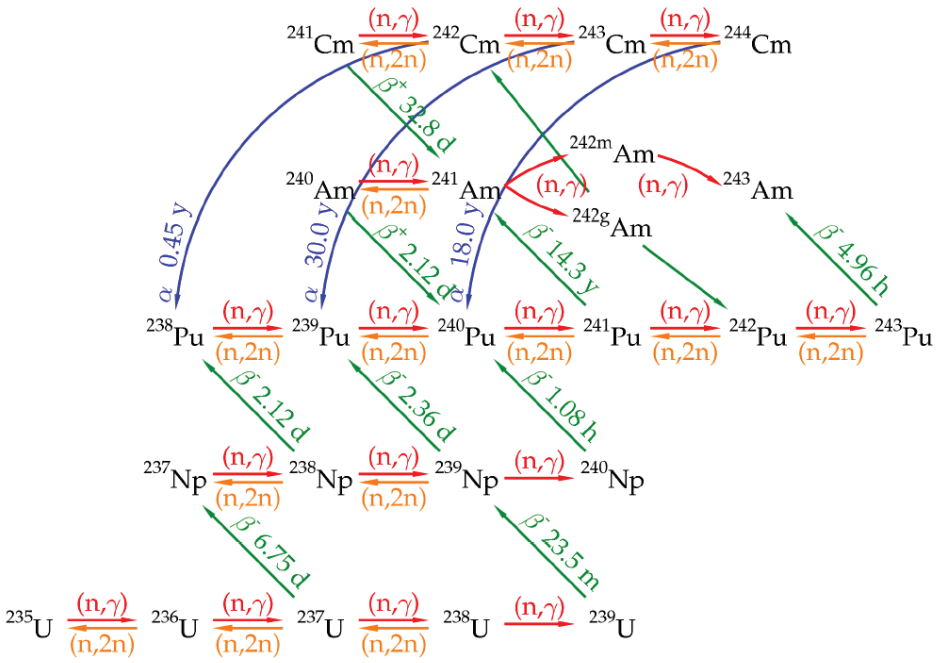


**Fig. 16. Dominant actinide transmutation chains in a thermal reactor.**

Table 5 shows the sensitivity coefficients for this problem.

**Table 5. Sensitivities of the $^{238}$Pu concentration after 3 years irradiation and 3 years decay**

| Parent nuclide | Product nuclide | Data type (α) | $S_\alpha$ |
|---|---|---|---|
| $^{235}$U | $^{236}$U | (n,γ) | 0.5928 |
| $^{236}$U | $^{237}$U | (n,γ) | 0.5877 |
| $^{237}$Np | $^{238}$Np | (n,γ) | 0.6136 |
| $^{241}$Pu | $^{241}$Am | Half life | 0.2132 |
| $^{238}$U | $^{239}$U | (n,γ) | 0.2155 |
| $^{242}$Cm | $^{238}$Pu | Decay branch | 0.2182 |
| $^{241}$Pu | $^{241}$Am | Decay branch | 0.2176 |
| $^{242}$Am | $^{242}$Cm | Decay branch | 0.2175 |
| $^{239}$Pu | $^{240}$Pu | (n,γ) | 0.1740 |
| $^{238}$U | $^{237}$U | (n,2n) | 0.1576 |
| $^{238}$Pu | $^{239}$Pu | (n,γ) | -0.1475 |

It can be seen that the final $^{238}$Pu concentration is most sensitive to the capture cross sections of $^{237}$Np, $^{235}$U, and $^{236}$U, which indicates that the major buildup chain for $^{238}$Pu in this system, and at this burnup starts with $^{235}$U:

$$^{235}\text{U}\ (\text{n},\gamma) \rightarrow {}^{236}\text{U}\ (\text{n},\gamma) \rightarrow {}^{237}\text{U}\ (\beta^-) \rightarrow {}^{237}\text{Np}\ (\text{n},\gamma) \rightarrow {}^{238}\text{Np}\ (\beta^-) \rightarrow {}^{238}\text{Pu}. \quad (16)$$

High sensitivities for decay branching-fractions of $^{242}$Cm alpha decay, $^{241}$Pu, and $^{242}$Am indicate that the $^{238}$Pu buildup from the chain beginning with $^{238}$U is also significant. In this case, the specific nuclear data in this particular chain are identified as being of greatest importance to the final $^{238}$Pu concentration.

The current version of ORSEN is a prototype that demonstrates the feasibility and utility of a sensitivity code–based perturbation theory for uncertainty analysis of fission event modeling and reactor-based material production calculations. Important development work is still needed in several areas, including (a) comprehensive verification and validation studies, (b) the capability to use burn-dependent cross sections required for accurate simulations, and (c) extension of theory and methodology to address the impact of data perturbations on the flux magnitude.

Another important development area is the addition of methods to compute response uncertainties (rather than sensitivities) using the sensitivity coefficients. ORSEN provides the sensitivities of each nuclear data parameter to a response. However, these sensitivities do not consider the accuracy of the nuclear data. For example, a parameter may have a very large *sensitivity* to a given response, but the parameter may be very well known and not contribute significantly to *uncertainty* in the response. Uncertainty analysis can be included in ORSEN by integrating the covariance data into the analysis. This addition will enable the calculation of not only the total uncertainties in the calculated quantities but will also enable users to identify the specific data that contribute to the uncertainty. This capability is necessary for prioritizing measurements to reduce modeling uncertainties. Continued development on this capability is planned in FY2016, however, extending the sensitivity capability to include the covariances for all nuclear data used to solve these problems is beyond the current resources of the project.

# 4. ANALYSIS OF THE NEUTRON MULTIPLICITY COUNTER (ENMC)

Initial demonstration of the data and methods was completed using a model for the Epithermal Neutron Multiplicity Counter (ENMC) at LANL with the case of plutonium oxide as a source. Reactor-grade and weapons-grade plutonium were analyzed, and different sample masses were used to assess the impacts of different levels of subcritical neutron multiplication on nuclear data uncertainties. The ENMC was selected in order to *demonstrate the mechanics of integrating uncertainty data* developed at the different labs in a real application. This will also allow the uncertainty results to be compared to measurements, providing a validation benchmark of uncertainty results.

The ENMC was selected as a detector type of interest because it exercises many of the nuclear data parameters being evaluated under this project, with the exception of irradiated material inventories. Selection of ENMC explicitly allowed many LLNL-developed data uncertainty components to be integrated and tested independently of ORNL data and methods development. Broader integration involving more complex applications is in the project plan for FY2016.

Neutron coincidence and multiplicity counting is widely used to measure plutonium materials and is used for nonproliferation applications and arms control measurements. The technique uses the time structure of the detected neutrons to distinguish spontaneous fission, (α,n) production, and induced fission contributions to the total counting rate to determine Pu mass. The measurement method considered here is based on the determination of (auto-) correlations in the counting rate that gives the total number of counts recorded (singles), the number of pairs of pulses recorded (doubles), and the number of threefold coincidences recorded (triples). Further details can be found in the *Manual of Multiplicity Counting* [38].

## 4.1 ENMC COUNTER

High quality neutron coincidence and multiplicity measurements require detectors with high efficiency and short die-away times to minimize statistical error. For this study, we have chosen the ENMC [39] as the state-of-the-art case. This detector consists of a large number of high pressure $^{3}$He tubes dispersed in a polyethylene matrix. It has a detection efficiency of around 65% and a die-away time of about 19 μs. The detector configuration is shown in Fig. 17. This detector gives measurements of counting rates with good statistical precision in a relatively short measurement time, as reflected in the simulation calculations. This reduces statistical uncertainties to see systematic effects. The ENMC is available to perform experimental measurements so that differences between simulations and measurements can be assessed.

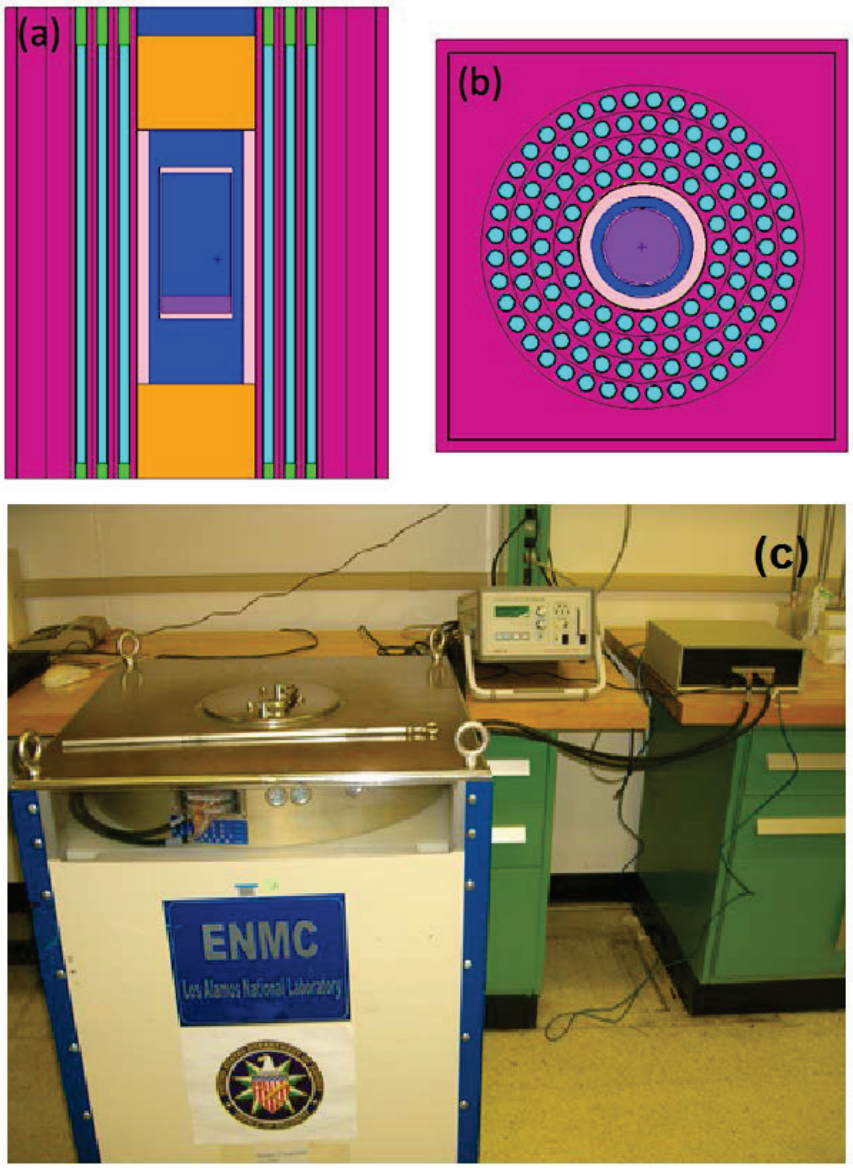


**Fig. 17. Cross section views of the ENMC MCNP6 geometry (a and b), showing $PuO_2$ canister measurement cavity (a) and 121 $^3$He tubes in four rings (b); and the ENMC counter at LANL (c).**

These measured counting rates are analyzed to produce values for the $^{240}$Pu effective mass, the ratio of (α,n) to spontaneous fission neutrons, and the neutron multiplication of the sample. In plutonium with typical reactor-grade isotopic compositions, the majority of the spontaneous fission neutrons are produced by $^{240}$Pu in the item, with $^{238}$Pu and $^{242}$Pu making significant but smaller contributions. Therefore, work is performed in terms of effective $^{240}$Pu mass ($^{240}Pu_{eff}$) as a quantity to represent the actual spontaneous fission source contribution from all isotopes as an equivalent amount of $^{240}$Pu. It is calculated using the equation:

$$^{240}Pu_{eff} = 2.52\,^{238}Pu + {}^{240}Pu + 1.68\,^{242}Pu \qquad (17)$$

Each spontaneous fission event has a probability of producing a certain number of neutrons between 0 and ~6. The notation P(ν) is used for the probability that a fission produces ν neutrons.

The alpha particle emission of all of the plutonium isotopes can create neutrons from (α,n) reactions if light elements are present in the sample. The term *alpha ratio* is used here to denote the ratio of (α,n) to spontaneous fission neutrons created in the sample.

To calculate the effect of nuclear data uncertainties, uncertainty is considered in the prediction of counting rates and measured quantities—$^{240}$Pu effective mass, the ratio of (α,n) to spontaneous fission neutrons and the neutron multiplication— caused by uncertainties in relevant nuclear data. The widely encountered case of plutonium oxide is analyzed to consider the following data effects:

- plutonium and oxygen neutron reaction cross sections,
- neutron-induced fission data for plutonium isotopes,
- $^{240}$Pu spontaneous fission neutron spectrum,
- P(ν) for $^{240}$Pu spontaneous fission,
- absolute intensity of spontaneous fission neutrons,
- intensity of neutrons emitted from (α,n) reactions, and
- the neutron spectrum from (α,n) reactions.

## 4.2 UNCERTAINTY ANALYSIS

MCNP6 [25] was used to calculate the probabilities of single, double and triples counts. The MCNP code contains specific tallies used to determine the number of correlated counts produced by a source event. The calculation takes into account the source process and all neutron transport, including induced fission (multiplication) up to the detection of a neutron in a $^{3}$He detector. The multiplicity of the source event and the neutron energy spectrum can be set in the input file description. The transport cross sections are obtained from a set of external nuclear data files, which also include details on the induced fission process, such as the energy dependence of the average number of neutrons per fission.

The tally results from the MCNP runs, which are performed on a per source event basis, were converted to actual counting rates (singles, doubles and triples) for a number of different sample cases. These counting rates were then analyzed using the point model equations to derive a *measured* Pu mass, alpha ratio and neutron multiplication. Three analysis methods are widely used for plutonium mass determination based on these measured rates:

- passive calibration curve,
- known alpha or multiplication corrected, and
- multiplicity analysis.

The Pu mass measured by a passive calibration curve depends only on the doubles rate and the calibration curve constants. The Pu mass determined by the known alpha method depends on singles, doubles, and the known alpha value. The Pu mass (as well as the alpha value and neutron multiplication) determined by multiplicity counting depends on nuclear data and detector parameters (efficiency, doubles gate fraction, and triples gate fraction). Since the area of interest concerns the change from a reference value (obtained with a nominal set of nuclear data), the analysis was performed without changing each of these input parameters. Therefore, the absolute values of the results, particularly in the case of the passive calibration curve with its nonlinear calibration, can differ considerably from the true value. This does not affect determination of the sensitivity of the technique to the uncertainty in the data.

Several different sample cases were considered. The calculations covered a range of three different sample masses and two isotopic compositions for the plutonium. All samples consisted of plutonium dioxide with a density of 2.2 g/cm$^3$ and a diameter of 11.9 cm. The sample heights were 0.0046, 2.84, and 23.7 cm for the small, medium and large samples respectively. Further details of the sample characteristics are given in Table 6 and 7.

### 4.2.1 Cross Section Data Uncertainty

To calculate the effect of the uncertainties in the cross section data values, LLNL generated 100 cross section libraries were using the Kiwi code with ENDF/B-VII.1-based covariance data. This included cross section perturbations for $^{236}$Pu, $^{237}$Pu, $^{238}$Pu, $^{239}$Pu, $^{240}$Pu, $^{241}$Pu, $^{242}$Pu, and $^{16}$O. These libraries were developed for use by MCNP. The intention was to determine the effect of the cross section changes on the neutron transport inside the item itself and not in the detector. Therefore, the cross section uncertainties were not included for materials of the detector.

A summary of the covariance data available in ENDF/B-VII.1 for the materials in this initial demonstration problem is presented in Table 8. Most covariance data in ENDF/B-VII.1 pertain to reaction cross sections, but prompt fission multiplicity (ν) and prompt fission neutron energy distribution (PFNS) also have covariance terms. Cross reaction covariance data are available for all isotopes except $^{241}$Pu. However, not all neutron *reactions* have covariance data.

**Table 6. Summary of covariance data available in ENDF/B-VII.1 for materials in initial demonstration**

| Sample | $PuO_2$ mass g | Pu mass (g) | $^{240}Pu_{eff}$ mass (g) (iso #1) | $^{240}Pu_{eff}$ mass (g) (iso #2) |
|---|---|---|---|---|
| Small | 1.12555 | 0.9831 | 0.1693 | 0.0583 |
| Medium (standard) | 694.902 | 606.95 | 104.5 | 35.988 |
| Large | 5799.02 | 5065.08 | 872.3 | 300.32 |

**Table 7. Isotopic Compositions used for EMNC simulations**

| Case | $^{238}$Pu% | $^{239}$Pu% | $^{240}$Pu% | $^{241}$Pu% | $^{242}$Pu% | $^{241}$Am% | $^{240}Pu_{eff}$% |
|---|---|---|---|---|---|---|---|
| Iso#1 | 0.0449 | 82.8144 | 16.504 | 0.2762 | 0.3601 | 1.1012 | 17.22 |
| Iso#2 | 0.008578 | 94.09164 | 5.797022 | 0.071941 | 0.030819 | 2.86E-05 | 5.87 |

**Table 8. Covariance data for selected target materials available in ENDF/B-VII.1.**

| Isotope | Reactions with covariance matrices |
|---|---|
| $^{16}$O | Total, elastic, (n,γ), (n,2n), (n,nα), (n,n3α), (n,np), (n,2np), (n,n2p), (n,nd), (n,pα), (n,p*), (n,d*), (n,t*), (n,α*), … |
| $^{236}$Pu | Total, elastic, (n,γ), (n,2n), (n,f), (n,3n), (n,n'), nubar, PFNS |
| $^{237}$Pu | Total, elastic, (n,γ), (n,2n), (n,f), (n,3n), (n,n'), nubar, PFNS |
| $^{238}$Pu | Total, elastic, (n,γ), (n,2n), (n,f), (n,3n), nubar, PFNS |
| $^{239}$Pu | Total, elastic, (n,γ), (n,2n), (n,f), (n,3n), (n,4n), nubar, PFNS |
| $^{240}$Pu | Total, elastic, (n,γ), (n,2n), (n,f), nubar, PFNS |
| $^{241}$Pu | Total, elastic, (n,γ), (n,2n), (n,f), (n,3n), nubar, PFNS |
| $^{242}$Pu | Total, elastic, (n,γ), (n,2n), (n,f), (n,3n), (n,4n), (n,n'), nubar, PFNS |
| $^{244}$Pu | Total, elastic, (n,γ), (n,2n), (n,f), (n,3n), (n,4n), (n,n'), nubar, PFNS |
| $^{246}$Pu | Total, elastic, (n,γ), (n,2n), (n,f), (n,3n), (n,4n), (n,n'), nubar, PFNS |

Neutron transport calculations were carried out with MCNP6 for the plutonium oxide source masses and isotopic compositions. These calculations did not include the effect of (α,n) neutrons from $^{17}O$ and $^{18}O$. These calculations were performed to limit the sensitivity effect to only spontaneous and induced fission neutrons. Subsequent calculations (described below) were carried out to investigate (α,n) effects.

Figure 18 shows the plutonium mass determined from the calculated counting rates for the 100 perturbations. The standard deviation of the resulting measured Pu mass is 0.04%, which corresponds to a 3-sigma input cross section variation.

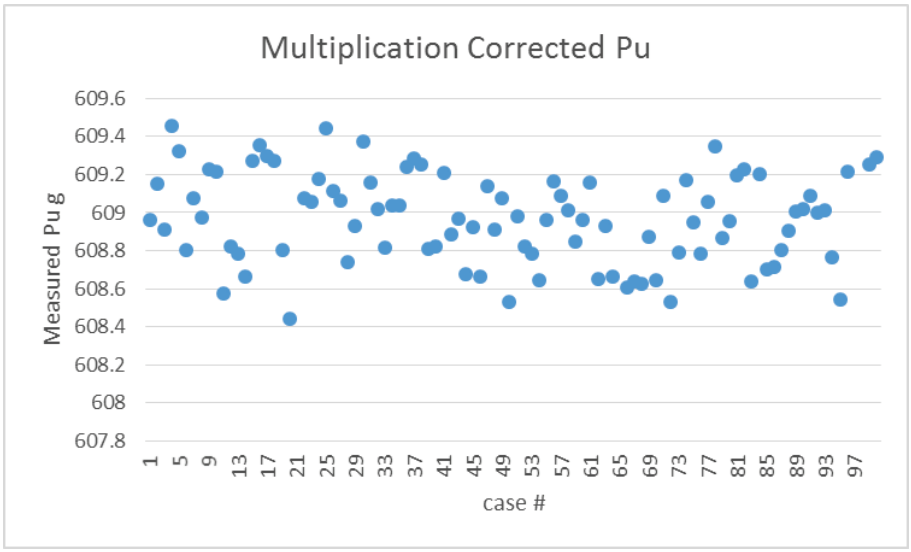


**Fig. 18. The measured Pu mass based on 100 samples of cross section data uncertainties.**

For the nonmultiplication corrected plutonium mass the standard deviation is 0.6% and for multiplicity determined mass is 0.09%. This indicates that the passive calibration curve (or "nonmultiplication corrected") analysis technique is the most sensitive to uncertainties in the nuclear data.

These variations include the effects of all nuclear data uncertainties for the isotopes and data types listed in Table 8.

### 4.2.2 Correlation Analysis

Analysis of the neutron singles, gated doubles, and gated triples indicates that the results are sensitive to changes in the $^{239}Pu$ prompt fission neutron spectrum (PFNS) as is indicated in Fig. 19 (and to a lesser extent to the $^{240}Pu$ PFNS). Correlations were generated using a 618 energy group covariance library. Later studies were performed using 40 groups. Softening of the PFNS (i.e., higher probability of neutrons at lower energies) is observed to be positively correlated with number of detected neutrons, while hardening of the spectrum is anti-correlated with counts. These were the only correlations deemed statistically significant based on the analysis of the first iteration.

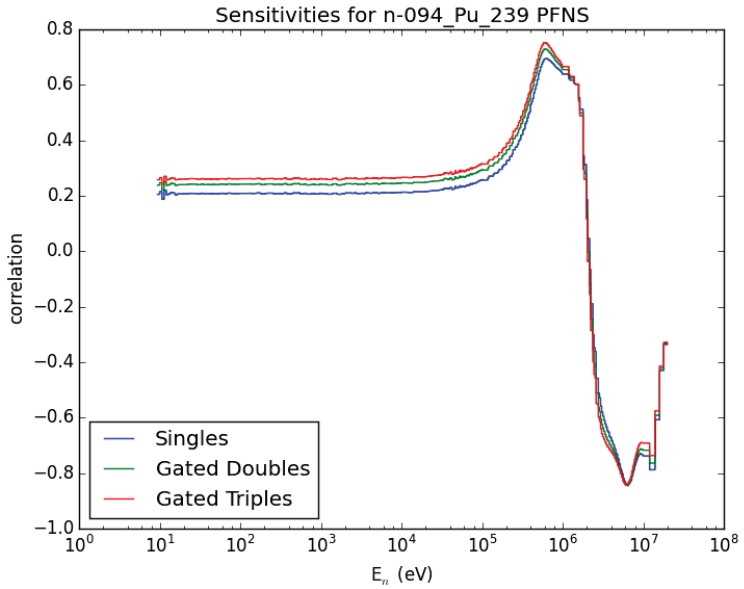


**Fig. 19. Correlation coefficients between number of detected neutrons and changes to the $^{239}$Pu prompt fission neutron spectrum at various outgoing energies.**

Analysis of the results began by scanning through all inputs to search for the largest correlations with output. The most significant correlation factor (r = 0.41) was for the $^{240}$Pu(n, 3n) cross section above 20 MeV. In order to understand the reason for this result, a scatter plot was generated (Fig. 20) that shows the distribution of multiplication-corrected Pu mass vs. variations in this input. The figure indicates that the cross sections became zero in three cases (Kiwi sets negative cross sections to zero), and the measured Pu mass for these three realizations is low compared to other runs. The output in this case is for a Pu mass of 606 g and standard isotopic composition (Iso#1).

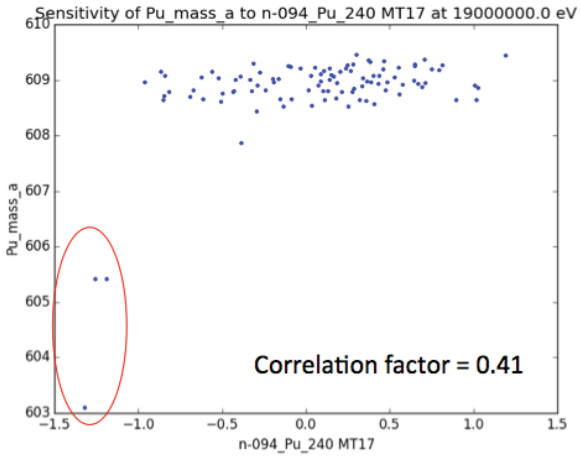


**Fig. 20. Distribution of multiplication-corrected Pu mass for standard-sized sample ('Pu_mass_a', in grams) vs. size of the relative variation in the $^{240}$Pu(n,3n) cross section from 18 MeV to 20 MeV for each realization (cross section set to zero in the three realizations circled in red).**

Since the three outliers in Fig. 20 correspond to the zero cross sections cases, these three runs were removed, and the analysis was continued using the remaining 97 realizations. After removal of the outliers, the remaining correlation coefficients were automatically rescaled, and other input variables

became more important. These correlations are summarized in Tables 9 and 10 for the standard mass case (606 g) at two different isotopic compositions.

**Table 9. Summary of significant correlations for multiplication-corrected Pu mass from the 606 g sample (standard isotopic composition) after removing three outlier runs**

| Isotope | Quantity | # of energy bins with correlation > 0.3 or < -0.3 | Max (anti) correlation |
|---|---|---|---|
| $^{239}$Pu | PFNS | 10 | 0.706 |
| | (n,γ) | 2 | -0.398 |
| $^{240}$Pu | (n,γ) | 18 | -0.413 |
| | $\bar{\nu}$ | 1 | -0.301 |
| $^{239}$Pu | elastic | 1 | -0.308 |

**Table 10. Summary of significant correlations for the multiplication-corrected Pu mass from the 606 g sample (enriched) after removing outlier runs**

| Isotope | Quantity | # of energy bins with correlation > 0.3 or < -0.3 | Max (anti) correlation |
|---|---|---|---|
| $^{239}$Pu | PFNS | 31 | 0.81 |
| | (n,γ) | 5 | -0.498 |
| $^{239}$Pu | elastic | 2 | -0.323 |
| $^{242}$Pu | total | 1 | -0.312 |
| $^{244}$Pu | (n,3n) | 1 | -0.302 |

The largest correlation is seen in the $^{239}$Pu PFNS (consistent with results shown in Fig. 20). Other important contributions include $^{239}$Pu (n,γ) and various reactions on other Pu isotopes. An interesting result is the sensitivity to $^{240}$Pu (n,γ) where it decreases for the weapons grade sample.

The tables above show that sensitivities are not necessarily identical for different isotopic compositions. Another test is to look for correlations between the 6 experiments performed by LANL (3 different sample sizes at two isotopic compositions). These results are shown in Fig. 21, revealing that the standard and large samples are all correlated with each other, but mostly uncorrelated to the small mass runs.

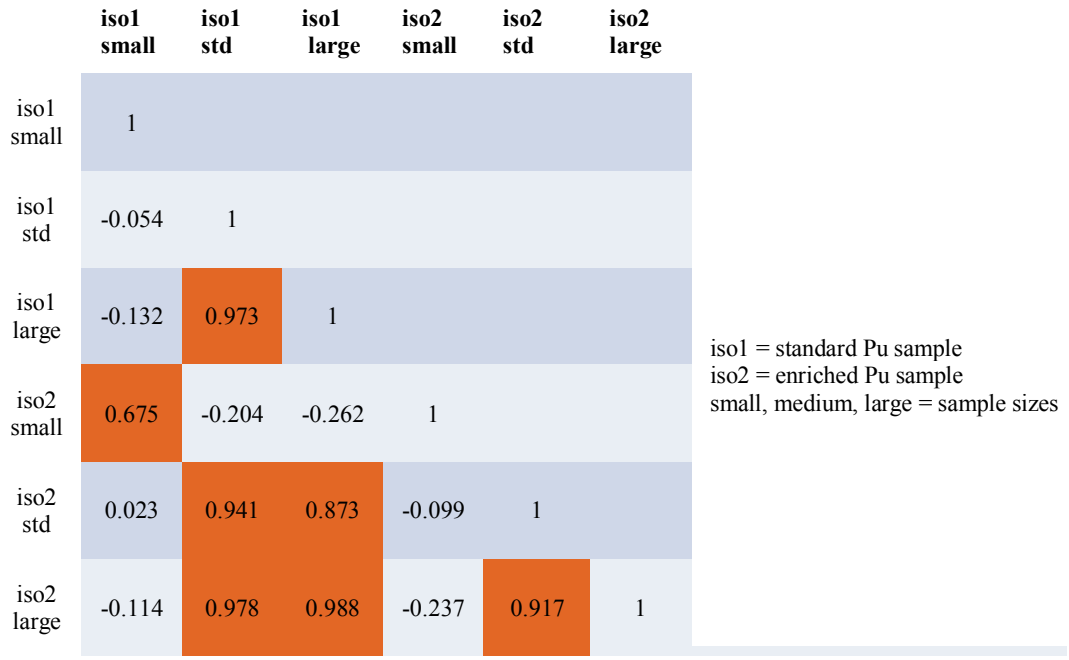


**Fig. 21. Correlation coefficients between different sets of MCNP simulations.**

Comparing different masses and isotopic compositions reveals other interesting differences:

- Both the large and small mass configurations are less sensitive to the $^{239}$Pu PFNS compared to the standard configuration.
- The only significant sensitivities to $^{16}$O appear for the small mass, where $^{16}$O(n,γ) is anti-correlated with multiplication-corrected Pu mass.
- No single nuclear data quantity dominates the sensitivity for the small mass simulations. The largest anti-correlation for standard enrichment is $^{240}$Pu(n,γ), with r = -0.375 around 600 keV. For higher enrichment, the largest correlation is to $^{244}$Pu(n,n'), with r = 0.364 around 1.8 MeV.

During analysis, a question arose as to whether there was evidence of nonlinear response to any of the input parameters. To address this question, each distribution of the detected Pu mass vs. input parameters was fitted with a second order polynomial using the Python *scipy.optimize.curve_fit* package that produced polynomial coefficients and their covariance matrix. The uncertainties for each coefficient were extracted from the covariance matrix, and the second order coefficient for each fit was filtered out unless it was more than 3*σ away from 0. While some fits pass this filter, after reviewing the information, no convincing evidence was found for any nonlinear response. A sample fit is shown in Fig. 22. Although this fit does show nonlinear behavior (C2 coefficient = -0.76 +/- 0.21), the fit is dominated by one point at the lower left that may be an outlier. No clear evidence of nonlinear response was observed for any parameters.

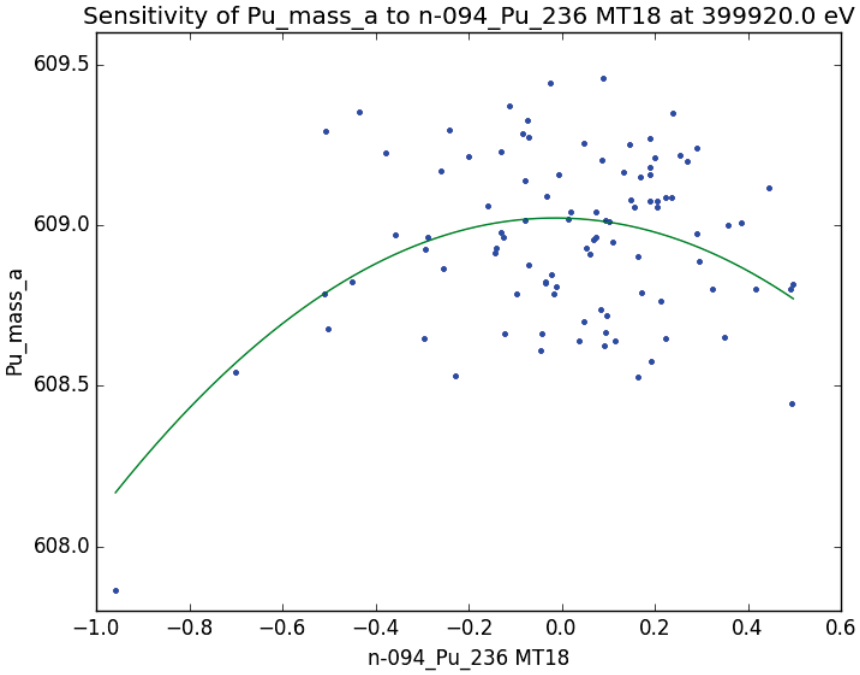


**Fig. 22. Second-order polynomial fit used to test for possible nonlinear responses.**

LLNL and LANL plan to generate and analyze additional realizations using the plutonium dioxide sample simulations to investigate the following:

- Sampling from a normal distribution of σ = 1 will be evaluated instead of sampling from a σ = 3 normal distribution when creating realizations. (Resultant realizations will agree better with the

covariance estimates from nuclear data evaluation and will be less likely to sample negative cross sections or probabilities.)

- The energy group structure of the covariance data may be refined to give more detail in some energy regions of interest.
- In addition to oxygen and plutonium isotopes, reactions on $^{241}$Am (usually present in samples from $^{241}$Pu decay) should also be varied.
- The method employed by Kiwi of preserving consistency between the total cross section and the sum of the constituent cross sections will be reviewed since some discrepancies in the consistency of data were identified during these studies.

### 4.2.3 Spontaneous Fission Neutron Spectrum

Uncertainties in the spontaneous fission neutron yield and energy spectrum are not included in the analyses using ENDF/B-VII.1 covariance data. The approach adopted to determine the effect of the spectrum of spontaneous fission neutrons was to determine the effect using a single parameter analysis rather than the overall correlated (combined) perturbation as carried out for analysis of the cross section data. For the ENMC model source, $^{240}$Pu is the dominant spontaneous fission source. The uncertainty in the mean energy of neutrons from $^{240}$Pu spontaneous fission is estimated to be 50 keV [34]. A Watt fission spectrum, as normally used in MCNP, was used to represent the neutron energy distribution for these calculations, where

$$N(E) = C\, e^{-E/a} sinh\sqrt{bE}. \qquad (18)$$

In a previous version of MCNP, a different set of parameters ($a = 0.799\ MeV$, $b = 4.903\ MeV^{-1}$) was used as the default. These parameters give an energy about 50 keV higher than the current default parameter set for $^{240}$Pu. Therefore, this parameter was set as the hard spectrum case and to create another soft spectrum case, with the same (but inverted sign) numerical differences in the parameters about the nominal values. The three cases are summarized in Table 11.

**Table 11. Watt parameters for $^{240}$Pu neutron spectrum simulation**

| Parameter set | *a*, MeV | *b*, MeV$^{-1}$ | Mean energy, MeV |
|---|---|---|---|
| Soft | 0.79086 | 4.47554 | 1.886 |
| Nominal | 0.79493 | 4.68927 | 1.933 |
| Hard | 0.799 | 4.903 | 1.981 |

These Watt parameters were used to define the spontaneous fission neutron energy of $^{238}$Pu, $^{240}$Pu and $^{242}$Pu to avoid any unwanted effect from the (small) contributions of $^{238}$Pu and $^{242}$Pu. Table 12 shows the calculated counting rates from each of the cases. The harder spectrum gives a lower count rate because the detector efficiency falls slightly with energy.

**Table 12. Simulated counting rates from different Watt parameters for $^{240}$Pu neutron spectrum**

| Case | Singles | Doubles | Triples | Mean SF energy, MeV |
|---|---|---|---|---|
| Nominal | 74,890 | 31,787 | 10,134 | 1.9329 |
| Hard | 74,715 | 31,651 | 10,108 | 1.9807 |
| Soft | 75,067 | 31,903 | 10,164 | 1.8858 |
| | **Relative to nominal** | | | |
| Hard | -0.23% | -0.43% | -0.26% | 2.47% |
| Soft | 0.24% | 0.37% | 0.29% | -2.44% |

Somewhat surprisingly, the change in singles and triples is about the same (0.25%), whereas the doubles changes are greater at 0.4%. These rates were used to calculate the plutonium mass from each of the three analysis methods; the results are shown in Table 13.

**Table 13. Pu masses determined from different $^{240}$Pu neutron spectra**

| Case | Multiplication corrected Pu mass (g) | Difference | Nonmultiplication corrected Pu mass (g) | Difference | Ratio (a,n) to SF | Multiplicity calculated Pu mass (g) | Difference |
|---|---|---|---|---|---|---|---|
| Nominal | 605.05 | -0.31% | 392.49 | -35.3% | -0.011 | 617.76 | 1.78% |
| Hard | 604.02 | -0.48% | 390.81 | -35.6% | -0.008 | 614.35 | 1.22% |
| Soft | 606.22 | -0.12% | 393.93 | -35.1% | -0.013 | 620.40 | 2.22% |
| | **Relative to nominal** | | | | | | |
| Hard | -0.17% | | -0.43% | 0.78% | | -0.55% | |
| Soft | 0.19% | | 0.37% | -0.67% | | 0.43% | |

The change in the nonmultiplication-determined mass is necessarily the same as that in the doubles rate (0.4%). The change in the known alpha result is 0.2%, and the multiplicity determined mass changes by 0.5%.

### 4.2.4 Effect of P(ν) for $^{240}$Pu Spontaneous Fission

A sensitivity study was made to determine the effect of the multiplicity distribution, P(ν), of spontaneous fission of $^{240}$Pu. The above calculations were carried out with the spontaneous fission probability for the plutonium spontaneous fission isotopes ($^{238}$Pu, $^{240}$Pu and $^{242}$Pu corresponding to their fractional content in the material). To make the effect of the change in P(ν) more clear, for these calculations, the multiplicity distribution of all of these isotopes was set to that of $^{240}$Pu. The first reference calculation was therefore not exactly that of the unperturbed medium mass sample in the previous section because of this change in the P(ν) distribution. Several calculations were carried out.

First, a reference P(ν) distribution was prepared (shown in Table 14). This was then perturbed to increase and decrease $\overline{\nu}$ by 1 standard deviation. This gave three P(ν) distributions that were used to determine the effect of $\overline{\nu}$ on the measurement. The size of the effect for all calculated quantities (singles, doubles, triples, Pu mass, etc.) was determined by taking half of the difference between the two extremes divided by the reference case.

**Table 14. Nominal and perturbed values for P(ν) for $^{240}$Pu**

| ν | P(ν) | P(ν) | P(ν) |
|---|---|---|---|
| | Nominal | nu-bar +sigma | nu-bar −sigma |
| 0 | 0.063185 | 0.063725 | 0.062649 |
| 1 | 0.231964 | 0.232974 | 0.230956 |
| 2 | 0.333323 | 0.333533 | 0.333107 |
| 3 | 0.252821 | 0.251975 | 0.253664 |
| 4 | 0.098646 | 0.097941 | 0.099354 |
| 5 | 0.01802 | 0.01784 | 0.018201 |
| 6 | 0.002041 | 0.002012 | 0.002069 |
| ν-bar | 2.15435 | 2.14934 | 2.15935 |

These distributions were used in MCNP6 to calculate the probabilities of single, double, and triple counts for a plutonium oxide sample with a Pu mass of 606.95 g and isotopic composition type 1 (Table 7). These probabilities were then converted into actual count rates by multiplying them by the spontaneous fission rate of the sample. The change in the singles, doubles and triples rates were 0.23%, 0.44%, and 0.57% respectively. The singles rate directly follows the change in $\overline{\nu}$, as expected. The correlated counting rates increase by a larger percentage.

The usual analysis methods were used to calculate the results. Table 15 shows the counting rates, the measured Pu masses, and the differences from the reference value. The absolute difference is not an important value here, as it can be corrected by a change in calibration constants. The important information is the relative change in the results caused by the change in $\overline{\nu}$. This is 0.16% for known alpha (multiplication corrected), 0.44% for nonmultiplication corrected (directly following the doubles change), and 0.38% for multiplicity analysis.

**Table 15. Counting rates and deduced Pu mass from perturbed P(ν) distributions for $^{240}$Pu**

| Case | S | D | T | Multi-plication-corrected Pu mass (g) | Difference from declared value | Nonmulti-plication-corrected Pu mass (g) | Difference | Multiplicity calculated Pu mass (g) | Difference from declared value |
|---|---|---|---|---|---|---|---|---|---|
| STDNOM | 74,886 | 31,788 | 10,142 | 604.989 | -0.32% | 392.507 | -35.33% | 617.505 | 1.74% |
| STDM1 | 74,712 | 31,649 | 10,085 | 604.000 | -0.49% | 390.787 | -35.61% | 615.155 | 1.35% |
| STDP1 | 75,057 | 31,926 | 10,200 | 605.969 | -0.16% | 394.205 | -35.05% | 619.793 | 2.12% |

These effects are similar in magnitude to the effect of changing the $^{240}$Pu spontaneous fission spectrum.

### 4.2.5 Effect of Spontaneous Fission and (α,n) Intensity

A further sensitivity study was made to determine the effect of the absolute intensities of (α,n) and spontaneous fission emission rates. A simulation of the singles, doubles and triples counting rates from (α,n) events in the medium mass sample (with isotopic composition #1) above was carried out. The spectrum of (α,n) neutrons was calculated using SOURCES4C [20]. The overall counting rates from the sample including the (α,n) rate is simply the sum of the spontaneous fission rates (calculated above) and these (α,n) rates. The processes are independent. Each calculation includes the effect of neutron

multiplication from induced fission. An assessment [34] of the current status of the uncertainty in the $^{240}$Pu spontaneous fission rate and the O(α,n) rate was used to calculate the effect on the counting rates and hence the measured Pu mass. Table 16 shows the counting rates—spontaneous fission plus (α,n)—determined for the reference case, labelled Wilson (α,n), and for increases and decreases of 1.5% in the (α,n) rate, as well as increases and decreases of 1.1% in the spontaneous fission rate.

**Table 16. Counting rates from perturbations in (α,n) and spontaneous fission intensity**

| Case | Singles | Doubles | Triples |
|---|---|---|---|
| Wilson (a,n) | 114,242.74 | 34,010.22 | 11,061.86 |
| +1.5%an | 114,833.10 | 34,043.54 | 11,075.65 |
| -1.5%an | 113,661.11 | 33,977.38 | 11,048.27 |
| SF+1.1% | 115,066.48 | 34,359.89 | 11,173.43 |
| SF-1.1% | 113,427.96 | 33,664.35 | 10,951.50 |

Table 17 shows the measured Pu mass resulting from the analysis of these counting rates. With the neutron multiplication of this sample, the (α,n) neutrons mainly increase the singles counting rate and do not contribute much to the doubles and triples rates. The nonmultiplication-corrected Pu mass, which is a direct measure of the doubles rate, changes by about 0.1% for a 1.5% change in the (α,n) rate. The multiplication-corrected Pu mass uses the ratio of the singles to doubles rate to determine the neutron multiplication and is more affected by this change in (α,n) rate and changes by 0.62%. This is because the analysis assumes a ratio for the (α,n) to spontaneous fission ratio for plutonium oxide based on the isotopic composition using fixed constants. On the other hand, the multiplicity analyzed mass has an additional free parameter and determines the (α,n) to spontaneous fission ratio independently. In this case, the change in the Pu mass determined by the multiplicity method is only 0.004%.

**Table 17. Masses determined from the perturbation in (α,n) and spontaneous fission intensity**

| Case | Multiplication-corrected Pu mass (g) | Difference from declared value | Nonmultiplication-corrected Pu mass (g) | Difference from declared value | Ratio (a,n) to SF | Multiplicity calculated Pu mass (g) | Difference from declared value |
|---|---|---|---|---|---|---|---|
| Wilson (a,n) | 585.449 | -3.54% | 419.941 | -30.8% | 0.5043 | 619.321 | 2.04% |
| +1.5%an | 589.107 | -2.94% | 420.352 | -30.7% | 0.5120 | 619.347 | 2.04% |
| -1.5%an | 581.847 | -4.14% | 419.535 | -30.9% | 0.4967 | 619.296 | 2.03% |
| SF+1.1% | 589.207 | -2.92% | 424.258 | -30.1% | 0.4987 | 626.115 | 3.16% |
| SF-1.1% | 581.732 | -4.47% | 415.670 | -31.7% | 0.5099 | 612.601 | 0.60% |

The results for the change in absolute spontaneous fission rate are more uniform across the various analysis techniques. The changes in nonmultiplication-corrected and multiplicity Pu mass are 1.02% and 1.09%, respectively. These are essentially the same as the change in the spontaneous fission rate itself. However, the change in the multiplication-corrected plutonium mass is somewhat smaller, at 0.64%, presumably because of compensation in the calculation of multiplication.

### 4.2.6 Effect of (α,n) Spectrum

A further sensitivity study was made to determine the effect of the spectrum of (α,n) neutrons. The starting point was the thick target data of Jacobs and Liskien [40], which was measured at various mono-energetic incident alpha particle energies. In an actual plutonium item, the (α,n) neutron spectrum will depend on the combination of isotopes present and their corresponding alpha particle line energies. For typical plutonium compositions, the measured values at an incident alpha particle energy of 5.5 MeV would be appropriate, but for low $^{238}$Pu and $^{241}$Am compositions, the measured values at an incident alpha particle energy of 5.0 MeV could be more representative. In addition to the Jacobs and Liskien data, there are measured spectra for plutonium oxide by Herald [41] and Anderson [42]. A reasonable approach is to determine the counting rates and measured plutonium masses for each of these spectra and compare the differences between them and also to compare them with the results from the SOURCES4C spectrum used above. The results based on the measured spectra are expected to be more reliable than the model calculation of Wilson.

Table 18 shows the mean energy of the (α,n) source neutrons and the calculated counting rates —sum of spontaneous fission and (α,n)—from each case and the differences from the Wilson reference case and from the Jacobs and Liskien 5.5 MeV case.

**Table 18. Counting rates and mean energies for different (α,n) spectra**

| Case | Singles | Doubles | Triples | Mean E MeV |
|---|---|---|---|---|
| Wilson (a,n) | 114,243 | 34,010 | 11,062 | 2.3095 |
| J&L 5.0 | 115,189 | 33,915 | 11,009 | 1.8624 |
| J&L 5.5 | 114,956 | 33,929 | 11,026 | 2.0155 |
| Herald | 115,301 | 33,905 | 11,011 | 1.8483 |
| Anderson | 114,592 | 33,979 | 11,054 | 2.1598 |
| **Relative to Wilson** | | | | |
| Wilson (a,n) | 0.00% | 0.00% | 0.00% | 0.0% |
| J&L 5.0 | 0.83% | -0.28% | -0.48% | -19.4% |
| J&L 5.5 | 0.62% | -0.24% | -0.33% | -12.7% |
| Herald | 0.93% | -0.31% | -0.46% | -20.0% |
| Anderson | 0.31% | -0.09% | -0.07% | -6.5% |
| **Relative to J&L5.5** | | | | |
| Wilson (a,n) | -0.62% | 0.24% | 0.33% | 14.6% |
| J&L 5.0 | 0.20% | -0.04% | -0.15% | -7.6% |
| J&L 5.5 | 0.00% | 0.00% | 0.00% | 0.0% |
| Herald | 0.30% | -0.07% | -0.14% | -8.3% |
| Anderson | -0.32% | 0.15% | 0.25% | 7.2% |

The difference between the rates from the Jacobs and Liskien 5.5 MeV and 5.0 MeV cases is very small, but there is a noticeable difference between these and the Wilson case. Interestingly the Herold and Anderson cases are close to, and bracket, the Jacobs and Liskien cases.

These counting rates were analyzed with the three analysis methods described above, and the results for plutonium mass and alpha value are shown in Table 19, together with the differences from the Wilson reference case and the Jacobs and Liskien 5.5 MeV case.

The results of the analysis reflect the counting rate changes above. The effect of the incident energy of Jacobs and Liskien is 0.27% on the multiplication corrected plutonium mass and effectively zero on the nonmultiplication-corrected and multiplicity plutonium masses. The alpha value derived from multiplicity analysis is changed by 0.6%.

**Table 19. Measured plutonium masses and alpha ratio from the different (α,n) spectra**

| Case | Multiplication-corrected Pu mass (g) | Difference from declared value | Nonmultiplication-corrected Pu mass (g) | Difference from declared value | Ratio (a,n) to SF | Multiplicity-calculated Pu mass (g) | Difference from declared value |
|---|---|---|---|---|---|---|---|
| Wilson (a,n) | 585.45 | -3.54% | 419.94 | -30.81% | 0.5043 | 619.32 | 2.04% |
| J&L 5.0 | 591.97 | -2.5% | 418.77 | -31.00% | 0.5221 | 617.36 | 1.72% |
| J&L 5.5 | 590.41 | -2.7% | 418.94 | -30.98% | 0.5188 | 617.35 | 1.71% |
| Herold | 592.75 | -2.3% | 418.64 | -31.03% | 0.5249 | 616.81 | 1.62% |
| Anderson | 587.84 | -3.1% | 419.55 | -30.87% | 0.5115 | 618.24 | 1.86% |
| | **Relative to Wilson** | | | | | | |
| Wilson (a,n) | 0.00% | | 0.00% | | 0.00% | 0.00% | |
| J&L 5.0 | 1.11% | | -0.28% | | 3.53% | -0.32% | |
| J&L 5.5 | 0.85% | | -0.24% | | 2.88% | -0.32% | |
| Herold | 1.25% | | -0.31% | | 4.08% | -0.41% | |
| Anderson | 0.41% | | -0.09% | | 1.44% | -0.17% | |
| | **Relative to J&L5.5** | | | | | | |
| Wilson (a,n) | -0.84% | | 0.24% | | -2.80% | 0.32% | |
| J&L 5.0 | 0.27% | | -0.04% | | 0.64% | 0.00% | |
| J&L 5.5 | 0.00% | | 0.00% | | 0.00% | 0.00% | |
| Herold | 0.40% | | -0.07% | | 1.17% | -0.09% | |
| Anderson | -0.44% | | 0.15% | | -1.40% | 0.14% | |

### 4.2.7 Summary of Perturbation Effects

Table 20 presents a summary of the individual nuclear data effects on the measurement of a medium-size plutonium sample. The results indicate that the uncertainty in the absolute intensity of spontaneous fission and (α,n) emission are the major contributors on this list. The (α,n) intensity only contributes significantly to the uncertainty on the multiplication-corrected plutonium mass. However, this is a widely used technique. This level of uncertainty is comparable with the observed measurement uncertainty on good quality measurements.

The uncertainty of the multiplicity distribution and energy spectrum of $^{240}$Pu spontaneous fission contributes almost equally to the uncertainty of all three techniques, but at a level less than the observed measurement error on all but the most careful measurements. The uncertainty on the (α,n) spectrum only contributes to the multiplication-corrected plutonium mass at a modest level.

For comparison, the global data perturbation that includes the cross section and prompt fission parameter uncertainties described above changes the nonmultiplication corrected value significantly, by 0.6%, whereas the multiplication corrected and multiplicity analyses are much less affected.

**Table 20. Summary of sensitivity study**

| Nuclear data | Multiplication-corrected Pu mass uncertainty | Nonmultiplication-corrected Pu mass uncertainty | Multiplicity calculated Pu mass uncertainty |
|---|---|---|---|
| Spontaneous fission neutron intensity | 0.64% | 1.02% | 1.09% |
| (α,n) neutron intensity | 0.62% | 0.10% | 0.00% |
| P(v) $^{240}$Pu | 0.16% | 0.44% | 0.38% |
| Spontaneous fission energy $^{240}$Pu | 0.18% | 0.40% | 0.50% |
| Energy spectrum for (α,n) | 0.27% | 0.04% | 0.00% |
| Cross section and prompt fission parameters | 0.04% | 0.61% | 0.09% |

## 4.3 INDEPENDENT MODEL VERIFICATION

The ENMC used in this study was modeled independently using the MAVRIC [43] neutron/gamma transport module of the SCALE code package [44] to verify the results from MCNP. The cross section covariance data used in the verification was also developed independently and is included in the SCALE code.

The $PuO_2$ powder sample was modeled with a density of 2.2 g/cm$^3$ at the bottom of an iron can and is cylindrical in shape, with a height of 2.84 cm and a radius of 5.95 cm. The dimensions and composition of the MAVRIC model were identical to the MCNP model. For the verification analysis case, the total $PuO_2$ source mass was 694.9 grams, and the plutonium vector was 82.2% $^{239}$Pu (Iso#1).

The starting source spectrum was calculated in 300 energy groups using equally spaced lethargy as calculated using the ORIGEN [24] code of SCALE. The spectrum generated by ORIGEN uses the methods in SOURCES4C and Watt fission spectrum parameters that are identical to those used internally by MCNP. The total spontaneous fission neutron yield was calculated to be 177.67 n/s/g of plutonium. The source is uniformly distributed in the source volume. The SCALE/MAVRIC model of the ENMC is shown in Fig. 23.

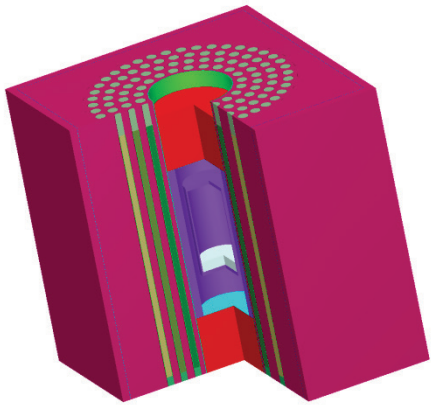

**Fig. 23. SCALE 3-dimensional model of the ENMCC detector system.**

Four detector responses corresponding to each of the four rings of detectors, as well as the total response calculated with SCALE/MAVRIC, all agree within ~1% with the corresponding results calculated with the MCNP6 code, as shown above in Table 21. For the outermost ring response, the difference is slightly larger at 1.79%.

**Table 21. SCALE and MCNP comparison for the results in the four detector rings**

| Response ring # | SCALE | | MCNP | | (MCNP-SCALE)/MCNP |
|---|---|---|---|---|---|
| | Value | Relative standard deviation | Value | Relative standard deviation | |
| 1 | 0.20583 | 0.00039 | 0.20543 | 0.0006 | -0.20% |
| 2 | 0.21845 | 0.00038 | 0.21918 | 0.0006 | 0.33% |
| 3 | 0.15636 | 0.00046 | 0.15726 | 0.0007 | 0.57% |
| 4 | 0.12325 | 0.00052 | 0.12549 | 0.0008 | 1.79% |
| Total | 0.70389 | 0.00019 | 0.70735 | 0.0004 | 0.49% |

The spontaneous fission spectrum neutrons produced in the volume are capable of inducing secondary fissions in the source material. It was determined that for this source, the induced fission neutrons account for about 10% of the total response at the detectors for the 694.9 gram case. The primary and secondary neutrons are transported to the detector tubes, where they are detected via an $^{3}$He (n,p) reaction. The SCALE calculations described in this report were performed with SCALE6.2 beta4 release. The nuclear data libraries used are standard continuous energy (for the initial MAVRIC model) and multigroup SCALE libraries based on the ENDF/B-VII.1 nuclear data library for the uncertainty calculations [45]. AMPX modules [46] are used to generate the standard SCALE libraries, which are part of the SCALE package.

The MAVRIC model for the ENMC was used to analyze the uncertainties in the model results *induced by uncertainties in the nuclear data*. The SAMPLER module [45] of SCALE was used for this purpose. SAMPLER propagates uncertainties in nuclear data to the results of the simulation by Monte Carlo sampling of the data within the uncertainty distributions. SAMPLER uses a 56-energy-group covariance data library of pregenerated perturbation factors derived from ENDF/B-VII.1 to modify the nuclear data and generate new runtime perturbed nuclear data libraries. These libraries replace the standard library in the transport simulation of the detection assembly. The simulation result will thus be affected by the uncertainties in the nuclear data.

The initial SCALE model of the ENMC detection system was developed using a continuous energy library based on ENDF/B-VII.1. However, in SCALE, uncertainty analysis is only performed using multigroup calculations. To be able to use the ENMC model in SAMPLER, a 252-group cross section library based on ENDF/B-VII.1 was used. The results for the 4 detector rings with the multigroup library are within 1–2 standard deviations from the corresponding results obtained with the continuous energy model, as shown in Table 22. The standard deviations listed in Table 22 are the Monte Carlo errors.

**Table 22. Differences between continuous energy and multigroup results for the 4 detector rings of the ENMC detection system**

| Ring | Continuous energy | | Multigroup | | Differences |
|---|---|---|---|---|---|
| | Value | Standard deviation | Value | Standard deviation | |
| 1 | 0.20583 | 0.00008 | 0.20601 | 0.00008 | 0.09% |
| 2 | 0.21845 | 0.00008 | 0.21832 | 0.00008 | -0.06% |
| 3 | 0.15636 | 0.00007 | 0.15665 | 0.00007 | 0.19% |
| 4 | 0.12325 | 0.00006 | 0.12398 | 0.00006 | 0.59% |
| Total | 0.70389 | 0.00014 | 0.70496 | 0.00013 | 0.15% |

Using the 56-group perturbation factors library containing 1,000 realizations in the SCALE6.2 beta4, the SAMPLER model was used to obtain satisfactory statistics of the results with different realizations of the nuclear data library. A *realization* in this context means a MAVRIC calculation using one of the 1,000 available perturbed cross section libraries. The results thus obtained were analyzed statistically and are shown in Tables 23 and 24.

**Table 23. Values and standard uncertainties of the 4 detector responses predicted using SCALE6.2**

| Ring | Value | Standard uncertainties | Relative standard uncertainties |
|---|---|---|---|
| 1 | 0.2060 | 0.0013 | 0.63% |
| 2 | 0.2183 | 0.0008 | 0.39% |
| 3 | 0.1565 | 0.0004 | 0.23% |
| 4 | 0.1237 | 0.0007 | 0.53% |
| **Total counts in all $^{3}$He detectors** | 0.7045 | 0.0020 | 0.29% |

The LLNL libraries contain perturbed cross section data but with the $\bar{\nu}$ data unperturbed. For comparison with the LLNL-based calculations, an assessment was performed of the impact on statistics of removing the $\bar{\nu}$ data from the perturbation factors library.

**Table 24. Values and standard uncertainties of the 4 detector responses predicted using SCALE6.2 (no $\bar{\nu}$ perturbation)**

| Ring | Value | Standard uncertainties | Relative standard uncertainties |
|---|---|---|---|
| 1 | 0.2030 | 0.0016 | 0.77% |
| 2 | 0.2157 | 0.0012 | 0.56% |
| 3 | 0.1554 | 0.0008 | 0.51% |
| 4 | 0.1241 | 0.0009 | 0.73% |

Again, the impact is not significant, as demonstrated in Table 24. The low impact of removing the $\bar{\nu}$ data from the perturbation factors library is due to the type of problem that is run. Since only ~10% of the response is affected by the $\bar{\nu}$ data, the impact on the final results is expected to be small.

Each of the realizations described above was initially simulated using 400,000 particles. The total runtime for 1,000 realizations was close to 1 week on a single processor. An inspection of the random statistical uncertainty for each realization shows that this has a relatively large size, comparable with the total effect produced by the perturbation of the cross sections. This random statistical uncertainty is compounded with the uncertainty due to the cross sections. Because the statistical uncertainty is large, and to ensure consistency of comparison with LANL results, the number of particles simulated was increased 100 times, to 40 million. The statistical uncertainty was thus decreased by a factor of 10 to about 0.02% for each of the total responses.

The number of realizations is also important when small effects are to be analyzed. From the simulations performed with the increased number of particles, it can be observed that using only 100 realizations can affect the standard deviation by ~10% when compared with the standard deviation calculated with a larger number of realizations.

The impact of uncertainties in nuclear data on the total ENMC count rate was evaluated. The impact is below 1% for each of the four rings. The random uncertainties due to the number of particles simulated may have a large impact for this particular problem. The impact of the perturbation factors library version of the cross section library and the $\bar{\nu}$ data was estimated to be minor for this problem.

The neutron source used in the simulation is a fixed source in a multiplicative medium with induced fissions enabled. About 10% of the response is due to secondary neutrons emitted from the source. The spectrum of the primary neutrons was obtained from an ORIGEN simulation and corresponds to the spontaneous fission source used in the MCNP simulations. The contribution of the (α,n) reaction is neglected in these preliminary verification studies.

# 5. SUMMARY AND CONCLUSIONS

This project provides for development of the analysis tools and code infrastructure to perform comprehensive nuclear data uncertainty analysis for applications in nuclear nonproliferation. Although several previous investigations have been conducted to identify nuclear data needs in safeguards and security, these investigations have generally been limited to narrow ranges of an application space, or they have only considered a small subset of nuclear data. This work expands the data analysis domain to include most nuclear data used in a broad spectrum of nuclear security applications. This is accomplished by evaluating the impact of nuclear data uncertainties as determined by the uncertainty in the data on applications of interest. This has not been accomplished previously because the complete covariance data necessary to perform these studies has not been available, and the computational tools necessary to analyze the results from these studies are not available. The work described in this report represents an important advance in providing the data and computing framework necessary for quantitative nuclear data uncertainty analysis. This effort has demonstrated initial integration of the data uncertainty components to a benchmark problem of a neutron multiplicity counter.

Specific accomplishments documented in this report include:

- advancement of the Kiwi code for covariance data analysis and uncertainty data development for the analysis of data uncertainties for problems using the MCNP code;
- development of processing tools to analyze correlations between nuclear data used in the model and the model results to identify key data importance;
- performance of an uncertainty analysis for (α,n) reactions and demonstration using oxide sources;
- preparation of a draft journal paper documenting the (α,n) uncertainty research;
- preliminary investigation of the potential application of the FREYA code to develop covariance data for spontaneous fission sources;
- integration of the wide range data uncertainty information in a practical problem of the neutron multiplicity coincidence counter using MCNP;
- performance of a parallel verification of the neutron counter uncertainty analysis using SCALE; and
- significant progress in the extension of inverse uncertainty analysis methods to the problem of reactor-based material production and post-detonation forensics.

## REFERENCES


[1] M. B. Chadwick et al., "ENDF/B-VII.1 Nuclear Data for Science and Technology: Cross Sections, Covariances, Fission Product Yields and Decay Data," *Special Issue on ENDF/B-VII.1 Library Nuclear Data Sheets*, 112(12) (2011): 2887–3152

[2] International Workshop on Nuclear Data Covariances, April 28 – May 1, 2014, Santa Fe, New Mexico, USA. http://t2.lanl.gov/cw2014/, *Nuclear Data Sheets*, 123 (January 2015) Special Issue on International Workshop on Nuclear Data Covariances (2015): 1–238.

[3] P. Schillebeeckx, M. Looman, and A. Ravazzani, "Nuclear Data Required for Non Destructive Assay of Fissile and Fertile Material," *World Scientific* (2000).

[4] *American National Standards for Plutonium-Bearing Solids Calibration Techniques for Calorimetric Assay*, ANSI-15.22 (1987).

[5] P. De Bièvre and A. Verbruggen, "A new measurement of the half-life of 241Pu using isotope mass spectrometry," *Metrologia*, 36 (1999): 25–31.

[6] S. Croft and P. M. J. Chard, "Neutronic Characterisation of Plutonium Oxide Samples at Harwell," *ESARDA Proceedings*, 26 (1993): 511–519.

[7] R. T. Perry and W. B. Wilson, "Neutron production from (α,n) reactions in $ThO_2$, $UO_2$, $(U,Pu)O_2$ fuels," LA-8869-MS (1981).

[8] P. Santi, "Sensitivity of Modeling Neutron Emissions to Uncertainties in Nuclear Data," LANL, LA-UR-08-06802 (September 2008).

[9] W. Parker, "Nuclear Data Needs: Source Term Library/Uncertainty Analysis," LLNL, Safeguards Working Group Meeting, Idaho State University, Pocatello, Idaho, (March 17–18, 2009).

[10] R. Bahran, "A Survey of Nuclear Data Deficiencies Affecting Nuclear Non-Proliferation," LA-UR-14-26531, *Proceedings of the 2014 INMM Annual Meeting*, Atlanta, GA (July 20–24).

[11] B. Sleaford, "Nuclear Data Needs and Capabilities for Applications 2015 – Gamma Spectroscopic Data for Non-Proliferation Applications." LLNL (May 28, 2015).

[12] Workshop on Nuclear Data Needs and Capabilities for Applications, NDNCA 2015, Department of Energy Office of Science, Berkeley, May 27–29, 2015, http://bang.berkeley.edu/events/ndnca/

[13] P. Talou, P. G. Young, T. Kawano, M. Rising, M. B. Chadwick, "Quantification of Uncertainties for Evaluated Neutron-Induced Reactions on Actinides in the Fast Energy Range," *Nuclear Data Sheets*, 112 (2011): 3054–3074.

[14] R. C. Little et al., "Low-fidelity Covariance Project," *Nuclear Data Sheets*, 109, 12 (2008): 2828–2833.

[15] T. R. England and B. F. Rider, "ENDF-349 Evaluation and Compilation of Fission Product Yields," LA-UR-94-3106, LANL (1994).

[16] IAEA Nuclear Data Section, Coordinated Research Project (CRP), Fission product yield data for transmutation of minor actinide nuclear waste, https://www-nds.iaea.org/fycrp/crp.html

[17] OECD/NEA Working Party on International Nuclear Data Evaluation Co-operation (WPEC), Improved fission product yield evaluation methodologies, WPEC Subgroup 37, https://www.oecd-nea.org/science/wpec/sg37/.

[18] M. Pigni, M. W. Francis, I. C. Gauld, "Investigation of Inconsistent ENDF/B-VII.1 Independent and Cumulative Fission Product Yields with Proposed Revisions," Nuclear Data Sheets 1 (2015): 123.

[19] J. M. Verbeke, J. Randrup, R. Vogt, FREYA, *User Manual*, Lawrence Livermore National Laboratory, LLNL-TM-654899 (2006).

[20] W. B. Wilson, R. T. Perry, W. S. Charlton and T. A Parish "SOURCES: A code for calculating (α,n), spontaneous fission and delayed neutron sources and spectra," *Progress in Nuclear Energy,* 51 (2009): 608.

[21] K. A. Miller, M. T. Swinhoe, and S. Croft, "Measured F(α,n) Yield from $^{234}$U in Uranium Hexafluoride," *Nuclear Science and Engineering* 176, 98–105 (2014).

[22] J. A. Winger et al., "Large β-Delayed Neutron Emission Probabilities in the $^{78}$Ni Region," *Phys. Rev. Letters,* 102, 142502 (2009).

[23] Bignan, G. et al., "Plutonium Isotopic Determination using Gamma Spectrometry: Recommendations for the $^{242}$Pu Content Evaluation using a New Algorithm," *ESARDA Bulletin* No. 28 (1998).

[24] I.C. Gauld et al., "Isotopic Depletion and Decay Methods and Analysis Capabilities in SCALE," *Nuclear Technology*, 174, 2, 169 (2011).

[25] J. T. Goorley, M. R. James, T. E. Booth, F. B. Brown, J. S. Bull, L. J. Lawrence, J. W. Durkee, Jr., J. S. Elson, M. L. Fensin, R. A. Forster, III, J. S. Hendricks, H. G. Hughes, III; R. C. Johns, B. C. Kiedrowski, R. L. Martz, S. G. Mashnik, G. W. McKinney, D. B. Pelowitz, R. E. Prael, J. E. Sweezy, L. S. Waters, T. Wilcox, A. J. Zukaitis. "Initial MCNP6 Release Overview - MCNP6 version 1.0," *Los Alamos National Laboratory Report,* LA-UR-13-22934, April 2013.

[26] R. E. Macfarlane, A. C. Kahler, "Methods for Processing ENDF/B-VII with NJOY," *Nuclear Data Sheets*, 111, Issue 12, 2739 (2010).

[27] C. M. Mattoon et al., "Covariance Applications with Kiwi," *EPJ Web of Conferences* 27 (2012)

[28] B. R. Beck, "FUDGE: A Program for Performing Nuclear Data Testing and Sensitivity Studies," Lawrence Livermore National Laboratory, UCRL-PROC-206797 (2004).

[29] N. M. Larson, "Updated Users Guide For SAMMY: Multilevel R-Matrix Fits To Neutron Data Using Bayes Equations," Oak Ridge National Laboratory, ORNL/TM-9179/R8, Oak Ridge, TN (October 2008).

[30] T. Murata, H. Matsunobu and K. Shibata, "Evaluation of the (α,xn) Reaction Data for JENDL/AN-2005," JAEA-Research 2006-052 (July 2006).

[31] J. K. Bair and N. B. Willard, "Level Structure in $^{22}$Ne and $^{30}$Si from the Reactions $^{18}$O (α,n)$^{21}$Ne and $^{26}$Mg(a,n)$^{29}$Si," *Phys. Rev*. 128, 299 (1962).

[32] J. K. Bair and F. X. Haas, "Total Neutron Yield from the Reactions C-13(α,n) O-16 and O-17,O-18 (α,n) Ne-20,Ne-21," Phys. Rev. C7, 1356 (1973).

[33] J. K. Bair, G. Campo, "Neutron Yields From Alpha-Particle Bombardment," *Nucl. Sci. Eng.*71, (1979) 18–28.

[34] S. Croft, Oak Ridge National Laboratory, private communication.

[35] D. West and A. C. Sherwood, "Measurements of Thick-Target (α, n) Yields from Light Elements," *Ann. Nucl. Energy* 9, 551 (1982).

[36] M. J. Berger, J. S. Coursey, M. A. Zucker and J. Chang, "Stopping-Power and Range Tables for Electrons, Protons, and Helium Ions," National Institute of Standards and Technology (NIST), NISTIR4999.

[37] M. Pusa and J. Leppänen. An efficient implementation of the Chebyshev rational approximation method (CRAM) for solving the burnup equations, in: *Proc. PHYSOR 2012*, Knoxville, TN, Apr. 15–20 (2012).

[38] N. Ensslin, W. C. Harker, M. S. Krick, D. G. Langner, M. M. Pickrell and J. E. Stewart, "Application Guide to Multiplicity Counting, " LANL Report LA-13422-M, November 1998.

[39] H. O. Menlove, C. D. Rael, K. E. Kroncke, K. J. DeAguero, *Manual for the Epithermal Neutron Multiplicity Detector (ENMC) for Measurement of Impure MOX and Plutonium Samples*, LA-14088, LANL, (May 2004).

[40] G. J. H. Jacobs and H. Liskien "Energy spectra of neutrons produced by α-particles in thick targets of light elements," *Ann. Nucl. Energy* 10 (1983): 541–552.

[41] T. R. Herald "Neutron Spectrum of $^{238}PuO_2$" Nuclear Applications 4 (1968): 11–22.

[42] M. E. Anderson. "Neutron energy spectra of a $^{238}$Pu-$^{18}$O (alpha, n) source—unmoderated and polyethylene moderated." *Health Phys.* Sep; 39 (3) (1980): 537–42.

[43] D. E. Peplow, "Monte Carlo Shielding Analysis Capabilities with MAVRIC," *Nuclear Technology* 174, Number 2 (2011): 289–313.

[44] *SCALE: A Comprehensive Modeling and Simulation Suite for Nuclear Safety Analysis and Design*, ORNL/TM-2005/39, Version 6.1 ORNL, Oak Ridge, TN, 2011. (Available from Radiation Safety Information Computational Center at Oak Ridge National Laboratory as CCC-785.)

[45] M. L. Williams, G. Ilas, M. A. Jessee, B. T. Rearden, D. Wiarda, W. Zwermann, L. Gallner, M. Klein, B. Krzykacz-Hausmann, A. Pautz, "A Statistical Sampling Method For Uncertainty Analysis With SCALE And XSUSA," *Nuclear Technology* 183, 3, (Sept. 2013) 515–527.

[46] M. E. Dunn and N. M. Greene, "AMPX-2000: A Cross-Section Processing System for Generating Nuclear Data for Criticality Safety Applications," *Trans. Am. Nucl. Soc.*, 86, (2002): 118.

# APPENDIX A.

# NUCLEAR DATA AND PHENOMENA IDENTIFICATION AND RANKING TABLE

## APPENDIX A. NUCLEAR DATA AND PHENOMENA IDENTIFICATION AND RANKING TABLE

**Table A.1: Status of existing nuclear data – neutron-based NDA methods for nonproliferation applications**

| Neutron-based NDA process/data needs | Importance (High = H, Medium = M, Low = L) | NDA system design tools and instruments | Knowledge (Unknown = U Known = K, Partially known = P) | Commentary/discussion |
|---|---|---|---|---|
| <u>Fission process data</u><br>Fission product yields [3] (independent fission yield, cumulative fission yield, chain yield, and mass yield [6]) | H | Nuclear data libraries used by codes such as SCALE (ORIGEN), SOURCES, SAMMY, MCNP<br>Source term definition | P | Nuclear data are an essential part of nuclear fuel burnup and decay codes and nuclear transport codes. Such codes are routinely used for analysis of spent fuel and NDA instruments for nonproliferation. Hence, the uncertainties in the nuclear data used in these codes affect the accuracies of such analysis. In addition, nuclear data uncertainties represent the limiting (smallest) uncertainties that can be expected from nuclear code predictions and therefore define the highest attainable accuracy of the NDA instrument.<br>Build-up of neutron-absorbing fission products (e.g., $^{133}$Cs, $^{143}$Nd, $^{149}$Sm, $^{154}$Eu, and $^{155}$Gd) reduces the net neutron emission rate from the source, and therefore, the count rate measured by an NDA instrument. Accurate estimation of neutron-absorbing fission products is vital. The absorption cross sections of some of the fission products ($^{155}$Gd) have large uncertainties [7](~5.3%).<br>For $^{244}$Cm—the dominant source of spontaneous fission neutrons as well as delayed neutrons—the nuclear data uncertainties are relatively high (8%) compared to other actinides such as $^{239}$Pu (1%) [7]. Thus Cm predictions remain a challenge. The destructive assay capabilities of Cm are also relatively poor.<br>The stable neodymium and samarium isotopes were predicted with ORIGEN to within a few percent of the measured values. Accurate predictions were made for $^{133}$Cs and $^{153}$Eu. However, predicted values for stable Ru and Rh isotopes varied by ~10%, and $^{109}$Ag consistently over-predicted by as much as 170% [7].<br>Larger uncertainties in modeling radioactive FP vs actinides or stable FPs calculated/experimental (C/E) ratio for $^{106}$Ru and $^{125}$Sb were 67% and 100%, respectively (ORIGEN). |
| Neutron absorption cross sections of fission products (FP) | L | Decay heat calculations | | |

| | | | | |
|---|---|---|---|---|
| | | | | Inconsistencies with legacy nuclear fission yield data on noble gas FPs. $^{85}$Kr predicted to within 10% (not 5%) [7].<br>Direct and cumulative yields are highly correlated [13]. No covariance data are available. Retroactive generation has been performed by combining independent and cumulative yields uncertainties with Bayesian statistical methods.<br>These are some of the areas where more work is needed for improving the accuracy of available nuclear data. This has a direct impact on the performance of NDA instruments used in the nonproliferation arena. |
| <u>Fission cross sections</u><br>Effective group-averaged fission cross-sections [6]<br><br>Neutron-induced fission cross section of $^{235}$U<br><br>Neutron-induced fission cross section of $^{239,241}$Pu and others (non-Uranium–based fuel cycles such as Thorium) | H<br><br>H<br><br>H | Source term definition<br>Nuclear data libraries used by codes such as SCALE (ORIGEN), SOURCES, SAMMY, MCNP<br>Design of Active Neutron NDA systems | **P**<br><br>**K**<br><br>**P** | Fission cross sections are highly important for source term definition and interpretation of the response of active and passive neutron NDA system measurements. The Active Well Coincidence Counter and the Neutron Coincidence Collar are examples of key NDA instruments used in material verification and nonproliferation. High fidelity covariance matrices were developed for evaluated ENDF/B-VII files for 3 major actinides: $^{235,238}$U and $^{239}$Pu [11]. Both differential experimental data and theoretical model calculations were used to estimate the uncertainties and correlations associated with the evaluated cross sections. The results were compiled in the ENDF format for covariance matrices and processed into multigroup files for applications.<br>The neutron-induced fission cross section of $^{235}$U was evaluated by the IAEA Standards Group (Carlson et al., "International Evaluation of Neutron Cross Section Standards," *Nuclear Data Sheets*, 110, 3215, 2009), and the ENDF/B-VII.0 evaluation incorporates their findings without modification, including the associated covariance matrix for this reaction. Overall, the evaluated standard deviations are very small at less than 1%. The off-diagonal elements are all positive and very small due to the large number of experimental data sets incorporated in the evaluation. The estimation of uncertainties associated with the neutron-induced fission cross section of $^{235}$U is of major importance, as most other actinide fission cross section uncertainties are driven by it. |

| | | | | |
|---|---|---|---|---|
| | | | | While evaluation by the IAEA Standards Group is the result of major efforts from experts in the domain, unrecognized correlations between experiments can lead to an underestimation of the final uncertainties. The development of a time-projection chamber (TPC) for subpercent fission cross section measurements (e.g. ,TPC at the Large Hadron Collider) represents an important effort to evaluate this cross section in a very different approach than what was done in the past. In this sense, the results of a TPC measurement would be mostly uncorrelated to past data sets and would represent a strong test for the current evaluation.<br>In Talou's 2011 paper [11], the neutron induced fission cross section plot is given for $^{239}$Pu (n, fission), but the correlation matrix is not given. The correlation matrix for $^{241}$Pu is also not given. The paper states that "a new evaluation of neutron-induced reactions on $^{241}$Pu is in progress and will eventually be incorporated in later releases of the ENDF/B-VII library. However, at this time, a new covariance matrix evaluation for the neutron-induced fission cross-section only was performed and is included in the VII.1 library. It is based solely on a statistical analysis of the experimental fission cross section data using the GLUCS code."<br>For the $^{233}$U(n,f) reaction, Talou et al [11] state that uncertainty quantification and the covariance matrix were indeed generated using tools and methods identical to those used for $^{235}$U and other actinides. The uncertainty and covariance results for $^{233}$U(n,f) reaction are indeed given in ENDFB-VII.1, albeit preliminary. |
| Neutron capture or absorption cross section<br>Cross sections for (n,p), (n,α), (n, gamma), (n,n') and (n, 2n)<br>Cross sections for elastic and in-elastic scattering<br>Prompt neutron emission [3]<br>Nu bar, average number | H<br>H<br>H<br>H | Source term definition<br>Transport through medium<br>Detection | **P** | Besides fission, accuracy of other cross sections is also vital since they are used in modeling neutron transport, detector response, and source term definition. While reaction cross sections have been available in general, it is only recently that the work on the uncertainty quantification including covariances has been undertaken.<br>Nuclear data uncertainty represents the limiting accuracy that can be achieved in simulations of NDA methods and data analysis.<br>The most comprehensive report on covariance matrix |

| | | | | |
|---|---|---|---|---|
| of neutrons per fission [4]<br>Prompt gamma ray emission [3] | H<br>H | | | evaluations for a large number of actinides is a publication titled "Quantification of Uncertainties for Evaluated Neutron-Induced Reactions on Actinides in the Fast Energy Range" by Talou et al. in 2011 [11]. All major reaction cross sections were considered in the Talou studies: total, capture, fission, elastic, total inelastic, and (n,xn), but neither angular distribution nor discrete inelastic reaction uncertainties were considered. In addition, for some actinides (i.e., n+$^{238-240}$Pu and n+$^{235,238}$U), the prompt fission neutron spectrum covariance matrix was evaluated at 0.5 MeV incident neutron energy following an approach similar to that developed for cross section uncertainties. Talou et al. also evaluated the average prompt fission neutron multiplicity ν_bar ($Ei_{nc}$) through a statistical analysis of experimental data when available.<br>"One should still consider the covariance matrices (in ENDFB-VII.1) as a first attempt at assessing uncertainties in evaluated nuclear data files in a scientific-based approach.<br>Much work remains to improve upon those matrices in order to represent the full evaluation process as faithfully as possible. A particular effort should be devoted to a better representation of the experimental uncertainties and of their correlations in and between experiments." – Talou et al [11]. |

| | | | | |
|---|---|---|---|---|
| Uncertainties and covariances in evaluated nuclear library data ENDFB-VII | H | Source term definition<br>Design tools such as SCALE, MCNP<br>Sensitivity and uncertainty analysis | **P** | In addition to the comments highlighted above in regard to the completeness of the uncertainty and covariance values in the ENDF/B-VII library, it is important to examine the summary by Talou et al. [11].<br>"In many cases, the evaluation of the nuclear data was performed prior to the quantification of uncertainties, thereby creating a somewhat inconsistent approach.<br>While such detailed approach (for uncertainty quantification and covariance calculation) has been used for the standards evaluation, much less has been done for other reactions and isotopes.<br>The unresolved resonance region represents an interesting challenge where much progress can be made by accounting for the matching between different reaction models where they overlap in this energy range.<br>Such work would lead to correlations between the resolved resonance range and the fast energy range, which are totally absent from the current covariance matrices." |
| <u>Radioactive decay data and decay heat</u><br>Decay half-lives<br><br>Decay constants, branching fractions/ratios<br>Production via alpha and beta decay | H | Decay heat predictions SCALE (ORIGEN) | **P**<br><br>**P** | Decay constants and branching ratios are among the fundamental nuclear data required in estimating the activities/masses of isotopes of interest.<br>$^{241}$Pu is short lived and is required for Pu mass decay and $^{241}$Am in-growth calculations. Inconsistencies in the uncertainties in the half-life of $^{241}$Pu have been revisited by Croft et al. [12] and addressed based on robust statistical principles.<br>Decay data were revised in ENDF/B-VII.1 (2011). Fission yield and decay data in ENDF/B-VII.1 are inconsistent [13].<br>Most experimental measurements of nuclear structure and decay-scheme data focus on the emission of discrete gamma rays. This type of spectral measurement dominates FP decay-scheme studies because of the difficulties and scarcity of facilities throughout the world that can measure the corresponding beta transition energies and emission probabilities accurately. However, the inability to detect weak high-energy gamma-ray |

| | | | | |
|---|---|---|---|---|
| Structurally based activation products [6] | L | | **K** | emissions satisfactorily impacts the β- decay data calculated from such measurements [6].<br>A generalized assessment was made of a radionuclide with a complex decay scheme (labelled *pandemonium*): approximately 20% of the gamma-ray emissions above 1.7 MeV were estimated to remain undetected within the background and would be omitted from the proposed decay scheme. Under these conditions, every complex β- decay scheme derived through gamma-ray studies must be regarded with some doubt: the recommended β--decay scheme may be inaccurate and might explain anomalies that sometimes occur between calculated and measured decay heat [6].<br><br>The radioactive decay of the activation products generated from structural materials of a thermal-reactor core represents an extremely minor contribution to the resulting decay heat. This source is more significant following shutdown of a fast reactor, with the formation of $^{22}$Na and $^{24}$Na by activation of the sodium coolant, and $^{58}$Ni(n,p)$^{58}$Co and $^{59}$Co(n,γ)$^{60}$Co from the activation of the nickel content of the steel structures in the reactor core. However, the production cross sections and decay data of all the main contributors are sufficiently well known that uncertainties in these parameters pose no problems in summation calculations. |
| <u>Neutron emission</u><br>- Spontaneous fission<br>- Induced fission<br>- (α, n)<br>Neutron multiplicity distribution [4]<br>Nu bar, average number of neutrons per fission [4]<br>Spontaneous fission neutron yields [1]<br><br>(α, n) neutron yields [1]<br><br>Thick-target yields from | H<br><br><br><br>H<br><br>H<br>H<br><br>H<br><br>**H** | ORIGEN, SOURCES4C, SAMMY, MCNP, GEANT4<br>Passive and Active neutron total and coincidence counters, neutron multiplicity counters | **P**<br><br><br><br><br><br>**P**<br><br><br>**P**<br><br>**P** | Nuclear data related to neutron emission are vital in accurate definition of the source term and the detector response. Before an NDA instrument can be configured and deployed, the use of modeling and simulation codes can provide a good estimate of performance characteristics. The emitted neutron signals ultimately help in the determination of the amount of nuclear material present. Therefore, accurate uncertainty quantification in nuclear data will establish the accuracy achievable using an NDA instrument.<br>SOURCES code used for spontaneous fission and (α,n) has no covariances, and in fact has no uncertainty guidance at all.<br>ENDF/B-VII.1 contains SF covariance data for $^{252}$Cf only. Its veracity and impact have not been tested. |

| | | | | |
|---|---|---|---|---|
| (α, n) reactions [1]<br><br>**Oxides**<br>$^{17}O(\alpha, n)$ and $^{18}O(\alpha,n)$<br><br>**Fluorides**<br>$^{19}F(\alpha, n)\ ^{22}Na$ cross-section as a function of energy [3]<br>$^{19}F(\alpha, n)\ ^{22}Na$ neutron yield [3]<br>$^{19}F(\alpha, n)\ ^{22}Na$ neutron spectra [3]<br><br>(α, n) reactions on other low Z elements (Li,N,Na,K..) | H<br><br>H<br><br>H<br><br>H | Uranium and Plutonium oxide measurements<br><br>Passive neutron counting for $UF_6$ canisters<br><br>Measurements associated with non-oxide fuel; pyro-processing | **P**<br><br>**U (very poorly known)**<br><br>**U** | A retroactive covariance data generation performed using the SAMMY code with R-Matrix evaluation for (α,n) cross sections is being undertaken to develop the methodology [14].<br>To get thick target yields, one has to generate microscopic cross sections and integrate over the slowing down in the material of interest, which involves using mass stopping powers that are not well known for the materials of interest to safeguards.<br>New thick target yield measurements over a broader energy range, 1.5 to 10 MeV, are needed for both $UO_2$ and $U_3O_8$ to adequately validate both the low energy range for $UO_2$ and the $UO_2$ to $U_3O_8$ scaling rules that depend on uncertain stopping power data. Yields for different oxygen compounds and from oxides of transuranic elements would be especially interesting to measure [15]. An accurate benchmark would be a measurement of $AmO_2$.<br>Croft has compiled the O(α, n) spectrum in the spreadsheet Oxanspec.XLS based on the data from Jacobs & Liskien [18]. This has been done by averaging the data for incident alpha energies of 4.5 and 5.0 MeV.<br>Improved spectral measurements are desired.<br>Fluorine is a very important (α, n) target for the fuel cycle. Nuclear data for $^{19}F(\alpha, n)\ ^{22}Na$ reaction are not well known. Data on emission spectra are sparse.<br>The thick-target yield from the $^{19}F(\alpha,n)$ reaction reported in the literature are systematically different by 54% to 35% as the energy of alpha increases from 4 MeV to 8 MeV [16], [17]. The differences are attributed in part due to the differences in the stopping powers used.<br>Both improved yield and spectrum data are desired.<br>Croft has compiled the F(α, n) spectrum in the spreadsheet Oxanspec.XLS, based on the data from Jacobs & Liskien [18] for an incident alpha energy of 5.0 MeV.<br><br>Data are needed for (α, n) reactions on elements other than O and F. These will be emphasized for other scenarios (e.g. pyro-processing). |

| | | | | |
|---|---|---|---|---|
| Delayed neutron yields | H | Active neutron measurement systems; e.g. $^{252}$Cf shuffler<br><br>Cross cutting NDA technique with applications in nuclear forensics | **U**<br>**(very poorly known)** | Each fissile isotope has a unique delayed neutron signature. The overall number of delayed neutrons per fission as well as their distribution among the delayed neutron groups varies. Development of delayed neutron NDA techniques used to estimate the isotopic composition of an uncharacterized sample is still an active topic [19]. It has been shown before that the delayed neutron signal of a sample can be unfolded to arrive at isotopic mass estimates [20].<br>The relative delayed neutron group abundances are among the poorest known nuclear data and have large associated uncertainties.<br>Kelley et al [19] carried out an analysis of the uncertainties associated with the delayed neutron NDA technique using a genetic algorithm. They observed that their genetic algorithm is sensitive to some of the delayed neutron group abundances. The overall uncertainties of the mass estimates were 15%, 5%, and 30% for $^{235}$U, $^{238}$U, and $^{239}$Pu, respectively. Reducing the first delayed neutron group abundances as proposed by Perret and Jordan [21] by a factor of three reduced the overall uncertainties to 10%, 3%, and 20%, respectively. |
| Energy spectrum of AmLi(α, n) neutron interrogation source [4]<br>Absolute neutron emission rate of AmLi(α, n) neutron interrogation source [4] | H<br><br>H | Active neutron measurement systems; (Active Well Coincidence Counter, Uranium Neutron Coincidence Collar) | **P**<br><br>**P** | Poorly studied from an applications perspective. |
| **Isotopes of interest: $^{3}$He, $^{10}$B, $^{6}$Li, $^{157}$Gd**<br><u>Neutron detection</u> | H | Thermal neutron | **K** | **Thermal neutron based detection:** gas proportional counters |

| | | | | |
|---|---|---|---|---|
| Absorption cross-sections<br><br>Elastic scattering cross sections H, Deuterium, He, C, O | H | detection; passive and active neutron coincidence counting<br><br>Fast neutron detection via neutron scattering | **K** | ($^{3}$He, $BF_3$, and $^{10}$B lined) and scintillation counters ($^{6}$LiF:ZnS). There is ongoing research for alternatives to $^{3}$He-based neutron detectors because of the paucity of $^{3}$He gas globally. Passive neutron coincidence and multiplicity counting is a powerful NDA technique applied in radioactive waste assay and nuclear safeguards.<br>Thermal neutron detectors are also used in active systems such as the $^{252}$Cf Shuffler, Active Well Coincidence Counters (AWCC), and Differential Die-Away (DDA) systems. These instruments are used in waste assay, as well as in nuclear safeguards.<br>**Fast neutron based detection:** Organic and plastic scintillators with pulse shape discrimination to filter out gammas, capture gated neutron detectors, liquid scintillation detectors |

| Table A.2. Status of existing nuclear and atomic data – photon-based NDA methods for nonproliferation applications | | | | |
|---|---|---|---|---|
| **Photon based NDA process/data needs** | **Importance (High = H, Medium = M, Low = L)** | **NDA system design tools and instruments** | **Knowledge (Unknown=U Known = K, Partially Known = P)** | **Commentary/discussion** |
| Isotopes of interest: $^{238,239,240,241,242}$Pu, $^{233,235,238}$U, $^{241}$Am, FPs, activation products<br>Gamma ray emission<br>• Energy (keV)<br>• Emission probability (per decay)<br>• Half-life (s)<br>• Decay branching ratio<br>Specific activity (number of decays per second per unit mass)<br>Principal NDA gamma ray signatures [1] | H<br>H<br>H | Attributes, gamma ray spectrometry based NDA systems; hand-held radiation identifiers, enrichment meters, Isotopic codes | K | Accurate knowledge of gamma ray energies, half-life, and gamma ray yields is extremely important for identifying and quantifying radionuclides of interest for nonproliferation applications. NDA instruments based on gamma spectrometry and analysis software depend on gamma ray–related nuclear data and the uncertainties in them.<br>Nuclear data related to gamma ray emission are needed to set up libraries for nuclide identification in gamma ray analysis, and activity or mass determination.<br>Codes such as MGA, MGAU, and FRAM are used to determine the Pu and U isotopics. These codes resort to using the gamma ray intensities as variables in order to obtain consistency in the isotopic ratio results. However, this is a work around that has become necessary to overcome the shortcomings of the fundamental nuclear data available in the libraries. If accurate nuclear data and defensible uncertainty quantification become available, the isotopic codes (and other applications) can directly use them and propagate the uncertainties.<br>Better knowledge of emission probabilities of x-rays and gamma rays will result in lower systematic uncertainties in the results generated by the isotopic codes. One of the key lines used by the isotopic codes is the 258.227 keV gamma emitted by $^{234m}$Pa, a daughter of $^{238}$U. The gamma ray intensity in the NuDAT is 0.0764% with a relative uncertainty of 21%. The 258.227 keV line bridges the gap between the low and high energy sides of the relative efficiency curve when determining U isotopics. |

| | | | | |
|---|---|---|---|---|
| Photo-neutron (γ,xn) and Photo-fission (γ,f) reaction data | M | Radiation shielding and radiation transport<br>Safeguards and Inspection technologies (identification of radiation induced by photonuclear reactions using portable bremsstrahlung devices)<br>Safeguards: Photon induced neutron production on light nuclei | **P** | The need for more accurate photonuclear will become a high priority when photon-induced active interrogation methods become more widely used in nonproliferation technologies. Bremsstrahlung sources such as a microtron offer a simpler alternative to using neutron generators for active interrogation.<br>In the past, several efforts were carried out which aimed to provide accurate, reliable photonuclear data for the applications mentioned. An important project was by the Photonuclear Data Center at the US National Bureau of Standards (now called NIST) from 1955–1982. The results were published by E.G. Fuller and H. Gersternberg [30] in a series of 15 issues titled "Photonulcear Data – Abstract Sheets 1955–1982."<br>Comprehensive compilations of photo-neutron cross section data can be found in the work by Dietrich and Berman [31] and in the IAEA-TEC-DOC 1178 [32].<br>More recent works on photofission include relative measurements of bremsstrahlung induced photofission yield performed by A. S. Soldatov for 19 nuclei from $^{232}$Th to $^{249}$Cf with respect to $^{238}$U. This work included the photofission yields for U and Pu isotopes of interest in nuclear safeguards and nonproliferation [33].<br>No uncertainty or covariance information is available in the ENDFB-VII.1 database. |
| $^{242}$Pu correlations | H | Total Pu evaluations using NDA techniques for nonstandard reactor types; implications on nonproliferation | **P** | $^{242}$Pu content evaluation is now becoming one of the major problems in plutonium assay by NDA. This is particularly true as many nuclear power plants tend to increase the initial $^{235}$U enrichment (in $UO_2$ fuel) to close to 4% in order to reach higher burn-up (50GWd/tU). Under these circumstances, the $^{242}$Pu content is not negligible. It could reach 10% for typical burn-up. A lack of knowledge of $^{242}$Pu will generate a significant bias in the total Pu evaluation while measuring via passive neutron coincidence counting and gamma spectrometry.<br>$^{242}$Pu cannot be determined by high resolution gamma spectrometry since it has no gamma emissions. Therefore, it is determined via correlations to other Pu isotopes. Correlation algorithms have been worked out for standard reactor types [22]. However, in nonstandard reactor types, it is necessary to understand the plutonium production cycle in order to establish the correlations. |

| | | | | |
|---|---|---|---|---|
| **X-Rays**<br>Major K x rays of uranium and plutonium [1]<br>$K_\alpha$ x-ray energies, intensities and intrinsic line widths [1] | H<br>H<br>H | NDA methods for determining U, Pu and other actinides; (e.g.)Isotopics, Hybrid K-Edge Densitometry<br>Portable and fixed NDA instruments for measurement of U-Pu isotopics that use X-ray and gamma ray data. | **K**<br>**P** | X-ray peaks from U and Pu are used by the isotopic codes such as MGA, MGAU, and FRAM to build the relative efficiency curve. The x-ray yields are important nuclear data for these codes. Also, the Hybrid K-Edge Densitometry (HKED) uses K-x-rays to estimate U and Pu concentrations. Precisions on the order of 0.3% can be achieved using the HKED methods for U and Pu. Such high precisions are necessary when it comes to reducing the uncertainty in the materials inventory. HKED systems are used in reprocessing facilities around the world (Europe, Asia) and relied on by the IAEA for materials inventory.<br>An even more precise HKED analysis based on whole spectrum fitting has been developed for determining the concentrations of U, Pu and other actinides of interest in nuclear safeguards [23]. The overall uncertainty of the whole spectrum fitting method is limited by the uncertainty in mass attenuation coefficients of actinide elements near the K-edge [23],[24].<br>Uncertainty in MAC is typically on the order of 1%–5% at energies well above the edges. Near the K-edges ($1.1 \leq E/E_K \leq 1.2$), the uncertainty in the photoelectric cross section is ~3%, and for $E/E_K$ less than 1.1, the uncertainty is 10%–20%. At energies only 0.1% above the edge, the uncertainty in the photoelectric cross section is ~50% [25]. |
| **Gamma transport and detection**<br>Photoelectric absorption cross-section<br>Compton scattering cross-section<br>Pair production cross-section | H<br>H<br>H | Design of photon based NDA systems using tools such as MCNP, GEANT4. Transport through low, intermediate, and high Z media.<br>Simulations of gamma ray interactions with detection materials such as Ge, NaI, $LaBr_3$, CZT | **P** | Knowledge of cross sections for gamma ray interactions with matter are very important for understanding and estimating gamma ray transport through a medium and gamma ray detection. Measurement systems and computer codes such as MCNP and GEANT rely on photon cross section libraries. The gamma ray nuclear data are needed in a variety of applications besides nonproliferation, including health physics, radioactive waste assay, portal monitor (security), etc.<br><br>As stated in a publication by Physical Measurement Laboratory, NIST [25]:<br><br>"For high energies (the transition depends upon *Z*), the coherent and incoherent cross-sections dominate over the photoelectric cross-section. In this region the scattering coefficients of refs. [26]and [27]are recommended as a possibly higher precision computation. At this point the experimental evidence on this point is inconclusive, but we do not claim any higher accuracy than 5 % for these scattering estimates.<br><br>At 1 MeV energies and above, (or at $\gamma$-ray resonances), nuclear physics dominates and we recommend inclusion of corrections by Hubbell et al. [27],[28] for radiative and double-Compton contributions to incoherent |

| | | | | |
|---|---|---|---|---|
| | | etc., that are used in NDA measurements. | | cross-sections, reaching 1 % at 100 MeV energies, and those of nuclear-field pair production $\kappa_n$ beginning at $2m_ec^2$ = 1.022 MeV and becoming dominant around 10 MeV and above.<br><br>Electron-field pair production ("triplet production") begins at 2.044 MeV and contributes above this energy at the 1 % level for high $Z$ elements but up to 10 % for fluorine and 50 % for hydrogen [or $1/(1 + Z)$]. Nuclear photo-absorption consists of one (or a few) peaks (giant resonances) between 10 MeV to 24 MeV of width 3 MeV to 9 MeV, contributing up to 10 % of the total cross-section in this region. Elastic processes include high energy Delbrück and dipole resonance scattering in addition to Rayleigh and nuclear Thompson contributions mentioned above."<br><br>If coherent and incoherent scattering cross sections cannot be known to better than 5%, the results of transport calculations (and design of detection systems) cannot be known to accuracies better than 5%. (In the detector material, higher energy photons undergo multiple collisions, lose energy, and eventually undergo photo-electric absorption.) |

| Table A.3. Status of existing muclear and data – heat based NDA methods for nonproliferation applications | | | | |
|---|---|---|---|---|
| **Heat-based NDA process/data needs** | **Importance (High = H, Medium = M, Low = L)** | **NDA system design tools and instruments** | **Knowledge (Unknown=U Known = K, Partially Known = P)** | **Commentary/discussion** |
| Isotopes of interest: $^{238,239,240,241,242}$Pu, $^{241}$Am<br>Heat production in item<br>Radionuclide half-life<br>Specific thermal power [29]<br>Half-life of Pu isotopes<br>Half-life of $^{241}$Pu [2],[12]<br>Half-life of $^{241}$Am [2]<br>Specific thermal power of $^{241}$Pu [2]<br>Specific thermal power of $^{241}$Am [2]<br>Q-value, disintegration energy for α-decay (in MeV) [4]<br>Average energy of β-particles (in MeV) [4]<br>Thermal conductivity | | Heat Flow Calorimetry – the most accurate NDA method for measuring many physical forms of Pu.<br><br>Calorimetry has also been applied to measuring mixed $PuO_2$+$UO_2$. | **K** | Generally known for all other isotopes except $^{241}$Pu.<br><br>The accuracy of the results achieved by the calorimeter is limited only by the uncertainties in the nuclear decay parameters (half-life and isotopic specific power), as well as the uncertainties from gamma spectroscopy based isotopic ratios. |

## APPENDIX A REFERENCES


[1] T. Douglas Reilly, "Useful Nuclear Data for NDA," Addendum to *Passive Non-Destructive Assay (PANDA) Manual* (2007).

[2] S. Croft, P. A. Santi, and R. D. McElroy, Jr., "Determination of the half-life and specific thermal power of $^{241}$Pu by nuclear calorimetry," *ESARDA Bulletin*, No. 50 (December 2013).

[3] A. Dougan, *Long Term R&D for Safeguards*, IAEA-CN-220-221.

[4] P. Schillebeeckx, M. Looman, and A. Ravazzani, "Nuclear Data Required for Non Destructive Assay of Fissile and Fertile Material," *World Scientific* (2000).

[5] G. Gilmore, *Practical Gamma Ray Spectroscopy*, 2nd edition, John Wiley and Sons (2008).

[6] A. L. Nichols, "Nuclear Data Requirements for Decay Heat Calculations," Lectures at Workshop on Nuclear Reaction Data and Nuclear Reactors: Physics, Design and Safety, Trieste, 25 February – 28 March 2002, International Atomic Energy Agency, Nuclear Data Section, Department of Nuclear Sciences and Applications, Vienna, Austria, LNS0520003 (2002).

[7] M. W. Francis, C. F. Weber, M. T. Pigni, and I. C. Gauld, "Reactor Fuel Isotopics and Code Validation for Nuclear Applications," ORNL,, ORNL/TM-2014/464 (September 2014).

[8] D. Rochman, M. Herman, P. Oblozinsky, S. F. Mughabghab, "Preliminary Cross Section and n-bar Covariances for WPEC Subgroup 26," BNL-77407-2007-IR, Energy Sciences & Technology Department, National Nuclear Data Center, January 2007.

[9] P. Talou, T. Kawano, and P. G. Young, "Covariance Matrices for ENDF/B-VII 235, $^{238}$U and $^{239}$Pu Evaluated Files in the Fast Energy Range," *Proc. Int. Conf. on Nuclear Data for Science and Technology*, Apr. 22–27, 2007, Nice, France,(2008): 293–296.

[10] R. C. Little et al., "Low-fidelity Covariance Project," *Nuclear Data Sheets*, 109, Issue 12 (2008): 2828–2833.

[11] P. Talou, P. G. Young, T. Kawano, M. Rising, M. B. Chadwick, "Quantification of Uncertainties for Evaluated Neutron-Induced Reactions on Actinides in the Fast Energy Range," *Nuclear Data Sheets* 112 (2011): 3054–3074.

[12] S. Croft, T.L. Burr, A. Favalli, "Estimating the Half-life of $^{241}$Pu and Its Uncertainty," *Radiation Measurements*, 59 (2013): 94–102.

[13] M. Pigni, M. W. Francis, I. C. Gauld, "Investigation of Inconsistent ENDF/B-VII.1 Independent and Cumulative Fission Product Yields with Proposed Revisions," *Nuclear Data Sheets* 1 (2015): 123.

[14] Luiz C. Leal, "Uncertainty Propagation in Neutron Source Calculations with SOURCES4C Code," *Annals of Nuclear Energy* 2015 (exact reference TBD).

[15] S. Croft and R. D. McElroy, "The thick-target integrated-over-angle (α,n) yield curve for $U_3O_8$ over the energy range from 1.5 to 10 MeV and associated specific (α,n) yields of the uranium isotopes," *Proc. 54th Annual Meeting of INMM*, July 14–18, 2013, Palm Desert, CA, USA.

[16] E. B. Norman et al., "$^{19}$F(α,n) thick target yield from 3.5 to 10.0 MeV," Applied Radiation and Isotopes 103 (2015 )177–178.

[17] J. K. Bair and G. Campo, "Neutron yields from alpha-particle bombardment," *Nucl. Sci. Eng.*71 (1979): 18–28.

[18] G. J. H. Jacobs and H. Liskien, "Energy spectra of neutrons produced by α-particles in thick targets of light elements," *Ann. Nucl. Energy* 10(10)(1983): 541–552.

[19] R. P. Kelley et al., "Uncertainty analysis of delayed neutron fissile material assay using a genetic algorithm," *Ann. Nucl. Energy* 80 (2015): 460–466.

[20] S. E. Aumeier and J. H. Forsmann, "Evaluation of Kalman filters and genetic algorithms for delayed-neutron nondestructive assay data analyses" *Nucl. Technol.* 122 (1998): 104–124.

[21] G. Perret, K. A. Jordan, "On the Combination of Delayed Neutron and Delayed Gamma Techniques for Fission Rate Measurement in Nuclear Fuel," *IEEE Transactions on Nuclear Science*, ANIMMA (2011).

[22] G. Bignan et al., "Plutonium Isotopic Determination using Gamma Spectrometry: Recommendations for the $^{242}$Pu Content Evaluation using a New Algorithm," *ESARDA Bulletin* 28 (1998).

[23] R. D. McElroy et al., "Spectral Fitting Approach to the Hybrid K-Edge Densitometer: Preliminary Performance Results," *Proc. of 56$^{th}$ Annual INMM Conference*, July 15–19, 2015, Indian Wells, CA, USA.

[24] S. Croft et al., "Mass Attenuation Coefficient Data for Hybrid K-Edge Densitometry," *Proc. of 37$^{th}$ Annual ESARDA Symposium*, May 18–21, 2015, Manchester, UK.

[25] C. T. Chantler et al., "X-Ray Form Factor, Attenuation, and Scattering Tables: Detailed Tabulation of Atomic Form Factors, Photoelectric Absorption and Scattering Cross Section, and Mass Attenuation Coefficients for Z = 1-92 from E = 1-10 eV to E = 0.4-1.0 MeV," Physical Measurement Laboratory, NIST, USA (2001).

[26] J. H. Hubbell et al., "Pair, triplet and total atomic cross sections (and mass attenuation coefficients) for 1 MeV - 100 GeV photons in elements Z = 1 to 100," *J. Phys. Chem. Ref. Data* 9 (1980): 1023–1147.

[27] J. H. Hubbell, I. and Øverbø, "Relativistic atomic form factors and photon coherent scattering cross sections," *J. Phys. Chem. Ref. Data* 8, (1979): 69–105.

[28] J. H. Hubbell et al., "Atomic form factors, incoherent scattering functions, and photon scattering cross sections," *J. Phys. Chem. Ref. Data* 4, (1975): 471–538.

[29] ASTM C1458: "Standard Test Method for Nondestructive Assay of Plutonium, Tritium and $^{241}$Am by Calorimetric Assay" (2015).

[30] E. G. Fuller and H. Gersternberg, "Photonuclear data – abstract Sheets 1955-1982," *Report of the US National Bureau of Standards*, NBSIR 83-2742, vol. I-XV (1983–1986), National Institute of Standards and Technology, Gaithersburg, MD, USA.

[31] S. S. Dietrich and B. L. Berman, "Atlas of Photoneutron cross sections obtained with monoenergetic photons," Atomic Data and Nuclear Data Tables 38 (1988): 199–338.

[32] *Handbook on Photonuclear data for applications – Cross sections and Spectra*, IAEA-TEC-DOC 1178, Final report of a coordinated research project, 1996–1999.

[33] A. S. Soldatov, "Relative measurements of Photofission Cross Sections with the Use of a Bremsstrahlung Spectrum," *Physics of Particles and Nuclei*, 39, No. 2 (2008): 173–220.